Fall 12-15-2023

Nonsmooth Epidemic Models with Evolutionary Game Theory

Cameron Morin
University of Maine, cameron.morin@maine.edu

NONSMOOTH EPIDEMIC MODELS WITH EVOLUTIONARY GAME THEORY

By

Cameron Morin

Unversity of Maine at Farmington, 2020

A THESIS

Submitted in Partial Fulfillment of the

Requirements for the Degree of

Master of Arts

(in Mathematics)

The Graduate School

The University of Maine

December 2023

Advisory Committee:

Peter Stechlinski, Associate Professor of Mathematics, Advisor

David Hiebeler, Professor of Mathematics

Brandon Lieberthal, Lecturer of Mathematics

NONSMOOTH EPIDEMIC MODELS WITH EVOLUTIONARY GAME THEORY

By Cameron Morin

Thesis Advisor: Professor Peter Stechlinski

An Abstract of the Thesis Presented
in Partial Fulfillment of the Requirements for the
Degree of Master of Arts
(in Mathematics)
December 2023

This thesis explores the utilization of game theory and nonsmooth functions to enhance the accuracy of epidemiological simulations. Traditional sensitivity analysis encounters difficulties when dealing with nondifferentiable points in nonsmooth functions. However, by incorporating recent advancements in nonsmooth analysis, sensitivity analysis techniques have been adapted to accommodate these complex functions. In pursuit of more accurate simulations, evolutionary game theory, primarily the replicator equation, is introduced, modeling individuals' decision making processes when observing others' choices. The SEIR model is explored in depth, and additional complexities are incorporated, leading to the creation of an expanded SEIR model, the Be-SEIMR model.

ACKNOWLEDGEMENTS

I am deeply grateful to my mother and father, whose unwavering support has been invaluable during my pursuit of a master's degree. To my best friend, your encouragement and camaraderie have made this journey more joyous. And to my soon-to-be wife, your love and support has been vital in my success. Thank you all for standing by me. Their unwavering support has been instrumental in my success.

I extend my deepest appreciation to my advisor, Dr. Peter Stechlinski, for his invaluable guidance during the course of this thesis. Working with him has been a truly wonderful experience. In moments of conceptual challenges, he consistently provided assistance and offered words of encouragement, helping me navigate through difficulties and persevere in the face of setbacks.

I extend my gratitude to Dr. David Hiebeler and Dr. Brandon Lieberthal for their contributions as members of my thesis committee.

Lastly, I am indebted to my friend, Philippe Nzarama, whose encouragement and support ensured that I stayed on the path to completing this journey.

TABLE OF CONTENTS

LIST OF TABLES

LIST OF FIGURES

CHAPTER 1
INTRODUCTION

Disease has wielded a profound influence on the course of human history. In antiquity, it often assumed the role of a divine force, revered as a deity by certain cultures or dreaded as a harbinger of pestilence, carried by the arrows of gods. As the world transitioned into the Renaissance era, the devastating impact of disease became painfully evident. The Black Death, a merciless scourge that claimed the lives of at least a third of Europe's population, stands as a somber testament to this era's vulnerability [23]. Similarly, the introduction of smallpox to the Americas decimated millions of indigenous people, altering the course of civilizations, sometimes eradicating these civilizations entirely [13]. Amidst the horrors of the Black Death, humanity's initial response was to ward off the perceived threat of miasma, or "bad air", through the use of aromatic substances enclosed in the infamous plague masks. During this period, hospitals served as grim waiting rooms for impending death, devoid of the treatment environments we recognize today [24]. The tide eventually turned as scientific understanding advanced. Miasma theory gave way to the revolutionary germ theory, unveiling an invisible realm teeming with microscopic viruses, bacteria, and fungi as the true culprits behind these afflictions. This pivotal shift marked the inception of a new era in disease-fighting, one characterized by relentless innovation and adaptation.

Advancements in our understanding have propelled us to a stage where we possess the capability to foresee the trajectory of disease within a population, employing intricate mathematical models. This journey commenced in 1760 when the pioneer of mathematical epidemiology, Daniel Bernoulli, conceptualized the first model [28]. The trajectory of progress continued with subsequent contributions from luminaries like Kermack and McKendrick, who further expanded the boundaries of this field, leading to monumental advancements [30]. These scholars made the crucial insight that an epidemic outbreak can be predicted based on a certain ratio of parameters in the mathematical model [21].

Emerging into the early 20th century, the advent of compartmental models marked a pivotal juncture, igniting an exponential surge in their application [28]. These models have emerged as indispensable tools, wielding their predictive power across an array of diseases, encompassing afflictions ranging from measles and chickenpox to pertussis, smallpox, rabies, and sexually transmitted diseases, among a myriad others [20].

In March 2020, the world bore witness to a major event as Coronavirus 2019 (Covid-19) swiftly transformed into a pandemic of unparalleled magnitude in the modern era. Prior to the discovery of a vaccine capable of halting the virus's spread, populations had to solely rely on plethora of disease mitigation strategies, each aiming to curb the spread of sickness. Across the globe, a multitude of mathematical models emerged, each rooted in its distinct set of assumptions, all aimed at illuminating the optimal course of action in the face of this viral adversary. Recent times have witnessed endeavors to systematize the construction of mathematical epidemic models [14], an endeavor undertaken with the intention of fostering the swift generation of models while concurrently mitigating the risk of compromising quality, reducing the total time it would take to create a model while keeping them accurate.

The central objective of this thesis revolves around the development of innovative mathematical epidemic models, integrating the realms of game theory and nonsmooth ordinary differential equation (ODE) theory. Our focus is sharply honed on infusing the model with the human decision making processes. This pivotal aspect enables us to accommodate the dynamic interplay between conventional behavior and disease aversion strategies within individuals. While Covid-19 stands as the cornerstone that motivated this thesis, our intent is to construct a versatile modeling framework capable of analyzing other diseases.

This thesis adds two major components to standard epidemic models: limited intervention resources and behavioral dynamics. Wang et al. [45, 43] introduce nondifferentiable, or nonsmooth, minimum functions to address the challenges posed by

constrained hospital and vaccine resources. By embracing these principles, Wang's contributions unveil an understanding of limited hospital capacities and constrained vaccine distribution, crucial aspects that mirror real world dynamics with finite resources. To introduce a heightened level of realism, we integrate human decision-making into epidemic modeling. This endeavor can take the form of segmenting populations into distinct groups, each characterized by varying probabilities of making specific decisions. Noteworthy examples that delve into this include works by Cai et al. [10], Ye et al. [46], and Vardavas et al. [40]. Furthermore, the spectrum widens as we examine scenarios where external influences prompt individuals towards certain choices. This dimension is explored in the studies by Bootsma and Ferguson [7], as well as Bentley et al. [5]. In this thesis, a pivotal tool in capturing the dynamics of imitation is the replicator equation, introduced as "evolutionary dynamics", by Hofbauer and Sigmund [22]. The essence of the replicator equation is rooted in the notion of individuals or groups copying the behaviors of other successful groups. This mechanism draws inspiration from observations wherein a group assesses the outcomes of another group's choices and, based on the results, individuals migrate between behaviors, emulating the more successful strategy. The replicator equation orchestrates a consensus or flocking behavior, mirroring the employment of ODEs akin to the compartmental models ubiquitous in epidemiology. Behavioral dynamics have been considered in epidemic modeling, such as by Bauch in [3] and Bauch and Bhattacharyya in [4].. These studies delineate the dynamics of individuals oscillating between their regular lifestyles and disease-avoidance behaviors. In this vein, the works of Poletti [35] and Schecter [37] investigated a similar approach to epidemic modeling. Notably, Poletti's framework lays the foundation for the subsequent replicator equation featured in this thesis.

At the heart of mathematical epidemiology lies the well-known Kermack-McKendrick model, often referred to as the SIR model. This model serves as the fundamental framework on which we build, aiming to capture a wider range of situations than the SIR model originally accounted for. This expanded framework introduces new aspects tailored

to the dynamics of Covid-19. For instance, we consider an incubation period, where individuals are affected by the virus but are not yet contagious, a concept supported by findings in [47]. Within this model, we also introduce a distinct compartment for hospitalizations, acknowledging the significant impact the virus has on some individuals [17]. Additionally, we incorporate a quarantine compartment to represent individuals who actively avoid potential contagion [29]. We further divide the group of infected individuals into two categories: symptomatic and asymptomatic [16]. We integrate compartments for vaccinations, a crucial strategy that contributes to reducing infection and mortality rates, as discussed in [8] and [27]. To introduce a dynamic layer of imitation dynamics, we draw from Poletti's work [35], which we adapt with the use of nonsmooth functions. In summary, this thesis amalgamates various insights to create a robust and flexible framework. Rooted in the SIR model, we enhance it by incorporating extensive variables, imitation dynamics, and intervention constraints.

With the new model in place, we perform a comprehensive analysis of this expanded model, with several key objectives in mind. Firstly, we use real world data to investigate the dynamics of our model. Secondly, our focus shifts towards analyzing the model's intrinsic dynamics. We calculate the basic reproductive number, a metric that uniquely quantifies a disease's infectiousness, for a submodel in which imitation dynamics are turned off. In this submodel, disease avoidance strategies will not be utilized It reveals the extent to which an infection would propagate within a fully susceptible population if a single infected individual were introduced. This critical value provides a lens through which we can grasp the inherent contagiousness of the disease. Although this model is rooted in Covid-19, we aimed to build a flexible framework that extends its applicability to other diseases. To this end, we compare our submodel basic reproductive number with those calculated for various other diseases, as documented in Earn et al. [33]. This comparative analysis will shed light on the relative contagiousness of different diseases and provide valuable insights. Lastly, a sensitivity analysis is conducted. This comprehensive

examination encompasses a majority of parameters, allowing us to discern the system's sensitivity to each parameter's variation. This undertaking provides insights into how the model responds to changes in different parameters, elucidating the robustness and fragility of the system.

As previously mentioned, our intention involves incorporating nonsmooth, nondifferentiable minimum and mid functions into our model. Classical sensitivity analysis relies on smooth functions, but given our context, this requirement presents challenges. While smoothing functions can approximate nonsmooth functions, they come paired with error functions that may lead to inaccuracies, particularly in the intricate landscape of our model. In addressing these complexities, we turn to Clarke's set-valued generalized derivative theory [11]. This theory operates with locally Lipschitz continuous functions instead of necessitating continuously differentiable functions. Elements of the Clarke derivative provide local first derivative information, proving especially useful within nonsmooth scenarios. The Clarke derivative encompasses useful calculus properties like the mean value theorem and the inverse function theorem. However, the calculus rules, such as the product rule, only hold as inclusions in most cases, and the computation of the elements can be challenging. Recent advancements in nonsmooth analysis have brought solutions to these challenges. Lexicographic derivatives, pioneered by Nestorov [31], bear strong resemblance to Clarke Jacobian elements. Moreover, lexicographical directional derivatives [2, 26] offer a systematic and accurate approach for computing lexicographical derivatives. These innovations have paved the way for nonsmooth ODE systems [25] to uncover generalized sensitivity functions suitable for locally Lipschitz continuous functions—a significantly expansive domain. This inclusion of locally Lipschitz continuous functions accounts for C^1, piecewise differentiable, and convex functions. Leveraging lexicographical sensitivity theory, we are poised to analyze our expanded epidemic model, even in instances where points of nondifferentiability arise.

The thesis will be organized into the following structured chapters:

- Chapter 2 will lay the groundwork by providing essential background information. It will delve into crucial concepts such as generalized derivative theory, nonsmooth ODE theory, game theory, and the SEIR model. These concepts serve as the building blocks for the subsequent chapters.

- Chapter 3 will constitute a pivotal section wherein the expanded SIR model takes shape. The additional components introduced, including the incubation period, hospitalization and quarantine compartments, different categories of infection, and vaccination compartments, will be detailed. This chapter aims to provide a comprehensive understanding of how these elements interact and shape the model's dynamics.

- Chapter 4 will focus on the rigorous analysis of the model. It will encompass the computation of the basic reproductive number—an indicator of the disease's infectivity— for the SEIMR submodel along with a comprehensive sensitivity analysis. These analyses will offer insights into the model's behavior, its responsiveness to various parameters, and its practical implications.

- Chapter 5 will bring the thesis to a close, summarizing the findings and insights derived from the preceding chapters. Concluding remarks will be made, highlighting the significance of the study's outcomes. Furthermore, potential avenues for future research directions will be suggested, aiming to spark further exploration and refinement of the developed model.

CHAPTER 2
MATHEMATICAL BACKGROUND

2.1 Preliminaries and Notation

For this section we will be considering an open set $E \subseteq \mathbb{R}^n$ and a function $\mathbf{f} : E \to \mathbb{R}^m$ unless stated otherwise. We also let

$$\mathbf{x} = (x_1, \cdots, x_n) = \begin{bmatrix} x_1 \\ x_2 \\ \vdots \\ x_n \end{bmatrix}$$

and given a function, $\mathbf{f}$,

$$\mathbf{f}(\mathbf{x}) = \begin{bmatrix} \mathbf{f}_1(\mathbf{x}) \\ \vdots \\ \mathbf{f}_m(\mathbf{x}) \end{bmatrix} = \begin{bmatrix} \mathbf{f}_1(x_1, \ldots, x_n) \\ \vdots \\ \mathbf{f}_m(x_1, \ldots, x_n) \end{bmatrix}.$$

Definition 2.1.1. *(Lipschitz Continuity). A function* $\mathbf{f}$ *is called Lipschitz continuous on* E *if there exists some constant* $L > 0$ *such that for all* $x, y \in E$,

$$\|\mathbf{f}(x) - \mathbf{f}(y)\| \leq L\|x - y\|.$$

The function f *is said to be locally Lipschitz on* E *if for each* $x_i \in E$ *there is an* ϵ*-neighborhood,* $N_\epsilon(x_i) \subseteq E$ *and a constant* L_i *such that for all* $x, y \in N_\epsilon(x_i)$,

$$\|\mathbf{f}(x) - \mathbf{f}(y)\| \leq L_i\|x - y\|.$$

If $\mathbf{f}$ is C^1 on E, then $\mathbf{f}$ is locally Lipschitz on E.

Example 2.1.2. *Let* $f : \mathbb{R} \to \mathbb{R}$ *be defied as* $f(x) = |3x + 2|$. *Then we have that by the reverse triangle inequality*

$$|f(x) - f(y)| = ||3x - 2| - |3y - 2|| \leq |3x - 2 - (3y - 2)| = |3x - 3y| = 3|x - y|.$$

Therefore for $L = 3$ our condition holds and f must be Lipshitz.

If a function f is locally Lipschitz on E, then f is also absolutely continuous.

Definition 2.1.3. *(Absolute Continuity). Let $E \subseteq \mathbb{R}$ be a connected set. A function $\mathbf{f} : E \to \mathbb{R}^n$ is called absolutely continuous on E if for any compact subinterval $Y \subset E$, and every $\epsilon > 0$ there exists $\delta > 0$ such that for each finite sequence of pairwise disjoint subintervals $\{[a_i, b_i] : i = 1, \ldots, q, q \in \mathbb{N}\}$ of Y satisfying $\sum_{i=1}^{q}(b_i - a_i) < \delta$ then*

$$\sum_{i=1}^{q} |\mathbf{f}(b_i) - \mathbf{f}(a_i)| < \epsilon.$$

Definition 2.1.4. *(Partial Derivative). Given a multivariable function, $\mathbf{f} : \mathbb{R}^n \to \mathbb{R}^m$, the partial derivative of $\mathbf{f}$ with respect to x_i is,*

$$\frac{\partial \mathbf{f}}{\partial x_i}(\mathbf{x}) = \lim_{h \to 0} \frac{\mathbf{f}(x_1, \ldots, x_i + h, \ldots, x_n) - \mathbf{f}(x_1, \ldots, x_n)}{h}. \tag{2.1}$$

When taking the partial derivative with respect to x_i all other variables, x_j $j \neq i$, are treated as constants.

Definition 2.1.5. *(Directional Derivative). Let $\mathbf{f}$ be a continuous mapping. Then the directional derivative of $\mathbf{f}$ at $\boldsymbol{x}$ in the direction $\boldsymbol{d} \in \mathbb{R}^n$ is*

$$\mathbf{f}'(\boldsymbol{x}; \boldsymbol{d}) = \lim_{\alpha \downarrow 0} \frac{\mathbf{f}(\boldsymbol{x} + \alpha \boldsymbol{d}) - \mathbf{f}(\boldsymbol{x})}{\alpha}.$$

We say $\mathbf{f}$ is directionally differentiable at $\boldsymbol{x}$ if $\mathbf{f}'(\boldsymbol{x}; \boldsymbol{d})$ exists for all $\boldsymbol{d} \in \mathbb{R}^n$, further we say that $\mathbf{f}$ is directionally differentiable on E if it is directionally differentiable for all $\boldsymbol{x} \in E$.

Definition 2.1.6. *(Gradient). Given a function, $f : \mathbb{R}^n \to \mathbb{R}$, the gradient $\nabla f : \mathbb{R}^n \to \mathbb{R}^n$ defined at a point $\boldsymbol{x}^* = (x_1^*, \ldots, x_n^*) \in \mathbb{R}^n$ is,*

$$\nabla f(\boldsymbol{x}^*) = \begin{bmatrix} \frac{\partial f}{\partial x_1}(\boldsymbol{x}^*) \\ \vdots \\ \frac{\partial f}{\partial x_n}(\boldsymbol{x}^*) \end{bmatrix}. \tag{2.2}$$

If we have multiple functions, $f_1, \ldots, f_m$, we can find a more complicated gradient called the Jacobian.

Definition 2.1.7. *(Jacobian Matrix). Given a function $\boldsymbol{f}\colon \mathbb{R}^n \to \mathbb{R}^m$, the Jacobian matrix evaluated at $\boldsymbol{x}^*$ is,*

$$\boldsymbol{J}\mathbf{f}(\boldsymbol{x}^*) = \begin{bmatrix} \frac{\partial f_1}{\partial x_1}(\boldsymbol{x}^*) & \cdots & \frac{\partial f_1}{\partial x_n}(\boldsymbol{x}^*) \\ \vdots & \ddots & \vdots \\ \frac{\partial f_n}{\partial x_1}(\boldsymbol{x}^*) & \cdots & \frac{\partial f_n}{\partial x_n}(\boldsymbol{x}^*) \end{bmatrix}.$$

Definition 2.1.8. *(Continuously Differentiable). For some function f, f is continuously differentiable (C^1) if the Jacobian matrix exists and is continuous on a neighborhood of x^*.*

Definition 2.1.9. *(C^1) A function, $\boldsymbol{f}$, is C^1 on E if $\boldsymbol{f}$ is C^1 for all $x \in E$.*

If f is C^1 then $f'(x;d) = \mathbf{J}\mathbf{f}(x)d$ and $\mathbf{f}$ is locally Lipschitz on E.

Definition 2.1.10. *(Convex). E is convex if for any $\boldsymbol{x}, \boldsymbol{y} \in E$, the line segment connecting $\boldsymbol{x}$ and $\boldsymbol{y}$ is also fully contained in E, that is $\lambda \in [0,1]$,*

$$\lambda\boldsymbol{x} + (1-\lambda)\boldsymbol{y} \in E$$

for all $\lambda \in [0,1]$. A function $\mathbf{f}$ is called convex if its domain is a convex set and for all $\boldsymbol{x}, \boldsymbol{y}$ in the domain and all $\lambda \in [0,1]$,

$$\mathbf{f}(\lambda\boldsymbol{x} + (1-\lambda)\boldsymbol{y}) \leq \lambda\mathbf{f}(\boldsymbol{x}) + (1-\lambda)\mathbf{f}(\boldsymbol{y}).$$

Many sets are not convex, but they can be converted into convex sets using the convex hull.

Definition 2.1.11. *(Convex Hull). The convex hull of E is E_c where E_c the smallest set such that $E \subseteq E_c$ and E_c is convex. If there is another convex set E_c' such that $E \subseteq E_c'$ then $E_c \subseteq E_c'$. If E is a finite set then the convex hull is,*

$$conv(E) = \{\sum_{i=1}^{|E|} \lambda_i \boldsymbol{x}_i \mid \sum_{i=1}^{|E|} \lambda_i = 1, \boldsymbol{x}_i \in E, \lambda_i \geq 0, \forall i = 1, 2, \ldots, |E|\}.$$

Definition 2.1.12. *(Piecewise Differentiable [38]). A continuous function* $\mathbf{f}$ *is called piecewise differentiable,* PC^1*, at* $\boldsymbol{x} \in E$*, if there exists a neighborhood* $N \subseteq E$ *around* $\boldsymbol{x}$ *and a finite collection of continuously differentiable,* C^1*, functions on* N*,* $\mathcal{F}_{\mathbf{f}} = \{\mathbf{f}_1, \ldots, \mathbf{f}_k\}$ *for some* $k \in \mathbb{N}$*,* $\mathbf{f}_i : N \to \mathbb{R}^m$ *for all* $i \in 1, \ldots, k$*, and*

$$\mathbf{f}(\boldsymbol{y}) \in \{\mathbf{f}_i(\boldsymbol{y}) \mid i \in [1, k] \cap \mathbb{N}, \forall \boldsymbol{y} \in N\}.$$

$\mathbf{f}$ *is said to be* PC^1 *on* E *if* $\mathbf{f}$ *is* PC^1 *for all* $\boldsymbol{x} \in E$*.*

Example 2.1.13. *Let* $f : \mathbb{R}^2 \to \mathbb{R}$ *be defined by* $f(x) = \min(x^2, y - 1)$*. When* $x^2 = y - 1$*,* f *is nondifferentiable. Note that* f *is* PC^1 *with neighborhood* $N = \mathbb{R}^2$ *and selection functions* $f_1 : (x, y) \to x^2$ *and* $f_2 : (x, y) \to y - 1$*.*

2.2 Generalized Derivatives Theory

The following material is from Clarke [11], unless stated otherwise.

Definition 2.2.1. *(B-Subdifferential). Given a locally Lipschitz continuous function* $\mathbf{f}$ *that is differentiable at each point in* $E \backslash Z_{\mathbf{f}}$*, with* $Z_{\mathbf{f}}$ *having Lebesgue measure zero, the Bouligand subdifferential, also referred to as the limiting subdifferential or limiting Jacobian, is,*

$$\partial_B \mathbf{f}(\boldsymbol{x})$$
$$= \{\boldsymbol{H} \in \mathbb{R}^{m \times n} \mid \lim_{i \to \infty} \mathbf{J}\mathbf{f}(x_{(i)}) = \boldsymbol{H} \text{ for some seq. } \{\boldsymbol{x}_{(i)}\} \text{ s.t. } \lim_{i \to \infty} \boldsymbol{x}_{(i)} = \boldsymbol{x}, \boldsymbol{x}_i \in X \backslash Z_{\mathbf{f}}, \forall i \in \mathbb{N}\}.$$

With the B-subifferential we can introduce Clarke's generalized derivative.

Definition 2.2.2. *(Clarke's Generalized Derivative). The Clarke generalized derivative, sometimes called Clarke's Jacobian, of* $\mathbf{f}$ *at* $\boldsymbol{x}$ *is,*

$$\partial \mathbf{f}(\boldsymbol{x}) = \text{conv}(\partial_{\text{B}} \mathbf{f}(\boldsymbol{x})).$$

In other words, the Clarke generalized derivative is the convex hull of the Bouligand subdifferential as defined in Definition 2.2.1. If $\mathbf{f}$ is C^1 at $\mathbf{x}$, then

$\partial \mathbf{f}(\mathbf{x}) = \partial_B \mathbf{f}(\mathbf{x}) = \{\mathbf{Jf}(\mathbf{x})\}$, that is all the sets would be singletons, which would result in the classical derivative, the Jacobian. The Clarke Jacobian is a generalized derivative that not only can handle nonsmooth objects, such as the absolute value function and max/min functions, but it is also equipped with helpful calculus properties such as the chain rule, mean value theorem and inverse function theorem.

Example 2.2.3. *For this example we will be looking at $f(x) = |x|$. We can see that the limiting derivatives would be $\partial_B f(0) = \{1, -1\}$. If we were to take the convex hull of these we would get the interval $[-1, 1]$. This means that the Clarke Jacobian is $\partial f(0) = [-1, 1]$.*

To recap, the Clarke Jacobian is used to describe the nearby derivative behavior of functions at points of nondifferentiability. If $\mathbf{f}$ is C^1 then $\mathbf{f}'(\mathbf{x}; \mathbf{d}) = \mathbf{Jf}(\mathbf{x})\mathbf{d}$. A C^1 function is a strong condition, as such, a more easily found condition, lexicographically smooth, can typically be used in its place. However, it is difficult in general to calculate Clarke Jacobian elements [2]. Motivated by this difficulty Khan and Barton [26] built the lexicographic directional derivative, bared on lexicographic differentiation [31].

Definition 2.2.4. *(Lexicographically Smooth Functions [31]). Let $\mathbf{f}$ be a locally Lipschitz continuous function. Then $\mathbf{f}$ is lexicographically smooth, or L-smooth, at $\boldsymbol{x} \in E$ if it is directionally differentiable at $\boldsymbol{x}$ and if for any $k \in \mathbb{N}$ and $\boldsymbol{M} = [\boldsymbol{m}_1 \quad \cdots \quad \boldsymbol{m}_k] \in \mathbb{R}^{n \times k}$,*

$$
\begin{aligned}
&\mathbf{f}^{(0)}_{\boldsymbol{x},\boldsymbol{M}} : \mathbb{R}^n \to \mathbb{R}^m : \boldsymbol{d} \to \mathbf{f}'(\boldsymbol{x}; \boldsymbol{d}),\\
&\mathbf{f}^{(1)}_{\boldsymbol{x},\boldsymbol{M}} : \mathbb{R}^n \to \mathbb{R}^m : \boldsymbol{d} \to [\mathbf{f}^{(0)}_{\boldsymbol{x},\boldsymbol{M}}]'(\boldsymbol{m}_1; \boldsymbol{d}),\\
&\mathbf{f}^{(2)}_{\boldsymbol{x},\boldsymbol{M}} : \mathbb{R}^n \to \mathbb{R}^m : \boldsymbol{d} \to [\mathbf{f}^{(1)}_{\boldsymbol{x},\boldsymbol{M}}]'(\boldsymbol{m}_2; \boldsymbol{d}),\\
&\quad \vdots\\
&\mathbf{f}^{(k)}_{\boldsymbol{x},\boldsymbol{M}} : \mathbb{R}^n \to \mathbb{R}^m : \boldsymbol{d} \to [\mathbf{f}^{(k-1)}_{\boldsymbol{x},\boldsymbol{M}}]'(\boldsymbol{m}_k; \boldsymbol{d}),
\end{aligned}
$$

are well defined. We call the sequence above the homogenization sequence. The function $\mathbf{f}$ is called L-smooth on X if it is L-smooth at each point $\boldsymbol{x} \in E$.

If a function is C^1, PC^1, convex it is L-smooth, and if a function is an integral or composition of C^1, PC^1 or convex functions then it is also L-smooth [31]. We call $\mathbf{M}$ the directions matrix. Each column of the directions matrix corresponds to a direction around the point and each step in the homogenization process changes the direction in which we probe. At a nondifferentiable point, we probe the nearby area to find derivative information to better understand what is going on when we cannot differentiate. If the columns of $\mathbf{M}$ span the space then we get the following [31].

Proposition 2.2.5. *([31]) Let $\mathbf{f}$ be an L-smooth function and $\boldsymbol{M} \in \mathbb{R}^{n\times k}$ have full row rank. Then the final differentiation of the homogenization sequence, $\mathbf{f}^{(k)}_{\boldsymbol{x},\boldsymbol{M}}$, in definition 2.2.4 is linear.*

Example 2.2.6. *Let $\mathbf{f} : \mathbb{R}^2 \to \mathbb{R}$ to be $\mathbf{f}(x_1, x_2) = x_1^2 + x_2^2$. We will also let the directions matrix be*

$$\boldsymbol{M} = \begin{bmatrix} \boldsymbol{m}_1 & \boldsymbol{m}_2 \end{bmatrix} = \begin{bmatrix} m_1 & m_2 \\ m_3 & m_4 \end{bmatrix}.$$

Taking the first directional derivative in the direction $\boldsymbol{d} = (d_1, d_2)$ at $\boldsymbol{x}^* = (x_1^*, x_2^*) = (1, 1)$, we would end up with:

$$\begin{aligned}
\mathbf{f}^{(0)}_{\boldsymbol{x}^*,\boldsymbol{M}}(d_1, d_2) &= \mathbf{f}'(\boldsymbol{x}^*; (d_1, d_2)) \\
&= \lim_{\alpha\downarrow 0} \frac{\mathbf{f}(\boldsymbol{x}^* + \alpha\boldsymbol{d}) - \mathbf{f}(\boldsymbol{x}^*)}{\alpha} \\
&= \lim_{\alpha\downarrow 0} \frac{(x_1^* + \alpha d_1)^2 + (x_2^* + \alpha d_2)^2 - (x_1^{*2} + x_2^{*2})}{\alpha} \\
&= \lim_{\alpha\downarrow 0} \frac{x_1^{*2} + 2\alpha x_1^* d_1 + \alpha^2 + d_1^2 + x_2^{*2} + 2\alpha x_2 d_2 + \alpha^2 d_2 - x_1^{*2} - x_2^{*2}}{\alpha} \\
&= \lim_{\alpha\downarrow 0} 2x_1^* d_1 + \alpha d_1^2 + 2x_2^* d_2 + \alpha d_2 \\
&= 2x_1^* d_1 + 2x_2^* d_2 \\
&= 2d_1 + 2d_2.
\end{aligned}$$

Therefore $\mathbf{f}^{(0)}_{\boldsymbol{x}^*,\boldsymbol{M}}(d_1,d_2) = 2d_1 + 2d_2$. *Since* $\boldsymbol{f}$ *is* C^1 *we can also solve this with:*

$$\mathbf{f}^{(0)}_{\boldsymbol{x}^*,\boldsymbol{M}}(d_1,d_2) = \mathbf{f}'(\boldsymbol{x}^*;d_1,d_2) = \boldsymbol{J}\mathbf{f}(\boldsymbol{x}^*)\begin{bmatrix} d_1 \\ \\ d_2 \end{bmatrix} = \begin{bmatrix} 2x_1^* & 2x_2^* \end{bmatrix}\begin{bmatrix} d_1 \\ \\ d_2 \end{bmatrix} = 2d_1 + 2d_2.$$

For the next step we find $\mathbf{f}^{(1)}_{\boldsymbol{x}^*,\boldsymbol{M}}$, *which from our definition is*

$$\begin{aligned}
\mathbf{f}^{(1)}_{\boldsymbol{x}^*,\boldsymbol{M}}(d_1,d_2) &= [\mathbf{f}^{(0)}_{\boldsymbol{x}^*,\boldsymbol{M}}]'(\boldsymbol{m}_1;\boldsymbol{d}) \\
&= \lim_{\alpha\downarrow 0}\frac{\mathbf{f}_{x^*,\boldsymbol{M}}(\boldsymbol{m}_1+\alpha\boldsymbol{d}) - \mathbf{f}_{x^*,\boldsymbol{M}}(\boldsymbol{m}_1)}{\alpha} \\
&= \lim_{\alpha\downarrow 0}\frac{2(m_1+\alpha d_1)+2(m_2+\alpha d_2)-(2m_1+2m_2)}{\alpha} \\
&= \lim_{\alpha\downarrow 0}\frac{2m_1+2\alpha d_1+2m_2+2\alpha d_2-2m_1-2m_2}{\alpha} \\
&= \lim_{\alpha\downarrow 0}\frac{2\alpha d_1+2\alpha d_2}{\alpha} \\
&= \lim_{\alpha\downarrow 0} 2d_1+2d_2 \\
&= 2d_1+2d_2.
\end{aligned}$$

Repeating this process reveals that $\boldsymbol{f}^{(2)}_{x^*,\boldsymbol{M}}(d_1,d_2) = 2d_1 + 2d_2$. *Note that* M *does not play a role here because* f *is* C^1.

With the concept of L-smooth in place we can now find lexicographical derivatives.

Definition 2.2.7. *(Lexicographical Derivative [31]). Let* $\mathbf{f}$ *be an L-smooth function and* $\boldsymbol{M} \in \mathbb{R}^{n\times k}$ *be a full row rank matrix. Then the lexicographical derivative, L-derivative, of* $\mathbf{f}$ *at* $\boldsymbol{x}$ *is*

$$J_L\mathbf{f}(\boldsymbol{x};\boldsymbol{M}) = J\mathbf{f}^{(k)}_{\boldsymbol{x};\boldsymbol{M}}(\mathbf{0}_n) \in \mathbb{R}^{m\times n}.$$

The choice $\mathbf{0}_n$ can be swapped out with any $\mathbf{v} \in \mathbb{R}^n$, since $J\mathbf{f}^{(k)}_{\mathbf{x};\mathbf{M}}$ has constant entries. We can note that the mapping $\mathbf{f}^{(k)}_{\mathbf{x};\mathbf{M}}$ is influenced by the choice of $\mathbf{M}$. As such, different acceptable choices of $\mathbf{M}$ can result in different L-derivatives.

Definition 2.2.8. *(Lexicographic Subdifferential [31]). Let* $\mathbf{f}$ *be an L-smooth function, then the lexicographic subdifferential, L-subdifferential, of* $\mathbf{f}$ *at* $\boldsymbol{x}$ *is given by*

$$\partial_L\mathbf{f}(x) = \{J_L\mathbf{f}(\boldsymbol{x};\boldsymbol{M}) : k\in\mathbb{N}, \boldsymbol{M}\in\mathbb{R}^{n\times k}, \boldsymbol{M} \text{ has full row rank}\},$$

and represents the set of all possible L-derivatives.

When evaluated at a point of nondifferentiabilty, the L-subdifferential is a nonempty and non-singleton set. Elements of the L-subdifferential are related to the elements of the Clarke Jacobian.

Proposition 2.2.9. *([31, 25]).Let $E \subseteq \mathbb{R}^n$ and let $\boldsymbol{f}\colon E \to \mathbb{R}^m$ be L-smooth. Then L-derivatives of $\boldsymbol{f}$ are identical to Clarke Jacobian elements with matrix-vector products such as*

$$\{\mathbf{A}_1\mathbf{v} : \mathbf{A}_1 \in \partial_L\mathbf{f}(\boldsymbol{x}), \mathbf{d} \in \mathbb{R}^n\} \subseteq \{\mathbf{A}_2\mathbf{v} : \mathbf{A}_2 \in \partial\mathbf{f}(\boldsymbol{x}), \mathbf{d} \in \mathbb{R}^n\}.$$

If $\mathbf{f}$ is PC^1, then we have that

$$\partial_L\boldsymbol{f}(\boldsymbol{x}) \subseteq \partial_B\boldsymbol{f}(\boldsymbol{x}) \subseteq \partial\boldsymbol{f}(\boldsymbol{x}).$$

A useful tool to find L-derivatives is the lexicographical directional derivative.

Definition 2.2.10. *(Lexicographic Directional Derivative [26]). Let $\mathbf{f}$ be an L-smooth function and let $\boldsymbol{M} = [\boldsymbol{m}_1 \quad \cdots \quad \boldsymbol{m}_k] \in \mathbb{R}^{n\times k}$. Then the lexicographical directional derivative, LD-derivative, of $\mathbf{f}$ at $\boldsymbol{x}$ in the directions given by $\boldsymbol{M}$ is*

$$\mathbf{f}'(\boldsymbol{x}; \boldsymbol{M}) = [\mathbf{f}^{(0)}_{\boldsymbol{x},\boldsymbol{M}}(\boldsymbol{m}_1) \quad \mathbf{f}^{(1)}_{\boldsymbol{x},\boldsymbol{M}}(\boldsymbol{m}_2) \quad \cdots \quad \mathbf{f}^{(k-1)}_{\boldsymbol{x},\boldsymbol{M}}(\boldsymbol{m}_k)].$$

Oftentimes, $k = m = n$ and $\mathbf{M} = \mathbf{I}$, where $\mathbf{I}$ is the identity matrix, but it is not required. When $k = 1$, $\mathbf{M}$ would be a single column vector and

$$\mathbf{f}'(\mathbf{x}, \mathbf{M}) = \mathbf{f}^{(0)}_{\mathbf{x},\mathbf{M}}(\mathbf{m}_1) = \mathbf{f}'(\mathbf{x}; \mathbf{m}_1).$$

Therefore if $k = 1$, then the LD-derivative gives the classical directional derivative.

Theorem 2.2.11. *(Connection between L-derivatives and LD-derivatives[26]) Let $\mathbf{f}$ be an L-smooth function and $\boldsymbol{M} = [\boldsymbol{m}_1 \quad \cdots \quad \boldsymbol{m}_k] \in \mathbb{R}^{n\times k}$ be a full row rank matrix. Then*

$$\mathbf{f}'(\boldsymbol{x}; \boldsymbol{M}) = \boldsymbol{J}_L\mathbf{f}(\boldsymbol{x}; \boldsymbol{M})\boldsymbol{M}$$

or equally,

$$\boldsymbol{J}_L\mathbf{f}(\boldsymbol{x};\boldsymbol{M}) = \mathbf{f}'(\boldsymbol{x};\boldsymbol{M})\boldsymbol{M}^{-1}. \tag{2.3}$$

where M is the right inverse.

The above theorem implies the importance of the LD-derivative, since a related L-derivative can be easily calculated using an LD-derivative as long as the directions matrix is full row rank. As such $\mathbf{M}$ is often chosen to be $\mathbf{I}$ and even further, since in this case, $\mathbf{M} = \mathbf{M}^{-1}$ implies that the LD-derivative is also an L-derivative. If all the requirements in Theorem 2.2.11 are satisfied and $\mathbf{f}$ is C^1, then Theorem 2.2.11 gives the special case of

$$\mathbf{f}'(\mathbf{x};\mathbf{M}) = \mathbf{J}\mathbf{f}(\mathbf{x};\mathbf{M})\mathbf{M}.$$

Example 2.2.12. *For this example we will be looking at the function*

$$\boldsymbol{g} : \mathbb{R}^2 \to \mathbb{R} : (x_1, x_2) \to |x_1 + x_2|.$$

The function $\boldsymbol{g}$ has the set of nondifferentiability,

$$Z_g = \{(x_1, x_2) : x_1 = -x_2\}$$

and essentially active selection functions

$$\mathcal{E}_g(\boldsymbol{x}) \subseteq \{x_1 + x_2, -(x_1 + x_2)\} = \{g_1(\boldsymbol{x}), g_2(\boldsymbol{x})\}.$$

Since this function is PC^1, we can find the Bouligand subdifferential and the Clarke Jacobian. We have that the Jacobians of the essentially active functions are $\boldsymbol{J}g_1(x) = [1 \quad 1]$ and $\boldsymbol{J}g_2(x) = [-1, -1]$ therefore $\partial_B\boldsymbol{g}(\boldsymbol{x}) = \{[1 \quad 1], [-1 \quad -1]\}$. From here we can find the convex hull of $\partial_B\boldsymbol{g}(\boldsymbol{x})$ to find that the Clarke Jacobian is $\{[a \quad 1-a] \mid a \in [-1, 1]\}$. Let $\boldsymbol{x}_0 = (1, -1) \in Z_g$ and let the full row rank directions matrix be $\boldsymbol{M} = \boldsymbol{I}_2$. We will find an L-derivative of $\boldsymbol{g}$ by first finding an LD-derivative as suggested in definition 2.2.11. First we find the two recursive directional derivatives of $\boldsymbol{g}$. For the

first directional derivative of $\boldsymbol{g}$ *at* $\boldsymbol{x}_0$ *we have*

$$\begin{aligned}
\mathbf{f}^{(0)}_{\boldsymbol{x}_0,\boldsymbol{M}}(d_1,d_2) &= \lim_{\alpha\downarrow 0}\frac{\boldsymbol{g}(\boldsymbol{x}_0+\alpha(d_1,d_2))-\boldsymbol{g}(\boldsymbol{x}_0)}{\alpha}\\
&= \lim_{\alpha\downarrow 0}\frac{|(1+\alpha d_2)+(-1+\alpha d_1)|-|1-1|}{\alpha}\\
&= \lim_{\alpha\downarrow 0}\frac{|\alpha(d_1+d_2)|}{\alpha}\\
&= \lim_{\alpha\downarrow 0}\frac{\alpha|d_1+d_2|}{\alpha}\\
&= \lim_{\alpha\downarrow 0}|d_1+d_2|\\
&= |d_1+d_2|.
\end{aligned}$$

In the direction $(1,0)$ *as given by the first column of the directions matrix* $\boldsymbol{M}$*, we have that*

$$\mathbf{f}^{(0)}_{\boldsymbol{x}_0,\boldsymbol{M}}(\boldsymbol{m}_1)=|1+0|=1.$$

The next directional derivative is found recursively giving us,

$$\begin{aligned}
\boldsymbol{f}^{(1)}_{\boldsymbol{x}_0,\boldsymbol{M}}(d_1,d_2) &= [\mathbf{f}^{(0)}_{\boldsymbol{x}_0,\boldsymbol{M}}]'(\boldsymbol{m}_1;(d_1,d_2)\\
&= \lim_{\alpha\downarrow 0}\frac{|(1+\alpha d_1)+(0+\alpha d_2)|-|1+0|}{\alpha}\\
&= \lim_{\alpha\downarrow 0}\frac{|1+\alpha d_1+\alpha d_2|-1}{\alpha}.
\end{aligned}$$

Since $\alpha\downarrow 0$*, the number* 1 *is the dominating term in* $|1+\alpha d_1+\alpha d_2|$ *and a positive result would be found as the limit is taken. Therefore,*

$$\boldsymbol{f}^{(1)}_{\boldsymbol{x}_0,\boldsymbol{M}}(d_1,d_2)=\lim_{\alpha\downarrow 0}\frac{1+\alpha d_1+\alpha d_2-1}{\alpha}=d_1+d_2.$$

With the above and given the second column of $\boldsymbol{M}$*, we have that,*

$$\boldsymbol{f}^{(1)}_{\boldsymbol{x}_0,\boldsymbol{M}}(m_2)=1.$$

With both directional derivatives found we can make the LD-derivative of $\mathbf{f}$ *at* $\boldsymbol{x}_0$ *in the directions given by* $\boldsymbol{M}$ *to be*

$$\mathbf{f}'(\boldsymbol{x}_0;\boldsymbol{M})=[\boldsymbol{f}^{(0)}_{\boldsymbol{x}_0,\boldsymbol{M}}(\boldsymbol{m}_1)\quad \boldsymbol{f}^{(1)}_{\boldsymbol{x}_0,\boldsymbol{M}}(\boldsymbol{m}_2)]=[1\quad 1].$$

Then from the LD-derivative, can use the inverse of $\boldsymbol{M} = \boldsymbol{I}$ to make an L-derivative

$$J_L\mathbf{f}(\boldsymbol{x}_0; \boldsymbol{M}) = [1 \quad 1]I^{-1} = [1 \quad 1].$$

Since L-derivatives are all Clarke jacobian elements, as seen in proposition 2.2.9, this means we can use L-derivatives and LD-derivatives to find information on nonsmooth functions. In order to find nonsmooth derivatives we must first understand lexicographical ordering.

Definition 2.2.13. *(Lexicographic Ordering). Let $\boldsymbol{a}, \boldsymbol{b} \in \mathbb{R}^k$ be vectors. Then $\boldsymbol{a}$ is lexicographically less than $\boldsymbol{b}$, written $\boldsymbol{a} \prec \boldsymbol{b}$, if $a_i < b_i$ for the first index $i \in \{1, 2, \ldots, i, \ldots, k\}$ such that $a_i \neq b_i$. We say $\boldsymbol{a}$ is lexicographically greater than $\boldsymbol{b}$, written $\boldsymbol{a} \succ \boldsymbol{b}$, if $a_i > b_i$ for the first index $i \in \{1, 2, \ldots, i, \ldots, k\}$ such that $a_i \neq b_i$. If equality is possible, $\succcurlyeq$ and $\preccurlyeq$ can be used.*

A helpful way to think of lexicographical ordering is to compare it to alphabetical ordering. Given the two words *grove* and *gross*, we know *gross* comes before *grove* in the dictionary because we compare the first letter that is different, in this case s and v, and it does not matter that, after that comparison, e in grove comes before the second s in gross. Similarly given two vectors, $[1 \quad -2 \quad 6]$ and $[1 \quad -2 \quad 4]$ we look at the first numbers that are different between them. Since $6 > 4$ we can conclude

$$[1 \quad -2 \quad 6] \succ [1 \quad -2 \quad 4].$$

For a couple more examples we can see that

$$[1 \quad -2 \quad 6] \prec [1 \quad 4 \quad -2]$$
$$[2 \quad 4 \quad 6] \succ [1 \quad 6 \quad 97].$$

With the notion of lexicographical ordering we can now introduce the functions lmax and lmin; for more details see Khan and Barton [26]. Much like max and min these

functions output either the lexicographical greatest or lexicographical least input. For example,

$$\begin{aligned}\text{lmax}([1 \quad -2 \quad 6], [1 \quad 4 \quad -2]) &= [1 \quad 4 \quad -2] \\ \text{lmin}([2 \quad 4 \quad 6], [1 \quad 6 \quad 97]) &= [1 \quad 6 \quad 97].\end{aligned}$$

We can also take the lmax and lmin of matrices. With matrices, lmax and lmin compare each row of the matrix and output the lexicographical max or lexicographical min from each matrix. As an example,

$$\text{lmax}\left(\begin{bmatrix} 2 & 3 \\ -1 & 2 \end{bmatrix}, \begin{bmatrix} 1 & -1 \\ -1 & 4 \end{bmatrix}\right) = \begin{bmatrix} 2 & 3 \\ -1 & 4 \end{bmatrix}.$$

We can also introduce the functions slmax and slmin, or the shifted lexicographical max and the shifted lexicographical min. These take the form of a left shift of the lmax and lmin functions. Using some previous examples,

$$\begin{aligned}\text{slmin}([2 \quad 4 \quad 6], [1 \quad 6 \quad 97]) &= [6 \quad 97] \\ \text{slmax}\left(\begin{bmatrix} 2 & 3 \\ -1 & 2 \end{bmatrix}, \begin{bmatrix} 1 & -1 \\ -1 & 4 \end{bmatrix}\right) &= \begin{bmatrix} 3 \\ 4 \end{bmatrix}.\end{aligned}$$

The LD-derivative of a minimum, or maximum, function composed with C^1 functions along matrices $(\mathbf{M}, \mathbf{N}) \in \mathbb{R}^{2n \times k}$ [2] is

$$\begin{aligned}[\min \circ(\mathbf{f}, \mathbf{g})]'(\mathbf{x}, \mathbf{y}; (\mathbf{M}, \mathbf{N})) = \text{slmin}([&\mathbf{f}(\mathbf{x}, \mathbf{y}) \quad \mathrm{J}_{\mathbf{x}}\mathbf{f}(\mathbf{x}, \mathbf{y})\mathbf{M} + \mathrm{J}_{\mathbf{y}}\mathbf{f}(\mathbf{x}, \mathbf{y})\mathbf{N}], \\ &[\mathbf{g}(\mathbf{x}, \mathbf{y}) \quad J_{\mathbf{x}}\mathbf{g}(\mathbf{x}, \mathbf{y})\mathbf{M} + J_{\mathbf{y}}\mathbf{g}(\mathbf{x}, \mathbf{y})\mathbf{N}]).\end{aligned}$$

The function fsign is important in the calculation of an LD-derivative of absolute value, and outputs the sign of the first nonzero entry. If all entries are zero, then it outputs zero.

For example,

$$\text{fsign}(0, -1, 4) = -1$$

$$\text{fsign}(2, -6, -7) = 1$$

$$\text{fsign}(0, 0, 0, 4) = 1$$

$$\text{fsign}(0, 0) = 0.$$

The LD-derivative of the absolute value function with a directions matrix $\mathbf{M} = [m_1 \quad \dots \quad m_k] \in \mathbb{R}^{1\times k}$ is

$$\text{abs}'(\text{x}; \mathbf{M}) = \text{fsign}(\text{x}, \text{m}_{1,1}, \dots, \text{m}_{1,\text{k}})\mathbf{M}.$$

2.3 ODE Theory

Unless stated otherwise, these definitions and theorems below are adapted from Perko [34]. In this section, we use the notation $\dot{x} = \frac{dx}{dt}$.

In this part we consider the following ODE system

$$\dot{\mathbf{x}} = \mathbf{f}(t, \mathbf{x}), \tag{2.4}$$

$$\mathbf{x}(t_0) = \mathbf{x}_0.$$

Where $\mathbf{x} = (x_1, \dots, x_n)$ is the state variable vector, t is the independent variable and $\mathbf{f} : E_t \times E_x \to \mathbb{R}^n$ with open sets $E_t \subseteq \mathbb{R}$ and $E_x \subseteq \mathbb{R}^n$, and initial values $t_0 \in E_t$ and $\mathbf{x}_0 \in E_x$.

Definition 2.3.1. *(Solution of an Initial Value Problem). A solution to the initial value problem (IVP) of the form* (2.4)*, on the connected interval $T \subseteq E_t$ is some function $\boldsymbol{x}(t)$ such that,*

i. $\boldsymbol{x}(t)$ is differentiable on T,

ii. $\boldsymbol{x}(t) \in E_x$ for each $t \in T$,

iii. $\boldsymbol{x}(t_0) = \boldsymbol{x}_0$ *with* $t_0 \in T$, *and*

iv. $\dot{\boldsymbol{x}}(t) = \mathbf{f}(t, \boldsymbol{x}(t))$ *for each* $t \in T$.

An IVP has a unique solution if f is sufficiently regular.

Theorem 2.3.2. *(Fundamental Existence-Uniqueness). Let* $\boldsymbol{x}_0 \in E_x$ *and let* $\mathbf{f}$ *be locally Lipshitz on* $E_t \times E_x$. *Then there exists an* $\epsilon > 0$ *such that the IVP* (2.4) *has a unique solution* $\boldsymbol{x}(t)$ *on the interval* $[t_0 - \epsilon, t_0 + \epsilon]$.

In many cases where an IVP has a solution, it can be incredibly difficult to find analytically using standard methods. As such we also can figure out the long-term behavior of DEs by analyzing equilibria.

Definition 2.3.3. *(Equilibria). A point* $\boldsymbol{x}^* \in E$ *is called an equilibrium point, or a critical point, of* $\dot{\boldsymbol{x}} = \mathbf{f}(\boldsymbol{x})$ *if* $\mathbf{f}(\boldsymbol{x}^*) = \mathbf{0}$.

Not only do equilibria tell us when an ODE is unchanging we can also use equilibria to find out the behavior of initial values around them.

Definition 2.3.4. *(Stability [34]). Given the equation* $\dot{\boldsymbol{x}} = \mathbf{f}(\boldsymbol{x})$, *the equilibrium,* $\boldsymbol{x}^*$ *is*

- *stable, if for each* $\epsilon > 0$, *there exists a* $\delta > 0$ *such that*
  $\|\boldsymbol{x}_0 - \boldsymbol{x}^*\| < \delta \implies \|\boldsymbol{x}(t) - \boldsymbol{x}^*\| < \epsilon$ *for all* $t \geq 0$
- *asymptotically stable if the equilibrium is stable and there exists* δ *such that*
  $\|\boldsymbol{x}_0 - \boldsymbol{x}^*\| < \delta \implies \lim_{t\to\infty} \boldsymbol{x}(t) = \boldsymbol{x}^*$
- *unstable otherwise.*

For the definition of stable, we must acknowledge the potential case of finite time blow up. If this were to occur we can rescale time with some $\tau = \alpha t$, allowing for global solutions and avoiding finite time blowup. Nonlinear equations are generally difficult to analyze when trying to figure out the nearby behavior, while linear equations are simple.

In order to utilize this simplicity we can linearize nonlinear equations around equilibria and find accurate nearby information.

Definition 2.3.5. *(Linearization). The linearization of* (2.4) *at an equilibrium* $\boldsymbol{x}^*$ *is the linear system,* $\dot{\boldsymbol{x}} = \boldsymbol{J}\mathbf{f}(\boldsymbol{x}^*)\boldsymbol{x}$.

The further away a solution is from the point of linearization the more inaccurate the information is, however in the local neighborhood the information is accurate. After linearization, we can find the behavior of nearby initial values.

Definition 2.3.6. *(Hyperbolic Equilibrium). An equilibrium point* $\boldsymbol{x}^*$ *is called a hyperbolic equilibrium point of* (2.4) *if none of the eigenvalues of* $\boldsymbol{J}\mathbf{f}(\boldsymbol{x}^*)$ *have zero real part.*

Definition 2.3.7. *An equilibrium point* $\boldsymbol{x}^*$

- *is called a sink if all of the eigenvalues of* $\boldsymbol{J}\mathbf{f}(\boldsymbol{x}^*)$ *have negative real part.*
- *is called a source if all the eigenvalues of* $\boldsymbol{J}\mathbf{f}(\boldsymbol{x}^*)$ *have positive real part.*
- *is called a saddle if it is a hyperbolic equilibrium point and if* $\boldsymbol{J}\mathbf{f}(\boldsymbol{x}^*)$ *has at least one positive and one negative eigenvalue.*

If the equilibrium point, $\mathbf{x}^*$, results in a sink, then $\mathbf{x}^*$ is asymptotically stable. If $\mathbf{x}^*$ is a source or a saddle then $\mathbf{x}^*$ is unstable.

We will now define a parametric initial value problem as

$$\begin{aligned} \dot{\mathbf{x}}(t, \mathbf{p}) &= \mathbf{f}(t, \mathbf{p}, \mathbf{x}(t, \mathbf{p})), \\ \mathbf{x}(t_0, \mathbf{p}) &= \mathbf{f}_0(\mathbf{p}) \end{aligned} \tag{2.5}$$

where $\mathbf{x} = (x_1, \ldots, x_n)$ is the vector of state variables and $\mathbf{p} = (p_1, \ldots, p_m)$ is the vector of parameters. We also suppose that $\mathbf{f} : E_t \times E_p \times E_x \to \mathbb{R}^n$, with E_t, E_p, E_x open, and $\mathbf{f}_0 : E_m \to E_x$, with E_t open, where $E_t \subseteq \mathbb{R}, E_p \subseteq \mathbb{R}^q$ and $E_x \subseteq \mathbb{R}^n$.

Definition 2.3.8. *(Sensitivity Functions). Let $\boldsymbol{x}(t, \boldsymbol{p})$ be a solution of the parametric IVP (2.5) on the interval $[t_0, t_1]$ and for $\boldsymbol{p}$ in the neighborhood of $\boldsymbol{p}^* \in E_p$, the forward-parametric sensitivity functions are*

$$\boldsymbol{S}_x(t) = \frac{\partial \boldsymbol{x}}{\partial \boldsymbol{p}}(t, \boldsymbol{p}^*) \in \mathbb{R}^{n \times q},$$

where $\boldsymbol{p}^* \in E_p$ are some chosen parameters of importance.

Sensitivity functions help figure out the importance of parameters in an IVP. If a system has two parameters p_1 and p_2, these sensitivity equations inform us which parameters, when perturbed slightly, cause a more drastic change to the solution of the system. With how helpful these equations are, once again we would like to easily check whether they are possible to find or not.

Theorem 2.3.9. *Suppose $\mathbf{f} : E_t \times E_p \times E_x \to \mathbb{R}^n$ and $\mathbf{f}_0 : E_p \to E_x$ are C^1, let $t_1 > t_0$ and suppose there exists a unique solution of the IVP, $\boldsymbol{x}^*(t) = \boldsymbol{x}(t, \boldsymbol{p}^*)$, on $[t_0, t_1] \subseteq E_t$ and for $\boldsymbol{p} = \boldsymbol{p}^*$. Then the solution $\boldsymbol{x}(t, \boldsymbol{p})$ is C^1 with respect to $\boldsymbol{p}$ near $\boldsymbol{p} = \boldsymbol{p}^*$, i.e., the sensitivity functions in Definition 2.3.8 exist. Moreover, the sensitivity functions are the unique solution of the sensitivity system*

$$\dot{\boldsymbol{S}}_x = J_{\boldsymbol{p}}\mathbf{f}(t, \boldsymbol{p}^*, \boldsymbol{x}^*(t)) + J_{\boldsymbol{x}}\mathbf{f}(t, \boldsymbol{p}^*, \boldsymbol{x}^*(t))\boldsymbol{S}_x,$$

$$\boldsymbol{S}_x(t_0) = J\mathbf{f}_0(\boldsymbol{p}^*)$$

on the time span $[t_0, t_1]$, where $\boldsymbol{J}_p\boldsymbol{f}$ and $\boldsymbol{J}_x\boldsymbol{f}$ are partial Jacobians with respect to $\boldsymbol{p}$ and $\boldsymbol{x}$ respectively.

Example 2.3.10. *For this example we look at the non-linear parametric IVP,*

$$\dot{x}(t, \boldsymbol{p}) = x(t, \boldsymbol{p})^{p_1}$$

$$x(0, \boldsymbol{p}) = p_2$$

with parameters $\boldsymbol{p} = (p_1, p_2)$. Once again, since this equation is separable we can find the closed form solution

$$x(t, p) = \sqrt[1-p_1]{p_2^{1-p_1} - p_1 t + t}.$$

Therefore we can calculate the sensitivity function by differentiating the closed form solutions by p_1 and p_2. This will give us,

$$\frac{\partial x}{\partial \boldsymbol{p}}(t,\boldsymbol{p}) = \begin{bmatrix} (-p_1 t + p_2^{1-p_1} + t)^{\frac{1}{1-p_1}} \left(\frac{\ln(-p_1 t + p_2^{1-p_1} + t)}{(1-p_1)^2} + \frac{-p_2^{1-p_1}\ln(p_2) - t}{(1-p_1)(-p_1 t + p_2^{1-p_1} + t)}\right) \\ \frac{(-p_1 t + p_2^{1-p_1} + t)^{\frac{1}{1-p_1}-1}}{p_2^{p_1}} \end{bmatrix}^T$$

Then once we choose our reference parameters of $p^* = (2,1)$ we have that

$$\frac{\partial x}{\partial \boldsymbol{p}}(t,\boldsymbol{p}^*) = \begin{bmatrix} \frac{t + (t-1)\ln(\frac{1}{1-t})}{(-t+1)^2} & \frac{1}{(-t+1)^2} \end{bmatrix}.$$

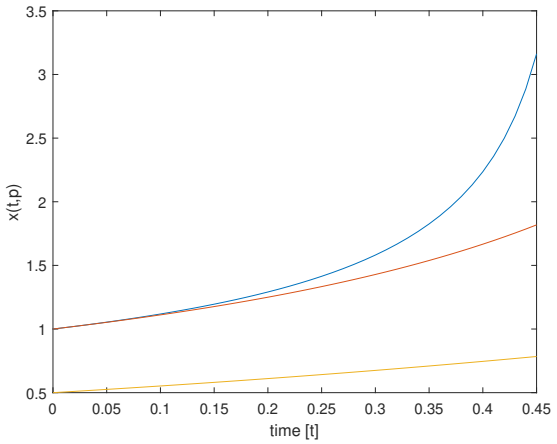

Figure 2.1: Solutions of the system with different values of $\mathbf{p}^*$. $\mathbf{p}^* = (1, .5)$ in yellow, $\mathbf{p}^* = (2,1)$ in red and $\mathbf{p}^* = (3,1)$ in blue.

Once again with different choices in parameter $\boldsymbol{p}^*$, long term behavior of solutions change. In order to calculate the sensitivity equations we first define $f(\boldsymbol{p}, x) = x^{p_1}$ and $f_0(\boldsymbol{p}) = p_2^*$. Then we have that

$$J_{\boldsymbol{p}} f(\boldsymbol{p}, x^*) = [x^{*p_1^*}\ln(x^*) \quad 0]$$

$$J_x f(\boldsymbol{p}, x^*) = [p_1^* x^{*p_1^*-1}]$$

$$J f_0(\boldsymbol{p}^*) = [0 \quad 1].$$

Then by substituting into the sensitivity system we have

$$\dot{\boldsymbol{S}}_x = [x^{*p_1^*} \ln(x^*) \quad 0] + [p_1^* x^{*p_1^*-1}]\boldsymbol{S}_x$$
$$\boldsymbol{S}_x(0) = [0 \quad 1].$$

We then split up the vector-valued IVP into

$$\dot{S}_x^{p_1} = x^{*p_1^*} \ln(x^*) + p_1^* x^{*p_1^*-1} S_x^{p_1}, S_x^{p_1}(0) = 0,$$
$$\dot{S}_x^{p_2} = p_1^* x^{*p_1^*-1} S_x^{p_2}, S_x^{p_2}(0) = 1.$$

Further we can plug in our closed form solution $\sqrt[1-p_1^*]{p_2^{*1-p_1^*} - p_1^* t + t}$ *for* x^* *resulting in*

$$\dot{S}_x^{p_1} = \sqrt[1-p_1^*]{p_2^{*1-p_1^*} - p_1^* t + t}^{\,p_1^*} \ln(\sqrt[1-p_1^*]{p_2^{*1-p_1^*} - p_1^* t + t}) + p_1^* \sqrt[1-p_1^*]{p_2^{*1-p_1^*} - p_1^* t + t}^{\,p_1^*-1} S_x^{p_1},$$
$$S_x^{p_1}(0) = 0,$$
$$\dot{S}_x^{p_2} = p_1^* \sqrt[1-p_1^*]{p_2^{*1-p_1^*} - p_1^* t + t}^{\,p_1^*-1} S_x^{p_2},$$
$$S_x^{p_2}(0) = 1.$$

Then once we plug in reference parameter $p^* = (2, 1)$ *then we find that*

$$\dot{S}_x^{p_1} = (\frac{1}{-t+1})^2 \ln(\frac{1}{-t+1}) + (\frac{2}{-t+1}) S_x^{p_1}$$
$$S_x^{p_1}(0) = 0,$$
$$\dot{S}_x^{p_2} = (\frac{2}{-t+1}) S_x^{p_2}$$
$$S_x^{p_2}(0) = 1.$$

These can be independently solved to get

$$S_x^{p_1}(t) = \frac{t + (t-1)ln(\frac{1}{1-t})}{(-t+1)^2}$$
$$S_x^{p_2}(t) = \frac{1}{(-t+1)^2}$$

which matches up with the sensitivity functions we found earlier.

Once again utilizing L-derivatives we can also find sensitivity information of parameters of nonsmooth functions. We will be following a similar evolution as before, where at first we introduced L-derivatives then LD-derivatives, however we will be looking at lexicographical sensitivity functions and then lexicographical directional sensitivity functions. First we must define L-smooth dependence of parameters.

Theorem 2.3.11. *(L-Smooth Dependence on Parameters [25]). Given the IVP* (2.5) *suppose that* $\mathbf{f} : E_t \times E_p \times E_x \to \mathbb{R}^n$ *and* $\mathbf{f}_0 : E_p \to E_x$ *are L-smooth on their domains. Then there exists* $\epsilon, \delta > 0$ *such that the IVP has a unique solution* $\boldsymbol{x}(t, \boldsymbol{p})$ *on* $[t_0, t_f]$*, with* $t_0 + \delta = t_f$*, for each fixed* $\boldsymbol{p} \in N_\epsilon(\boldsymbol{p}^*)$*, and* $\boldsymbol{x}(t, \boldsymbol{p})$ *is L-smooth with respect to* $\boldsymbol{p}$ *on* $N_\epsilon(\boldsymbol{p}^*)$ *for each fixed* $t \in [t_0, t_0 + \delta]$*.*

With L-smooth dependence on parameters, we can now introduce the lexicographic sensitivity functions.

Definition 2.3.12. *(Lexicographic Sensitivity Functions). Given the IVP* (2.5)*, the lexicographic sensitivity functions associated with a solution at chosen reference parameters,* $\boldsymbol{p}^* \in E_p$*,* $\boldsymbol{x}^* = \boldsymbol{x}(t, \boldsymbol{p}^*)$ *of the IVP, are*

$$\boldsymbol{S}_x(t) = \boldsymbol{J}_L[\boldsymbol{x}(t, \cdot)](\boldsymbol{p}^*; \boldsymbol{M}) \in \mathbb{R}^{n \times q},$$

for some $\boldsymbol{M} \in \mathbb{R}^{n \times k}$ *with full row rank.*

Lexicographical directional sensitivity function are easier to calculate and can be converted into the lexicographical sensitivity functions.

Definition 2.3.13. *(Lexicographical Directional Sensitivity Functions). Given the IVP* (2.5)*, the LD-sensitivity functions associated with a solution* $\boldsymbol{x}(t, \boldsymbol{p})$ *of the PIVP, if they exist, are*

$$\boldsymbol{X}(t) = [\boldsymbol{x}(t, \cdot)]'(\boldsymbol{p}^*; \boldsymbol{M}) \in \mathbb{R}^{n \times k}$$

with $\boldsymbol{p}^* \in E_p$ *as chosen reference parameters.*

Similarly to before, finding the LD-sensitivity functions require certain criteria to exist. So we define not only their existence criteria but also their calculation.

Theorem 2.3.14. *(Existence and Calculation of the LD-Sensitivity Functions [25]). Suppose that* $\mathbf{f} : E_t \times E_p \times E_x \to \mathbb{R}^m$ *and* $\mathbf{f}_0 : E_p \to E_x$ *are L-smooth on their domains and given* $t_f > t_0$*, there exists a unique solution of the IVP* (2.5) *on* $[t_0, t_f] \subset D_t$*. Then the solution* $\boldsymbol{x}(t, \boldsymbol{p})$ *is L-smooth with respect to* $\boldsymbol{p}$ *near* $\boldsymbol{p} = \boldsymbol{p}^*$*. That is, for any matrix* $\boldsymbol{M} \in \mathbb{R}^{n\times k}$*, the LD-sensitivity functions in definition 2.3.13 exist, are absolutely continuous and are the unique solution of the LD-sensitivity system*

$$\begin{aligned}\dot{\boldsymbol{X}}(t) &= [\mathbf{f}_t]'(\boldsymbol{p}^*, \boldsymbol{x}(t, \boldsymbol{p}^*); (\boldsymbol{M}, \boldsymbol{X}(t))),\\ \boldsymbol{X}(t_0) &= \mathbf{f}_0'(\boldsymbol{p}^*; \boldsymbol{M}),\end{aligned}$$

on the time interval $[t_0, t_f]$ *where* $\mathbf{f}_t : (\boldsymbol{p}, \boldsymbol{x}) \to \mathbf{f}(t, \boldsymbol{p}, \boldsymbol{x})$*.*

Even though calculating LD-sensitivity functions is easier, we still get more information from the L-sensitivity functions. We can easily convert between the two using the below.

Theorem 2.3.15. *(Existence and Calculation of the L-Sensitivity Functions). Suppose that* $\mathbf{f} : E_t \times E_p \times E_x \to \mathbb{R}^m$ *and* $\mathbf{f}_0 : E_p \to E_x$ *are L-smooth on their domains and given* $t_f > t_0$ *and that* $\boldsymbol{M} \in \mathbb{R}^{n\times k}$ *is full row rank. Then the results of Theorem 2.3.11 hold, both the L-sensitivity and LD-sensitivity functions exist, and for some fixed* t *on the time interval* $[t_0, t_f]$*, the L-sensitivity functions can be calculated as*

$$\boldsymbol{S}_x(t) = \boldsymbol{X}(t)\boldsymbol{M}^{-1} \in \mathbb{R}^{n\times q}.$$

where M^{-1} *is the right inverse of* M*.*

Remark 2.3.16. *If* $\mathbf{f}$ *and* $\mathbf{f}_0$ *are* C^1 *on their domains and* $\boldsymbol{M} = I$ *then we have that*

$$\boldsymbol{S}_x(t) = J_L[\boldsymbol{x}(t,\cdot)](\boldsymbol{p}^*; I) = \boldsymbol{X}(t)I^{-1} = [\boldsymbol{x}(t,\cdot)]'(\boldsymbol{p}^*; I) = \frac{\partial x}{\partial p}(t, p^*).$$

Therefore the result is the classical, smooth, sensitivity equations.

Example 2.3.17. *Let*

$$\dot{x}(t, \boldsymbol{p}) = \min(p_1 - 1, x^2(t, \boldsymbol{p}))$$
$$x(0, \boldsymbol{p}) = |p_2|$$

with reference parameters $\boldsymbol{p}^* = (1, 0)$.

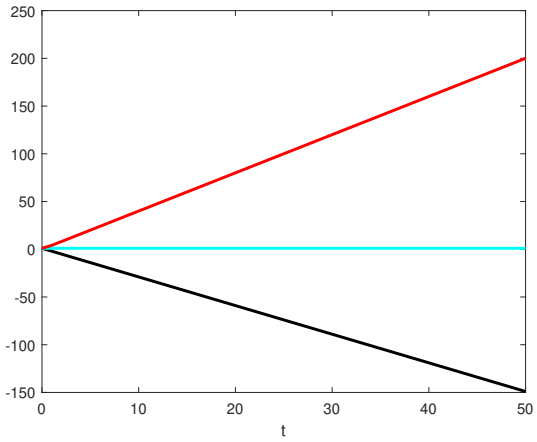

Figure 2.2: Solutions of the system with different values of p_1. We have $p_2 = 1$ for all and $p_1 = -2$ in black, $p_1 = 1$ in cyan and $p_1 = 5$ in red.

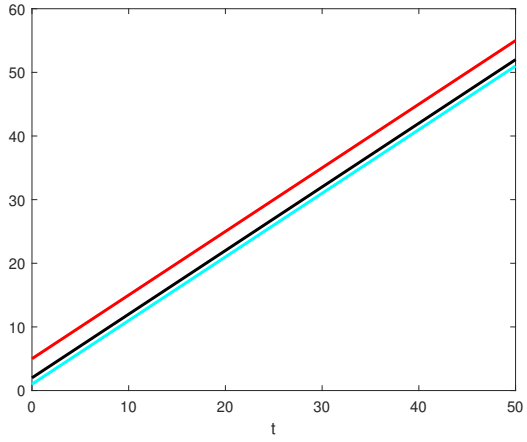

Figure 2.3: Solutions of the system with different values of p_2. We have $p_1 = 2$ for all and $p_2 = -2$ in black, $p_2 = 1$ in cyan and $p_2 = 5$ in red.

Since we have the reference parameter we can solve for x^*. At the reference parameters we have that

$$\dot{x}(t, \boldsymbol{p}^*) = \min(0, x^2(t, \boldsymbol{p}^*))$$
$$x(0, \boldsymbol{p}^*) = 0.$$

Since $x^2(t, \boldsymbol{p}^*) \geq 0$, $\min(0, x^2(t, \boldsymbol{p}^*)) = 0$ giving us

$$\dot{x}(t, \boldsymbol{p}^*) = 0$$
$$x(0, \boldsymbol{p}) = 0$$

which can be easily solved to find $x^* = 0$. To build the sensitivity system we introduce directions matrix

$$\boldsymbol{M} = \begin{bmatrix} \boldsymbol{M}_1 \\ \boldsymbol{M}_2 \end{bmatrix} = \begin{bmatrix} m_{1,1} & m_{1,2} \\ m_{2,1} & m_{2,2} \end{bmatrix}$$

and L-sensitivity matrix $\boldsymbol{S}_x = [S_x^{p_1} \quad S_x^{p_2}]$. Then following along with definition 2.3.13, we choose $u(\boldsymbol{p}, x) = p_1 - 1$ and $v(\boldsymbol{p}, x) = x^2$. Then we have that

$$\begin{aligned}
\dot{\boldsymbol{X}} &= \mathrm{slmin}([\mathrm{u}(\boldsymbol{p}^*, \mathrm{x}^*) \quad \mathrm{J_{p_1}u}(\boldsymbol{p}^*, \mathrm{x}^*)\boldsymbol{M}_1 + \mathrm{J_{p_2}u}(\boldsymbol{p}^*, \mathrm{x}^*)\boldsymbol{M}_2 + \mathrm{J_x u}(\boldsymbol{p}^*, \mathrm{x}^*)\mathrm{X}], \\
&\quad [v(\boldsymbol{p}^*, x^*) \quad J_{p_1}v(\boldsymbol{p}^*, x^*)\boldsymbol{M}_1 + J_{p_2}v(\boldsymbol{p}^*, x^*)\boldsymbol{M}_2 + J_x v(\boldsymbol{p}^*, x^*)X]) \\
&= \mathrm{slmin}([\mathrm{p}_1^* - 1 \quad 1[\mathrm{m}_{1,1} \quad \mathrm{m}_{1,2}] + 0[\mathrm{m}_{2,1} \quad \mathrm{m}_{2,2}] + 0[\mathrm{X}_1 \quad \mathrm{X}_2], \\
&\quad [x^{*2} \quad 0[m_{1,1} \quad m_{1,2}] + 0[m_{2,1} \quad m_{2,2}] + 2x^*[S_x^{p_1} \quad S_x^{p_2}]]) \\
&= \mathrm{slmin}([\mathrm{p}_1^* - 1 \quad [\mathrm{m}_{1,1} \quad \mathrm{m}_{1,2}]], [\mathrm{x}^{*2} \quad [\mathrm{X}_1 \quad \mathrm{X}_2]]) \\
&= \mathrm{slmin}([\mathrm{p}_1^* - 1 \quad \mathrm{m}_{1,1} \quad \mathrm{m}_{1,2}], [\mathrm{x}^{*2} \quad 2\mathrm{x}^*\mathrm{X}_1 \quad 2\mathrm{x}^*\mathrm{X}_2]).
\end{aligned}$$

Then at the chosen reference parameters $\boldsymbol{p}^* = (1, 0)$,

$$\dot{\boldsymbol{X}} = \mathrm{slmin}([0 \quad \mathrm{m}_{1,1} \quad \mathrm{m}_{1,2}], [0 \quad 0 \quad 0]).$$

Then for the initial conditions we have that

$$\begin{aligned}\boldsymbol{X}(0) &= \text{fsign}(\text{p}_2^*, \text{J}_\text{p}(\text{p}_2)\text{M})\text{J}_\text{p}(\text{p}_2)\boldsymbol{M} \\ &= \text{fsign}(\text{p}_2^*, [0 \quad 1]\text{M})[0 \quad 1]\boldsymbol{M} \\ &= \text{fsign}(\text{p}_2^*, \text{M}_2)\boldsymbol{M}_2.\end{aligned}$$

Once again at $\boldsymbol{p}^* = (1, 0)$*,*

$$\boldsymbol{X}(0) = \text{fsign}(0, \boldsymbol{M}_2)\boldsymbol{M}_2$$

Therefore we have at $\boldsymbol{p}^*$*,*

$$\begin{aligned}\dot{\boldsymbol{X}} &= \text{slmin}([-1 \quad \text{m}_{1,1} \quad \text{m}_{1,2}], [0 \quad 0 \quad 0]) \\ \boldsymbol{X}(0) &= \text{fsign}(0, \boldsymbol{M}_2)\boldsymbol{M}_2.\end{aligned}$$

If we choose $M = I$*, we get that*

$$\dot{X} = \text{slmin}([-1 \quad 1 \quad 0], [1 \quad 0 \quad 0]) = [1 \quad 0]$$

and

$$X(0) = \text{fsign}(0, \boldsymbol{M}_2)\boldsymbol{M}_2 = \text{fsign}(0, 0, 1)[0 \quad 1] = [0 \quad 1].$$

This gives us

$$\begin{aligned}\dot{X} &= [1 \quad 0] \\ X(0) &= [0 \quad 1]\end{aligned}$$

which can be solved to get

$$\begin{aligned}X_1(t) &= t \\ X_2(t) &= 1.\end{aligned}$$

To convert these from LD-sensitivity equations to L-sensitivity equations we need to multiply by the inverse of the directions matrix. In our case we would have that

$$S_x(t) = X(t)M^{-1} = [t \quad 1]M^{-1} = [t \quad 1]I^{-1} = [t \quad 1]I = [t \quad 1].$$

If we choose $M = -I$,

$$\dot{X} = \text{slmin}([-1 \quad -1 \quad 0], [1 \quad 0 \quad 0]) = [-1 \quad 0]$$

and

$$X(0) = \text{fsign}(0, \text{M}_2)\text{M}_2 = \text{fsign}(0, 0, -1)[0 \quad -1] = -[0 \quad -1] = [0 \quad 1].$$

This gives us

$$\dot{X} = [-1 \quad 0]$$
$$X(0) = [0 \quad 1]$$

which can be solved to get

$$X_1(t) = -t$$
$$X_2(t) = 1.$$

Then to find the LD-sensitivity function,

$$S_x(t) = X(t)M^{-1} = [-t \quad 1]M^{-1} = [-t \quad 1](-I^{-1}) = [-t \quad 1](-I) = [t \quad -1].$$

2.4 Evolutionary Game Theory

Game theory is the study of mathematical models that try to depict rational decision making. Traditionally, as first seen in Neumann's *On the Theory of Games and Strategies* [41], game theory was primarily used to study individuals playing various strategic games giving their best attempt to win or get the best reward. Since then, the field of study has expanded beyond traditional games of strategy and can be used to analyze human decision making processes applied to many mathematical fields. Evolutionary game theory expands game theory even further by allowing players to adapt based on the other players around them. In the field of mathematical epidemiology, evolutionary game theory is a way to incorporate human decision making and risk assessment into the model. Unless specified

otherwise all definitions are adapted from *Evolutionary Games and Population Dynamics* [22]. Below we introduce some terminology that will be used often in this section

- A game is a collection of circumstances that has results depending on the actions of two or more decision-makers [32].
- A player is a strategic decision-maker within the context of the game [32].
- An action is an available choice for a player. An action can also be called a move or a strategy given certain circumstances [32].

Definition 2.4.1. *(Payoff Matrix [18]). A payoff matrix for a two player game is a bi-matrix that shows the outcomes of both players, given their choices of action. A bi-matrix is a matrix where each cell contains two values, where the first value corresponds to the outcome of player 1 and the second value is the outcome for player 2.*

For a two player game, a payoff bi-matrix $M \in \mathbb{R}^{n\times m}$ would mean that player A would have n unique actions while player B has m unique actions. Any entry $m_{i,j} \in M$ would be an element of $\mathbb{R}^2$, representing the payoffs of both players given player A chose action i and player B chose action j. We denote $(m_{i,j})1$ to be the payoff for player A while $(m_{i,j})2$ would be the payoff for player B. This can be expanded to n players, by increasing the dimension of the bi-matrix to n-dimensional and allowing the individual entries of the matrix to be elements of $\mathbb{R}^n$.

Example 2.4.2. *Below is the payoff matrix for a game of Rock paper scissors between two players.*

	Rock	*Paper*	*Scissors*
Rock	$(0,0)$	$(0,1)$	$(1,0)$
Paper	$(1,0)$	$(0,0)$	$(0,1)$
Scissors	$(0,1)$	$(1,0)$	$(0,0)$

In this game we can see $m_{i,j} \in \mathbb{R}^2$ because there are two players. An element $m_{1,2}$ means that player A chose strategy 1, rock, while player B chose strategy 2, paper. This choice of strategies resulted in 0 points for A and 1 point for B. We can also see in this example that since the players have the same strategy options, this results in a square matrix.

Definition 2.4.3. *Given $n+1$ vertices, $s_0, \ldots, s_n$, such that $s_1 - s_0, \ldots, s_n - s_0$ are linearly independent, the simplex, S_n, is determined by*

$$S_n = \{\theta_0 s_0 + \cdots + \theta_k s_k \mid \sum_{i=0}^{n} \theta_i = 1 \text{ and } \theta_i \geq 0 \text{ for all } i.$$

The n-simplex, S_n, is a closed and bounded subset of $\mathbb{R}^n$. S_n contains all vectors with non-negative entries that sum to one. In other words, given an n-dimensional space, the n-simplex, S_n, is an n-dimensional polytope, a geometric objects with flat sides, which is the convex hull of the $n+1$ chosen vertices.

Example 2.4.4. *Some examples of simplexes are as follows:*

- *In 1 dimension the simplex is the line segment $\{x \mid x \in [0,1]\}$.*
- *In 2 dimensions the simplex is a triangle $\{(x,y) \mid x + y \leq 1, x, y \in [0,1]\}$.*
- *In 3 dimensions the simplex is a tetrahedron $\{(x,y,z) \mid x + y + z \leq 1, x, y, z \in [0,1]\}$.*

Definition 2.4.5. *(Pure Strategy). Given a set of actions, $\{x_1, \cdots, x_n\}$, a pure strategy is when a player only chooses a single action from the set to implement and never deviates. In any given game there will be finitely many actions.*

Since we define a pure strategy as a singular action, an action will be referred to as a strategy and a set of actions will be called a strategy set. We will use the terms strategy and strategy set from this point onward, unless action is needed to prevent confusion.

Example 2.4.6. *In the case of rock paper scissors our set of actions is rock,paper,scissors. Therefore there are three pure strategies, which are to always play rock, paper or scissors. In the case listed in definition 2.4.1 where our strategy set is $\{x_1, \cdots, x_n\}$, there are n pure strategies which are to always use action x_i for some $0 \leq i \leq n$.*

Definition 2.4.7. *(Mixed Strategy). Given a strategy set, $\{x_1, \cdots, x_n\}$, a mixed strategy is when a player picks multiple actions and assigns a probability of use to each $(p_1, \cdots, p_n) \in [0,1]^n$.*

A pure strategy can be seen as a special case of the mixed strategies where $p_i = 1$ for some i and $p_j = 0$ for $j \neq i$. Mixed and pure strategies can also be seen as points on a simplex, where the pure strategies correspond to the vertices, and mixed strategies correspond to the edges and interior space. Any given mixed strategy $\mathbf{p} = (p_1, \cdots, p_n)$ corresponds to a point in the simplex S_n such that,

$$S_n = \{\mathbf{p} = (p_1, \cdots, p_n) \in \mathbb{R}^n | p_i \geq 0 \text{ and } \sum p_i = 1\}.$$

Definition 2.4.8. *(Expected Value). Given an $n_1 \times n_2$ payoff matrix M, and mixed strategies $\mathbf{p}$ for player A and $\mathbf{q}$ for player B, then the expected value for player A is,*

$$E_A(\mathbf{p}, \mathbf{q}) = \sum_{j=1}^{n_2} \sum_{i=1}^{n_1} (m_{i,j})_1 p_i q_j. \tag{2.6}$$

Recall we denote $(m_{i,j})_1$ to be the payoff for player A while $(m_{i,j})_2$ to be the payoff for player B.

Example 2.4.9. *Define the payoff matrix for two players A and B,*

$$M = \begin{array}{|c|c|c|} \hline \textit{(0,4)} & \textit{(8,-2)} & \textit{(2,2)} \\ \hline \textit{(-4,10)} & \textit{(3,0)} & \textit{(4,4)} \\ \hline \end{array} \tag{2.7}$$

with mixed strategy probabilities,

$$P = (.5, .5) \tag{2.8}$$

$$Q = (.2, .3, .5). \tag{2.9}$$

Then,

$$E_A(P,Q) = 0(.5)(.2) + 8(.5)(.3) + 2(.5)(.5) + -4(.5)(.2) + 3(.5)(.3) + 4(.5)(.5) = 2.75$$

$$E_B(P,Q) = 4(.5)(.2) + -2(.5)(.3) + 2(.5)(.5) + 10(.5)(.2) + 0(.5)(.3) + 4(.5)(.5) = 2.6.$$

This means with the given mixed strategies we expect player A to average 2.75 *points per round and player B to average* 2.6 *points.*

Definition 2.4.10. *(Nash Equilibrium). Given a strategy set* $\boldsymbol{x} = \{x_1, \ldots, x_n\}$*, where* x_i *is a percentage of play, a Nash equilibrium is a collection of pure strategies* $\boldsymbol{x}^* = (\boldsymbol{x}_i, \cdots, \boldsymbol{x}_j)$ *each corresponding to a player* P_i*. The Nash equilibrium has the property that no player* P_i *can improve their expected value by choosing a strategy different from* x_k*,* $k \neq i$*, as long as every other player* P_j *adheres to* x_j*. Formally this means that*

$$E_{P_i}(\boldsymbol{x}^*) \geq E_{P_i}(\boldsymbol{x}').$$

for all $x^*, x' \in \boldsymbol{x}$*.*

Before going into an example of a Nash equilibrium, when doing classical game theory, we assume players are playing rationally. A player's goal is to get the most payout or to win the game, as such once a player chooses a strategy they will not change strategies unless the game is changed or a better strategy is discovered.

Example 2.4.11. *Consider the following payoff matrix,*

	b_1	b_2
a_1	*(2,2)*	*(1,3)*
a_2	*(3,1)*	*(5,5)*

(2.10)

From the perspective of player A, if player B chooses strategy b_1*, player A will want to choose strategy* a_2*. If player B chooses* b_2*, then once again player A would choose* a_2*. This would mean player A has no incentive to choose strategy* a_1 *and therefore would only choose* a_2*. From the perspective of player B, we can see* b_2 *would be the optimal strategy. This means that the Nash equilibrium is*

$$\boldsymbol{x}^* = (a_2, b_2). \tag{2.11}$$

Definition 2.4.12. *Given two players, A and B, each with mixed strategies, P_A^* and P_B^*, a mixed Nash equilibrium is (P_A^*, P_B^*), such that if either player changes strategies to any $P'_A \neq P_A^*$ and $P'_B \neq P_B^*$,*

$$E_A(P_A^*, P'_B) \leq E_A(P_A^*, P_B^*), \tag{2.12}$$

$$E_A(P'_A, P_B^*) \leq E_A(P_A^*, P_B^*), \tag{2.13}$$

$$E_B(P_A^*, P'_B) \leq E_B(P_A^*, P_B^*), \tag{2.14}$$

$$E_B(P'_A, P_B^*) \leq E_B(P_A^*, P_B^*). \tag{2.15}$$

Example 2.4.13. *Looking back at the payoff matrix for Rock paper scissors as seen in Example 2.4.2 the mixed Nash equilibrium would be (P_A^*, P_B^*), where $P_A^* = P_B^* = (1/3, 1/3, 1/3)$.*

Definition 2.4.14. *(Fitness). Given a population of competing individuals of type I_i, where a type corresponds to a mixed strategy, in a population of composition Q,*

$$Q = (p_1 I_1, p_2 I_2, \ldots p_n I_n) \tag{2.16}$$

where p_i is the frequency of I_i, $p_i \geq 0$ for all i and

$$\sum_{i=1}^{n} p_i = 1, \tag{2.17}$$

then the fitness of type I_i is

$$W(I_i, Q) = \sum_{j=1}^{n} x_j E_{I_i}(I_i, I_j). \tag{2.18}$$

Definition 2.4.15. *(Evolutionarily Stable). A population consisting of P-types, individuals using strategy $\mathbf{p}$, will be evolutionarily stable if, whenever a population of L-types, using strategy $\mathbf{l}$ is introduced, the P-types have higher fitness than the L-types. This means that for all $P \neq L$,*

$$W(L, Q) < W(P, Q). \tag{2.19}$$

A mixed strategy **p** is said to be evolutionarily stable if, whenever all members of the population use it, no other mixed strategies **l**, when introduced, can survive. This means that proportion of those using **l** will eventually drop to zero until those using **p** take up the entire population.

The replicator equation is a differential equation that allows for a fitness function to be considered in the distribution of mixed strategies. Instead of fixing a certain proportion of the population to a given strategy, it allows for players to replicate and switch to different strategies. Traditionally the replicator equation is written as,

$$\dot{x}_i = x_i[f_i(\mathbf{x}) - \phi(\mathbf{x})], \tag{2.20}$$

where x_i is the proportion of the population using strategy i, $\mathbf{x} = (x_1, \cdots, x_n)$ is the vector of strategies being used by the population, f_i is the fitness of the strategy **i** users and $\phi(x)$ is average population fitness and can be written,

$$\phi(\mathbf{x}) = \sum_{j=1}^{n} x_j f_j(\mathbf{x}). \tag{2.21}$$

Example 2.4.16. *Consider two types of players, A and B, using mixed strategies P_A and P_B. Also assume that across the entire population, $0 \leq k \leq 1$ is the proportion of the population in A and $(1-k)$ is the proportion of B. Finally assume that $W(A, Q) = w_a$ and $W(B, Q) = w_b$. Then,*

$$\boldsymbol{x} = (k, 1-k), \tag{2.22}$$

$$\phi(\boldsymbol{x}) = k(w_a) + (1-k)(w_b) = kw_a + w_b - kw_b. \tag{2.23}$$

Then the replicator equations take on the following forms:

$$\dot{x}_1 = k[w_a - (kw_a + w_b - kw_b)] = k(1-k)(w_a + w_b),$$

$$\dot{x}_2 = (1-k)[w_b - (kw_a + w_b - kw_b)] = -k(1-k)(w_a + w_b).$$

Observe that, $\dot{x}_1 = -\dot{x}_2$. When dealing with two group populations this will always be the case because of symmetry. See Figures 2.4 and 2.5 for simulations of the replicator equation over a span of 200 days.

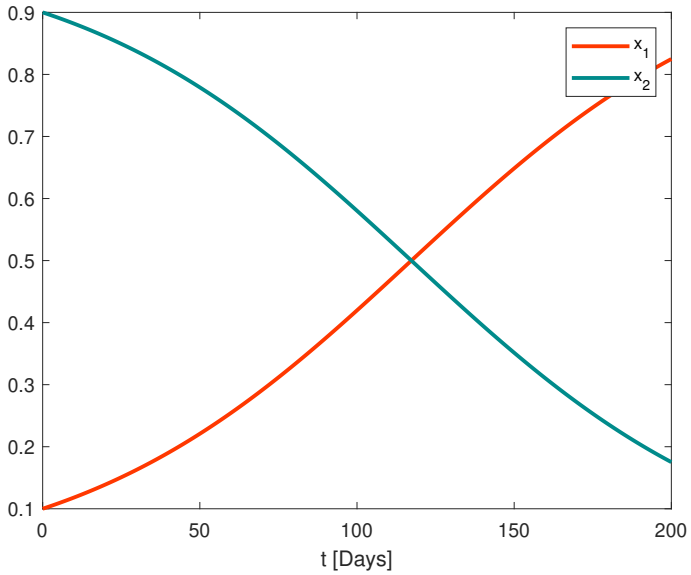

Figure 2.4: Here we have k = 0.1, $w_a = 1/3$ and $w_b = 0.3146$. Since $w_a > w_b$ we can see that the population starts to migrate to x_1, but as more people join x_1 the rate at which people are joining slows down. After 200 days, x_1 has yet to take over the entire population.

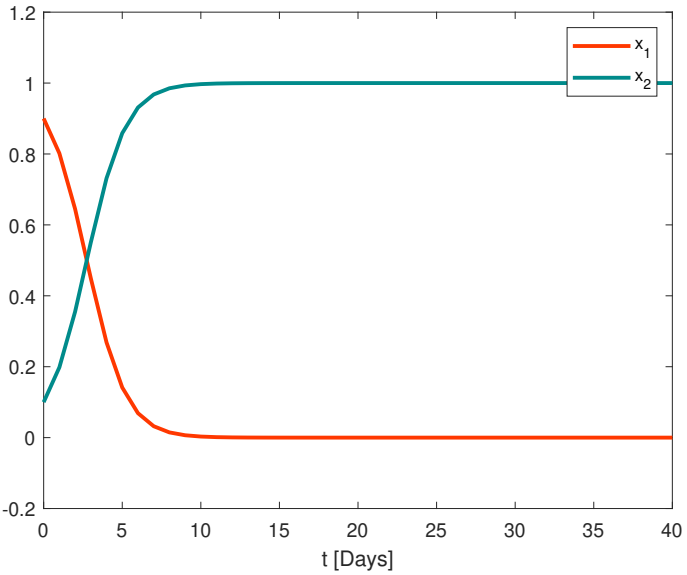

Figure 2.5: Here we have k = 0.9, $w_a = 0.1$ and $w_b = 0.9$. This time $w_b > w_a$, however the difference in w_a and w_b is much more significant than the previous graph. As such the population is shifting to x_2 at a faster rate. At day 10 the entire population is x_2.

2.5 Mathematical Epidemiology

This section is adapted from Brauer [9]. In mathematically modeling an infectious disease, a popular approach is to split the population into different compartments. A standard epidemic model is the SEIRS model,

$$\text{Susceptible} \to \text{Exposed} \to \text{Infected} \to \text{Recovered} \to \text{Susceptible},$$

given by the following ODEs:

$$\begin{aligned} \dot{S} &= \mu(S+E+I+R) - \beta SI + \zeta R - \mu S \\ \dot{E} &= \beta SI - \sigma E - \mu E \\ \dot{I} &= \sigma E - \gamma I - \mu I \\ \dot{R} &= \gamma I - \zeta R - \mu R \end{aligned} \tag{2.24}$$

where the state variables S, E, I, R correspond to the proportion of the population who are susceptible, exposed, infected and recovered. There are also parameters β, σ, γ, ζ and μ, where β is the average rate of contacts sufficient for infection, σ is the mean incubation rate, γ is the mean infectious rate, ζ is the mean waning immunity rate and μ is the natural death and birth rate. We assume that the birth and death rates are equal to allow for a constant population, as such $\mu(S+E+I+R)$ is added back into the susceptible compartment. Each state variable translates to a proportion of the population where,

$$S(t) + E(t) + I(t) + R(t) = 1.$$

If we want to see an exact population value, instead of a proportion, we can multiply each equation by our total population N. Keeping the state values as a proportion also helps simplify the susceptible compartment into

$$\dot{S} = \mu - \beta SI + \zeta R - \mu S.$$

Example 2.5.1. *The details that make up the standard SEIRS model can be made clearer with examples with parameter values in whatever units are chosen. For instance,* ζ

represents the reciprocal of the average amount of time it takes for individuals to lose immunity. This means that recovered individuals leave the recovered class at a rate of ζ per unit time. If we want to look at SEIRS in terms of days, and want the waning natural immunity period to be 30 days, then

$$30 = \frac{1}{\zeta} \implies \zeta = \frac{1}{30} \approx 0.033.$$

Let us say that we want to keep the units in days. We will say that we want there to be two sufficient contacts for infection a day, a five day incubation period, an eight day infectious period, a waning immunity period of 30 days and an average lifespan of 80 years. This will give us

$$\begin{aligned}
\beta &= 2 \\
\sigma &= 1/5 = 0.2 \\
\gamma &= 1/8 = 0.125 \\
\zeta &= 1/30 \approx 0.033 \\
\mu &= 1/(80(365)) = 1/29200.
\end{aligned}$$

Once we plug these into our model we will have that

$$\begin{aligned}
\dot{S} &= 1/29200 - 2SI + 0.033R - (1/29200)S \\
\dot{E} &= 2SI - 0.2E - (1/29200)E \\
\dot{I} &= 0.2E - 0.125I - (1/29200)I \\
\dot{R} &= 0.125I - 0.033R - (1/29200)R.
\end{aligned}$$

These sorts of ODE models can be impossible to solve analytically. In order to solve them we must solve them numerically, by simulating them, and analyze them qualitatively. If we assume that 90% is susceptible and 10% is exposed at the start of modeling we will have a model

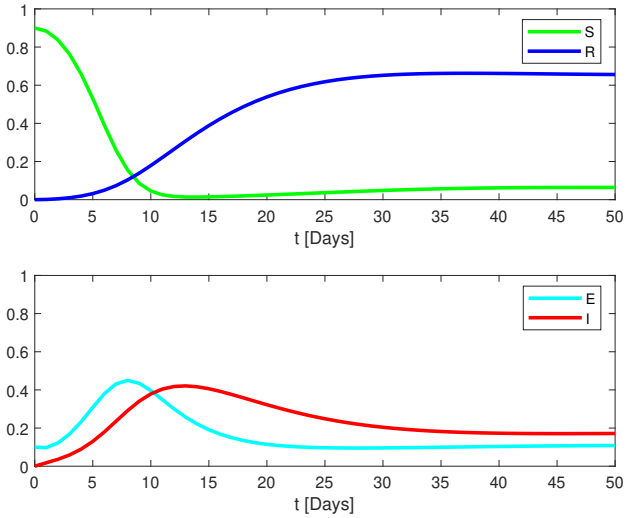

Figure 2.6: Simulation of the SEIR model.

As we can see in Figure 2.6, the susceptible population drops quickly with a high value of β and becomes exposed and infected. However the sick population starts to lower and due to such a long immunity period cannot return to the peak. After the SEIR model has been simulated, we can use the information to create other graphs to get a glimpse of different helpful information. For example below in Figure 2.7, is a bar graph of the daily change of the infected category.

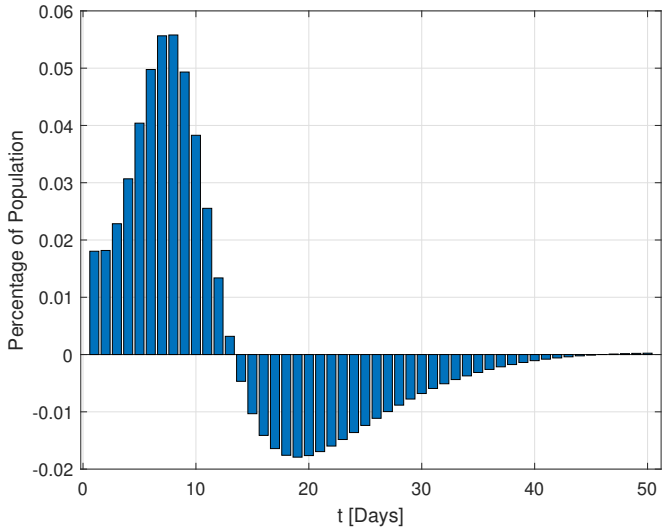

Figure 2.7: Net change of the infected population in population percentage per day.

As we can see the new daily infections spike in the first seven days, but after that they start losing individuals faster than they can get more.

In a system of ODEs, equilibria are very important in figuring out behavior of solutions. In mathematical epidemiology, two equilibria that are of interest are the endemic equilibrium and the disease free equilibrium. The endemic equilibrium is when a disease is always present in the population, or when $E(t) > 0$ or $I(t) > 0$ for all t. In order to find the endemic equilibrium for SEIRS we must first set all ODE's equal to zero and then solve for S,E,I and R. First we set all equations equal to zero and assume all parameters are nonzero:

$$0 = \mu - \beta SI + \zeta R - \mu S \tag{2.25}$$

$$0 = \beta SI - \sigma E - \mu E \tag{2.26}$$

$$0 = \sigma E - \gamma I - \mu I \tag{2.27}$$

$$0 = \gamma I - \zeta R - \mu R. \tag{2.28}$$

From equation (2.27) we can solve for E in terms of I:

$$E = \frac{\gamma + \mu}{\sigma} I, \tag{2.29}$$

and from equation (2.28) we solve I in terms of R:

$$I = \frac{\zeta + \mu}{\gamma} R. \tag{2.30}$$

If we take equation (2.26) and substitute equation (2.29) for E we have that

$$0 = \beta SI - \frac{(\sigma + \mu)(\gamma + \mu)}{\sigma} I = I(\beta S - \frac{(\sigma + \mu)(\gamma + \mu)}{\sigma}).$$

If we were to choose for $I = 0$ we would find the DFE, so we will assume $I \neq 0$ such that

$$0 = \beta S - \frac{(\sigma + \mu)(\gamma + \mu)}{\sigma} \implies S = \frac{(\sigma + \mu)(\gamma + \mu)}{\sigma}. \tag{2.31}$$

From here we substitute equation (2.31) into equation (2.25) for S:

$$\begin{aligned} 0 &= \mu - \frac{(\sigma + \mu)(\gamma + \mu)}{\sigma} \beta I + \zeta R - \mu \frac{(\sigma + \mu)(\gamma + \mu)}{\sigma} \\ \implies R &= \frac{\mu\sigma^2\gamma\beta - \mu\sigma\gamma(\sigma + \mu)(\gamma + \mu)}{\sigma\beta(\zeta + \mu)(\sigma + \mu)(\gamma + \mu) - \zeta\sigma^2\gamma\beta}. \end{aligned} \tag{2.32}$$

Now we can substitute equation (2.32) into equation (2.30) for R to get

$$I = \frac{\mu\sigma^2\gamma\beta(\zeta + \mu) - \mu\sigma\gamma(\sigma + \mu)(\gamma + \mu)(\zeta + \mu)}{\sigma\beta\gamma(\zeta + \mu)(\sigma + \mu)(\gamma + \mu) - \zeta\sigma^2\gamma^2\beta}. \tag{2.33}$$

Then we can substitute equation (2.33) into equation (2.29) for I to get

$$E = \frac{\mu\sigma^2\gamma\beta(\zeta + \mu)(\gamma + \mu) - \mu\sigma\gamma(\sigma + \mu)(\gamma + \mu)^2(\zeta + \mu)}{\sigma^2\beta\gamma(\zeta + \mu)(\sigma + \mu)(\gamma + \mu) - \zeta\sigma^3\gamma^2\beta}.$$

Therefore we have that the endemic equilibrium is

$$\mathbf{x}^*(S^*, E^*, I^*, R^*) = (S^*, E^*, I^*, R^*) = \begin{bmatrix} S^* \\ E^* \\ I^* \\ R^* \end{bmatrix} = \begin{bmatrix} \frac{(\sigma+\mu)(\gamma+\mu)}{\sigma} \\ \frac{\mu\sigma^2\gamma\beta(\zeta+\mu)(\gamma+\mu) - \mu\sigma\gamma(\sigma+\mu)(\gamma+\mu)^2(\zeta+\mu)}{\sigma^2\beta\gamma(\zeta+\mu)(\sigma+\mu)(\gamma+\mu) - \zeta\sigma^3\gamma^2\beta} \\ \frac{\mu\sigma^2\gamma\beta(\zeta+\mu) - \mu\sigma\gamma(\sigma+\mu)(\gamma+\mu)(\zeta+\mu)}{\sigma\beta\gamma(\zeta+\mu)(\sigma+\mu)(\gamma+\mu) - \zeta\sigma^2\gamma^2\beta} \\ \frac{\mu\sigma^2\gamma\beta - \mu\sigma\gamma(\sigma+\mu)(\gamma+\mu)}{\sigma\beta(\zeta+\mu)(\sigma+\mu)(\gamma+\mu) - \zeta\sigma^2\gamma\beta} \end{bmatrix}.$$

The disease free equilibrium (DFE) is exactly as it sounds, when there is no disease, as such we set any infective compartments equal to zero. In the case of SEIRS, we would set $E = I = 0$ and see where the rest of the population settles. Anyone in the susceptible

category would stay susceptible since there is no infective population to infect them, while anybody in the recovered category will eventually flow back into the susceptible category. This makes the DFE $\mathbf{x}^* = (S^*, E^*, I^*, R^*) = (1, 0, 0, 0)$. More formally, we assume that $I = 0$. Then we can plug I into equation (2.29):

$$E = \frac{\gamma + \mu}{\sigma}(0) = 0.$$

We can also plug I into equation (2.30):

$$0 = \frac{\zeta + \mu}{\gamma} R \implies 0 = R.$$

Now we can plug $R = I = E = 0$ into equation (2.25):

$$0 = \mu - \beta S(0) + \zeta(0) - \mu S = \mu - \mu S = \mu(1 - S).$$

Since $\mu \neq 0$, $S = 1$. Therefore the DFE is

$$\mathbf{x}^* = (S^*, E^*, I^*, R^*) = (1, 0, 0, 0).$$

Now that the idea of an endemic and disease free equilibrium have been discussed, one might wonder if there is a way we can tell if our disease is going to move towards the endemic equilibrium or the DFE. This brings us to the basic reproduction number.

Definition 2.5.2. *(Basic Reproduction Number [9]). The basic reproduction number, denoted $\mathcal{R}_0$, is the average number of secondary infections produced by one infected individual, during their infectious period, when introduced to a wholly susceptible population.*

The basic reproduction number can be calculated from the eigenvalue of special matrices associated with an epidemic model. Importantly, $\mathcal{R}_0$ specifically determines when the DFE is going to be attractive and stable, or when it will be unstable. More specifically, if $\mathcal{R}_0 < 1$ then the disease will die out (and the DFE is asymptotically stable) and if $\mathcal{R}_0 > 1$ then there will be an epidemic (and the DFE is unstable).

With variations of the epidemic model, $\mathcal{R}_0$ can take on many different forms. In order to find $\mathcal{R}_0$ we will follow along with the process seen in van den Driessche and Watmough [39]. Looking at the SEIRS model in equation (2.24), in order to solve for $\mathcal{R}_0$ we must first reorder our epidemic model such that the infected terms come first, this changes the model to

$$\begin{aligned}
\dot{E} &= \beta SI - \sigma E - \mu E \\
\dot{I} &= \sigma E - \gamma I - \mu I \\
\dot{S} &= \mu - \beta SI + \zeta R - \mu S \\
\dot{R} &= \gamma I - \zeta R - \mu R.
\end{aligned}$$

Now we must find vectors $\mathcal{F}$, $\mathcal{V}^+$ and $\mathcal{V}^-$, where $\mathcal{F}$ denotes the rates of new infections, $\mathcal{V}^+$ denotes the rate of transfer into the corresponding compartment and $\mathcal{V}^-$ denotes the rate of transfer out of the corresponding compartment. Both $\mathcal{V}^+$ and $\mathcal{V}^-$ ignore any terms used in $\mathcal{F}$. For the above, we have that

$$\mathcal{F} = \begin{bmatrix} \beta SI \\ 0 \\ 0 \\ 0 \end{bmatrix}, \mathcal{V}^+ = \begin{bmatrix} 0 \\ \sigma E \\ \mu + \zeta R \\ \gamma I \end{bmatrix}, \mathcal{V}^- = \begin{bmatrix} (\sigma + \mu)E \\ (\gamma + \mu)I \\ \mu S \\ (\zeta + \mu)R \end{bmatrix}.$$

We also have that

$$\mathcal{V} = \mathcal{V}^- - \mathcal{V}^+ = \begin{bmatrix} (\sigma + \mu)E \\ (\gamma + \mu)I - \sigma E \\ \mu S - \mu - \zeta R \\ (\zeta + \mu)R - \gamma I \end{bmatrix}.$$

Now we must take the Jacobian of $\mathcal{F}$ and $\mathcal{V}$ at the disease free equilibrium, $\mathbf{x}^* = (E, I, S, R) = (0, 0, 1, 0)$. This gives us the Jacobians

$$\mathbf{J}\mathcal{F}(\mathbf{x}^*) = \begin{bmatrix} 0 & \beta S & \beta I & 0 \\ 0 & 0 & 0 & 0 \\ 0 & 0 & 0 & 0 \\ 0 & 0 & 0 & 0 \end{bmatrix} = \begin{bmatrix} 0 & \beta & 0 & 0 \\ 0 & 0 & 0 & 0 \\ 0 & 0 & 0 & 0 \\ 0 & 0 & 0 & 0 \end{bmatrix}, \mathbf{J}\mathcal{V}(\mathbf{x}^*) = \begin{bmatrix} \sigma + \mu & 0 & 0 & 0 \\ -\sigma & \gamma + \mu & 0 & 0 \\ 0 & 0 & \mu & -\zeta \\ 0 & -\gamma & 0 & \zeta + \mu \end{bmatrix}.$$

To progress further we must find F, V and V^{-1} where F is the top left $k \times k$ matrix of $\mathcal{F}$ and V is the top left $k \times k$ matrix of $\mathcal{V}$. We determine k as the number of infected compartments. For SEIRS, we have E and I as the infected terms so $k = 2$. Therefore,

$$F = \begin{bmatrix} 0 & \beta \\ 0 & 0 \end{bmatrix}, V = \begin{bmatrix} \sigma + \mu & 0 \\ -\sigma & \gamma + \mu \end{bmatrix}, V^{-1} = \frac{1}{(\sigma + \mu)(\gamma + \mu)} \begin{bmatrix} \gamma + \mu & 0 \\ \sigma & \sigma + \mu \end{bmatrix}.$$

Now we can also find

$$FV^{-1} = \begin{bmatrix} \frac{\beta\sigma}{(\sigma+\mu)(\gamma+\mu)} & \frac{\beta}{\gamma+\mu} \\ 0 & 0 \end{bmatrix}.$$

The final step is to find $\mathcal{R}_0$ with the formula

$$\mathcal{R}_0 = \rho(FV^{-1})$$

where $\rho(FV^{-1})$ denotes the spectral radius of a matrix FV^{-1}, the max of the absolute values of the eigenvalues. In our case since FV^{-1} is upper triangular we can see we have only one nonzero eigenvalue and therefore

$$\rho(FV^{-1}) = \mathcal{R}_0 = \frac{\beta\sigma}{(\sigma + \mu)(\gamma + \mu)}. \tag{2.34}$$

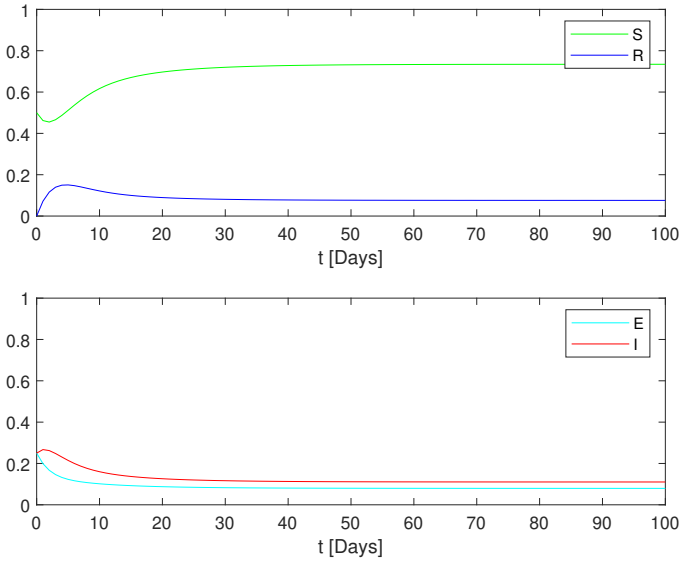

Figure 2.8: $\mathcal{R}_0 = 1.3617$ with $\beta = 0.5$, $\sigma = 0.5$, $\gamma = 0.35$, $\mu = 0.01$ and $\zeta = 0.5$.

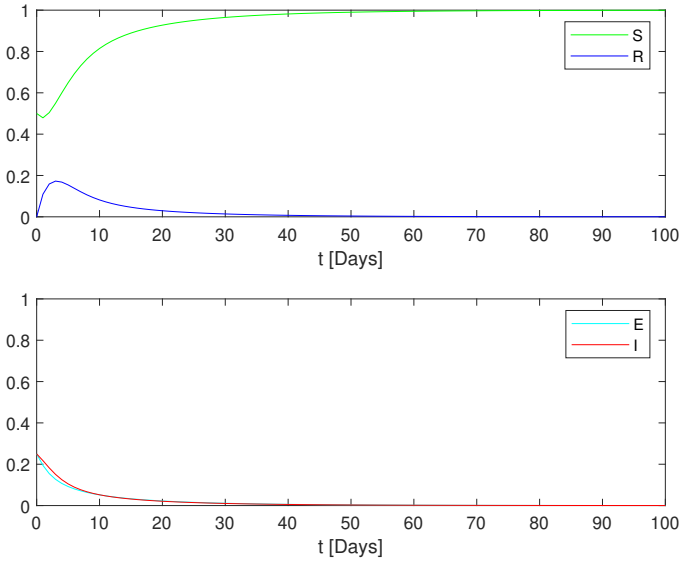

Figure 2.9: $\mathcal{R}_0 = 0.8036$ with $\beta = 0.5$, $\sigma = 0.5$, $\gamma = 0.6$, $\mu = 0.01$ and $\zeta = 0.5$.

As we can see from figure 2.8, when $\mathcal{R}_0 > 1$ the infected compartments asymptote to nonzero values while in figure 2.9 when $\mathcal{R}_0 < 1$, all compartments go to zero except for the susceptible compartment which converges to one. We also note that sometimes when

$\mathcal{R}_0 > 1$, the disease can still die out. The $\mathcal{R}_0$ only captures local behavior at the DFE and can say that it has unstable behavior. An example of when the $\mathcal{R}_0 > 1$ but the disease still dies out is when the average waning immunity is prolonged, and the virus spreads rapidly with a short incubation and infectious period. In such a scenario, the virus can exhaust its pool of susceptible individuals, eventually causing the number of infected cases to drop to zero. As we have done in other sections, we will be doing a sensitivity analysis with the basic SEIR model,

$$\begin{aligned}
\dot{S} &= \mu - \beta SI + \zeta R - \mu S =: f_1(\mathbf{p}, \mathbf{x}) \\
\dot{E} &= \beta SI - \sigma E - \mu E =: f_2(\mathbf{p}, \mathbf{x}) \\
\dot{I} &= \sigma E - \gamma I - \mu I =: f_3(\mathbf{p}, \mathbf{x}) \\
\dot{R} &= \gamma I - \zeta R - \mu R =: f_4(\mathbf{p}, \mathbf{x}).
\end{aligned}$$

For this model we will assume the reference parameter is

$$\mathbf{p}^* = (\beta^*, \sigma^*, \gamma^*, \zeta^*, S_0^*, E_0^*)$$

and we will assume μ, I_0 and R_0 are constant. We also will define

$$\begin{aligned}
\mathbf{x} &= (S, E, I, R), \\
\mathbf{f} &= (f_1, f_2, f_3, f_4), \\
\mathbf{f}_0 &= (f_{1_0}, f_{2_0}, f_{3_0}, f_{4_0}),
\end{aligned}$$

where $\mathbf{f}_0(\mathbf{p}) = (S_0, E_0, 0, 0)$.

Now we can calculate

$$\mathbf{J_p f}(\mathbf{p}, \mathbf{x}) = \begin{bmatrix} -SI & 0 & 0 & R & 0 & 0 \\ SI & -E & 0 & 0 & 0 & 0 \\ 0 & E & -I & 0 & 0 & 0 \\ 0 & 0 & I & -R & 0 & 0 \end{bmatrix}$$

$$\mathbf{J_x f}(\mathbf{p}, \mathbf{x}) = \begin{bmatrix} -\beta I - \mu & 0 & -\beta S & \zeta \\ \beta I & -\sigma - \mu & \beta S & 0 \\ 0 & \sigma & -\gamma - \mu & 0 \\ 0 & 0 & \gamma & -\zeta - \mu \end{bmatrix}$$

$$\mathbf{J f}_0(\mathbf{p}) = \begin{bmatrix} 0 & 0 & 0 & 0 & 1 & 0 \\ 0 & 0 & 0 & 0 & 0 & 1 \\ 0 & 0 & 0 & 0 & 0 & 0 \\ 0 & 0 & 0 & 0 & 0 & 0 \end{bmatrix}.$$

In this case,

$$\mathbf{S_x} = \begin{bmatrix} \mathbf{S}_S \\ \mathbf{S}_E \\ \mathbf{S}_I \\ \mathbf{S}_R \end{bmatrix} = \begin{bmatrix} S_S^\beta & S_S^\sigma & S_S^\gamma & S_S^\zeta & S_S^{S_0} & S_S^{E_0} \\ S_E^\beta & S_E^\sigma & S_E^\gamma & S_E^\zeta & S_E^{S_0} & S_E^{E_0} \\ S_I^\beta & S_I^\sigma & S_I^\gamma & S_I^\zeta & S_I^{S_0} & S_I^{E_0} \\ S_R^\beta & S_R^\sigma & S_R^\gamma & S_R^\zeta & S_R^{S_0} & S_R^{E_0} \end{bmatrix}.$$

From here we plug these into the sensitivity system as

$$\dot{\mathbf{S}}_S(t) = \begin{bmatrix} -S^*I^* & 0 & 0 & R^* & 0 & 0 \end{bmatrix} + \begin{bmatrix} -\beta^*I^* - \mu & 0 & -\beta^*S^* & \zeta^* \end{bmatrix} \mathbf{S_x}(t)$$

$$\dot{\mathbf{S}}_E(t) = \begin{bmatrix} S^*I^* & -E^* & 0 & 0 & 0 & 0 \end{bmatrix} + \begin{bmatrix} \beta^*I^* & -\sigma^* - \mu & \beta^*S^* & 0 \end{bmatrix} \mathbf{S_x}(t)$$

$$\dot{\mathbf{S}}_I(t) = \begin{bmatrix} 0 & E^* & -I^* & 0 & 0 & 0 \end{bmatrix} + \begin{bmatrix} 0 & \sigma^* & -\gamma^* - \mu & 0 \end{bmatrix} \mathbf{S_x}(t)$$

$$\dot{\mathbf{S}}_R(t) = \begin{bmatrix} 0 & 0 & I^* & -R^* & 0 & 0 \end{bmatrix} + \begin{bmatrix} 0 & 0 & \gamma^* & -\zeta^* - \mu \end{bmatrix} \mathbf{S_x}(t)$$

where S^*, E^*, I^* and R^* represent the state variables using the reference parameters. We also have initial conditions,

$$\mathbf{S}_S(0) = \begin{bmatrix} 0 & 0 & 0 & 0 & 1 & 0 \end{bmatrix}$$
$$\mathbf{S}_E(0) = \begin{bmatrix} 0 & 0 & 0 & 0 & 0 & 1 \end{bmatrix}$$
$$\mathbf{S}_I(0) = \begin{bmatrix} 0 & 0 & 0 & 0 & 0 & 0 \end{bmatrix}$$
$$\mathbf{S}_R(0) = \begin{bmatrix} 0 & 0 & 0 & 0 & 0 & 0 \end{bmatrix}$$

or, in component form, we first have S_S,

$$\begin{aligned}
\dot{S}_S^{\beta}(t) &= -S^*(t)I^*(t) - (\beta^* I^*(t) + \mu)S_S^{\beta}(t) + (-\beta^* S^*(t))S_I^{\beta}(t) + \zeta^* S_R^{\beta}(t), & S_S^{\beta}(0) = 0,\\
\dot{S}_S^{\sigma}(t) &= -(\beta^* I^*(t) + \mu)S_S^{\sigma}(t) + (-\beta^* S^*(t))S_I^{\sigma}(t) + \zeta^* S_R^{\sigma}(t), & S_S^{\sigma}(0) = 0,\\
\dot{S}_S^{\gamma}(t) &= -(\beta^* I^*(t) + \mu)S_S^{\gamma}(t) + (-\beta^* S^*(t))S_I^{\gamma}(t) + \zeta^* S_R^{\gamma}(t), & S_S^{\gamma}(0) = 0,\\
\dot{S}_S^{\zeta}(t) &= R^*(t) - (\beta^* I^*(t) + \mu)S_S^{\zeta}(t) + (-\beta^* S^*(t))S_I^{\zeta}(t) + \zeta^* S_R^{\zeta}(t), & S_S^{\zeta}(0) = 0,\\
\dot{S}_S^{S_0}(t) &= -(\beta^* I^*(t) + \mu)S_S^{S_0}(t) + (-\beta^* S^*(t))S_I^{S_0}(t) + \zeta^* S_R^{S_0}(t), & S_S^{S_0}(0) = 1,\\
\dot{S}_S^{E_0}(t) &= -(\beta^* I^*(t) + \mu)S_S^{E_0}(t) + (-\beta^* S^*(t))S_I^{E_0}(t) + \zeta^* S_R^{E_0}(t), & S_S^{E_0}(0) = 0,
\end{aligned}$$

then, for S_E,

$$\begin{aligned}
\dot{S}_E^{\beta}(t) &= S^*(t)I^*(t) + \beta^* I^*(t)S_S^{\beta} - (\sigma^* + \mu)S_E^{\beta} + \beta^* S^*(t)S_I^{\beta}, & S_E^{\beta}(0) = 0,\\
\dot{S}_E^{\sigma}(t) &= -E^*(t) + \beta^* I^*(t)S_S^{\sigma} - (\sigma^* + \mu)S_E^{\sigma} + \beta^* S^*(t)S_I^{\sigma}, & S_E^{\sigma}(0) = 0,\\
\dot{S}_E^{\gamma}(t) &= \beta^* I^*(t)S_S^{\gamma} - (\sigma^* + \mu)S_E^{\gamma} + \beta^* S^*(t)S_I^{\gamma}, & S_E^{\gamma}(0) = 0,\\
\dot{S}_E^{\zeta}(t) &= \beta^* I^*(t)S_S^{\zeta} - (\sigma^* + \mu)S_E^{\zeta} + \beta^* S^*(t)S_I^{\zeta}, & S_E^{\zeta}(0) = 0,\\
\dot{S}_E^{S_0}(t) &= \beta^* I^*(t)S_S^{S_0} - (\sigma^* + \mu)S_E^{S_0} + \beta^* S^*(t)S_I^{S_0}, & S_E^{S_0}(0) = 0,\\
\dot{S}_E^{S_0}(t) &= \beta^* I^*(t)S_S^{I_0} - (\sigma^* + \mu)S_E^{I_0} + \beta^* S^*(t)S_I^{I_0}, & S_E^{I_0}(0) = 1,
\end{aligned}$$

and for S_I,

$$\begin{aligned}
\dot{S}_I^{\beta}(t) &= \sigma^* S_E^{\beta} - (\gamma^* + \mu) S_I^{\beta}, & S_I^{\beta}(0) &= 0, \\
\dot{S}_I^{\sigma}(t) &= E^*(t) + \sigma^* S_E^{\sigma} - (\gamma^* + \mu) S_I^{\sigma}, & S_I^{\sigma}(0) &= 0, \\
\dot{S}_I^{\gamma}(t) &= -I^*(t) + \sigma^* S_E^{\gamma} - (\gamma^* + \mu) S_I^{\gamma}, & S_I^{\gamma}(0) &= 0, \\
\dot{S}_I^{\zeta}(t) &= \sigma^* S_E^{\zeta} - (\gamma^* + \mu) S_I^{\zeta}, & S_I^{\zeta}(0) &= 0, \\
\dot{S}_I^{S_0}(t) &= \sigma^* S_E^{S_0} - (\gamma^* + \mu) S_I^{S_0}, & S_I^{S_0}(0) &= 0, \\
\dot{S}_I^{E_0}(t) &= \sigma^* S_E^{E_0} - (\gamma^* + \mu) S_I^{E_0}, & S_I^{E_0}(0) &= 0,
\end{aligned}$$

and finally, for S_R,

$$\begin{aligned}
\dot{S}_R^{\beta}(t) &= \gamma^* S_I^{\beta} - (\zeta^* + \mu) S_R^{\beta}, & S_R^{\beta}(0) &= 0, \\
\dot{S}_R^{\sigma}(t) &= \gamma^* S_I^{\sigma} - (\zeta^* + \mu) S_R^{\sigma}, & S_R^{\sigma}(0) &= 0, \\
\dot{S}_R^{\gamma}(t) &= I^*(t) + \gamma^* S_I^{\gamma} - (\zeta^* + \mu) S_R^{\gamma}, & S_R^{\gamma}(0) &= 0, \\
\dot{S}_R^{\zeta}(t) &= -R^*(t) + \gamma^* S_I^{\zeta} - (\zeta^* + \mu) S_R^{\zeta}, & S_R^{\zeta}(0) &= 0, \\
\dot{S}_R^{S_0}(t) &= \gamma^* S_I^{S_0} - (\zeta^* + \mu) S_R^{S_0}, & S_R^{S_0}(0) &= 0, \\
\dot{S}_R^{E_0}(t) &= \gamma^* S_I^{E_0} - (\zeta^* + \mu) S_R^{E_0}, & S_R^{E_0}(0) &= 0,
\end{aligned}$$

In Figure 2.11, we can see that for all state variables, ζ exhibits the most dynamic curves. This would mean that ζ acts as the most influential parameter and when perturbed would cause the most change. After that we can see that γ would be the next most influential overall.

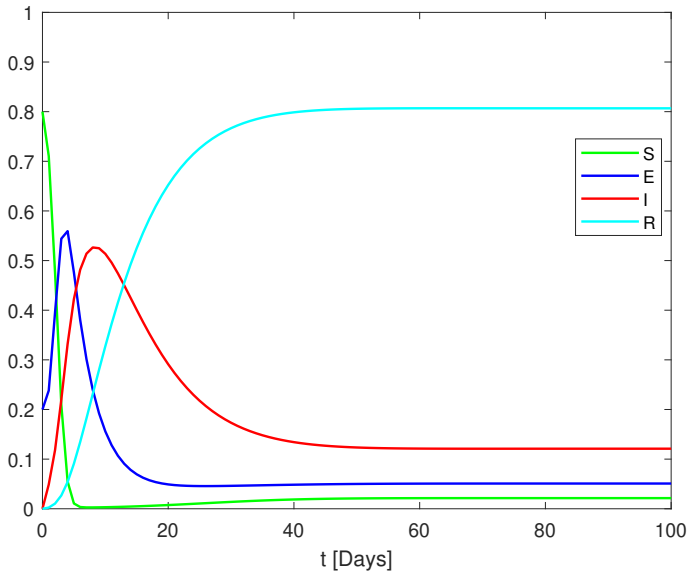

Figure 2.10: Numerical solutions of the state variables with $\mathbf{p}^* = (\beta^*, \sigma^*, \gamma^*, \zeta^*, S_0, E_0) = (5, 0.25, 0.1, 0.01, 0.8, 0.2)$ and $\mu = 0.005$.

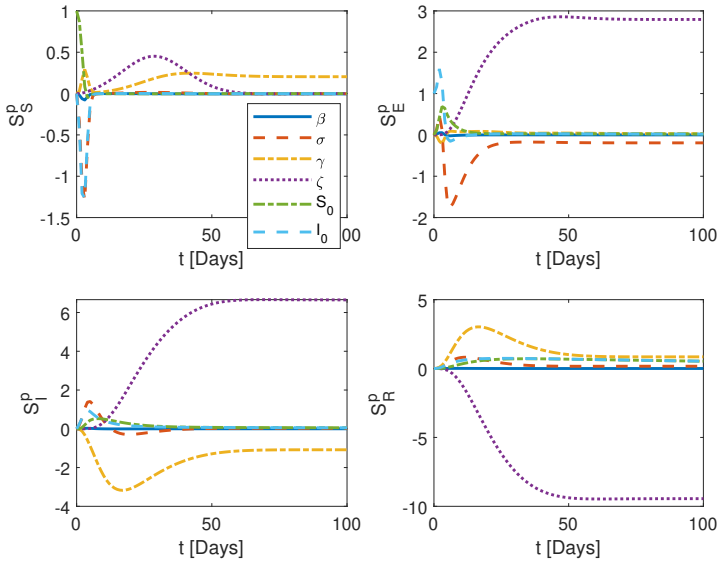

Figure 2.11: Numerical solutions of sensitivity functions with $\mathbf{p}^* = (\beta^*, \sigma^*, \gamma^*, \zeta^*, S_0, E_0) = (5, 0.25, 0.1, 0.01, 0.8, 0.2)$ and $\mu = 0.005$.

CHAPTER 3
BE-SEIMR MODEL FORMULATION

3.1 Base Model

In our expansion of the SEIR model, we want to incorporate when there are asymptomatic individuals and will be splitting the infected compartment into two groups: symptomatic, I_S and asymptomatic I_A. With this split we can still keep track of the total amount of infected individuals with $I_S + I_A = I$. We also need to introduce a new parameter Ξ, where Ξ is the ratio of individuals who become asymptomatic. This changes the basic SEIR model in equation (2.24) to

$$\begin{aligned}
\dot{S} &= \mu - \beta S[I_S + I_A] + \zeta R - \mu S \\
\dot{E} &= \beta S[I_S + I_A] - \Xi\sigma E - (1-\Xi)\sigma E - \mu E \\
\dot{I}_S &= (1-\Xi)\sigma E - \gamma I_S - \mu I_S \\
\dot{I}_A &= \Xi\sigma E - \gamma I_A - \mu I_A \\
\dot{R} &= \gamma[I_S + I_A] - \zeta R - \mu R,
\end{aligned}$$

where all state variables sum to one. In real world scenarios involving asymptomatic individuals, it is possible for these individuals to become aware of their infection. However, in our expanded SEIR model, we will make the assumption that asymptomatic individuals remain entirely unaware of their disease until they transition into the recovered compartment. In the SEIR model, we account for natural death, but we do not consider death induced by the disease. To address this, we will introduce a new parameter δ to account for disease induced mortality. Since asymptomatic individuals do not exhibit symptoms, we will assume that they do not experience an increased mortality rate while

sick. To balance the birth and death rates, we introduce the term Λ, defined as follows:

$$\Lambda = \mu + \delta I_S.$$

With this modification, the susceptible and symptomatic infected compartments will be updated as follows:

$$\dot{S} = \boxed{\Lambda} - \beta S[I_S + I_A] + \zeta R - \mu S,$$
$$\dot{I}_S = (1 - \Xi)\sigma E - \gamma I_S - \mu I_S - \boxed{\delta I_S}.$$

These adjustments allow us to account for disease induced mortality and maintain a balance between birth and death rates in the expanded SEIR model. In order to simulate this model we will be looking at the following parameter values pulled from Acuña-Zegarra et al. [1]:

Symbol	Meaning	Value
β_n	Average Contacts Sufficient for Infection	0.363282
σ	Average Exposed Period	0.196078
γ	Average Infected Period	0.167504
ζ	Average Waning Immunity Period	0.00273973
Ξ	Ratio of Asymptomatic Individuals	0.8787
μ	Natural Death and Birth Rate	0.0000391389
δ	Disease Death Rate	0.01017576

Table 3.1: Parameter values for Covid-19 from Acuña-Zegarra et al. [1].

For a comparison of the model with the present one, see Appendix C. A simulation of the revised model is given in Figure 3.1. We can see that the disease quickly spreads, but dies out over time due to the long immunity period.

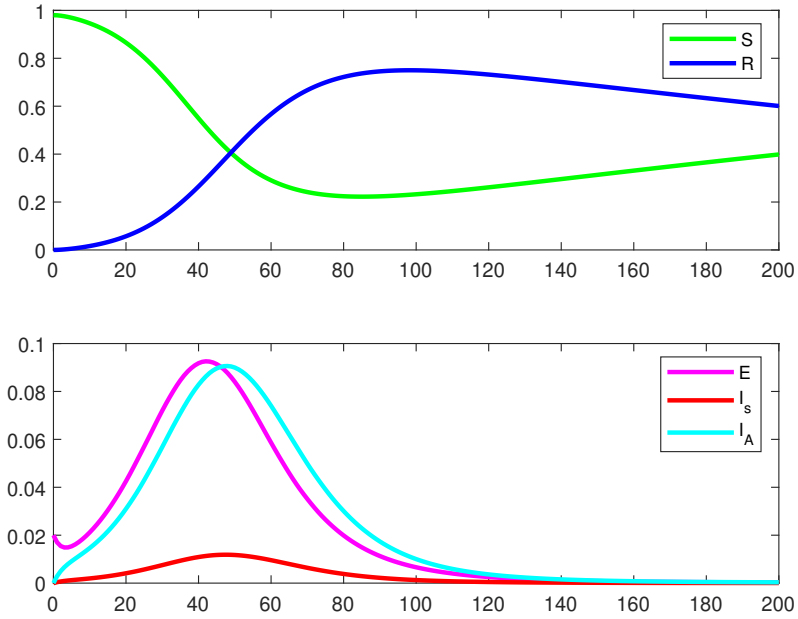

Figure 3.1: Here we used the parameters listed in the table above pulled from Acuña-Zegarra.

3.2 Adding a Behavioral Component

When faced with a highly severe or deadly disease, people often adapt their daily routines to protect themselves. Some individuals choose to wear masks, limit public outings, or engage in various disease avoidance practices. To account for these different choices, we will introduce two distinct groups, based on people's behavior: those with normal behavior denoted as b_n, and those with altered behavior denoted as b_a. We assume that individuals in the altered behavior group, b_a, are actively taking measures to reduce their risk of getting sick. In light of these groups, we will divide the susceptible population, S, into two subcompartments: S_n for individuals with normal behavior and S_a for those with altered behavior. This division is governed by the choices individuals make either following normal routines or adopting precautionary measures. The sum of these two subcompartments equals the total susceptible population, as expressed by the equation:

$$S_n + S_a = S. \tag{3.1}$$

Considering that altered behavior aims to minimize the likelihood of infection, we assume that individuals in the b_a group experience a reduced infection rate. To account for this difference, we define β_a as the infection rate for individuals with altered behavior b_a, and β_n as the infection rate for those with normal behavior, b_n. It is important to note that β_a is less than β_n, which is equal to the overall infection rate, β.

$$\beta_a < \beta_n = \beta.$$

By introducing these subcompartments and distinct infection rates, we can better model the impact of people's behavior on disease transmission in our SEIR model. We will also introduce the state variable:

$$x(t) = \frac{S_n(t)}{S_n(t) + S_a(t)},$$

where $x(t)$ represents the ratio of individuals who are susceptible and behaving normally to the total susceptible population at time t. This ratio will allow us to implement the behavioral assumptions into the model before adding the ability for individuals to switch between the two behavioral options, b_n and b_a. Now, our expanded SEIR model becomes:

$$\begin{aligned}
\dot{S} &= \Lambda - \boxed{S[\beta_n x + \beta_a(1-x)](I_S + I_A)} + \zeta R - \mu S \\
\dot{E} &= \boxed{S[\beta_n x + \beta_a(1-x)](I_S + I_A)} - \Xi\sigma E - (1-\Xi)\sigma E - \mu E \\
\dot{I}_S &= (1-\Xi)\sigma E - \gamma I_S - \mu I_S - \delta I_s \\
\dot{I}_A &= \Xi\sigma E - \gamma I_A - \mu I_A \\
\dot{R} &= \gamma[I_S + I_A] - \zeta R - \mu R.
\end{aligned}$$

Here, we use $x(t)$ to determine how the susceptible population is divided between S_n and S_a compartments. By incorporating this behavioral ratio, $x(t)$, into the model, we are able to represent the initial distribution of susceptible individuals based on their chosen behavior. We now consider the individuals who are asymptomatic and unaware of their sickness. Despite being able to spread the virus, they do not realize their condition and would also go through the process of choosing between b_n and b_a behavioral options. Even

though the infection rates for asymptomatic individuals do not change, their choice to adopt altered behavior (b_a) allows them to actively reduce their chances of spreading the virus. To account for this risk reduction, we introduce the parameter κ, which represents the extent of the reduction in their ability to transmit the virus when choosing b_a. By considering the parameter κ, we acknowledge that individuals who opt for altered behavior not only protect themselves but also contribute to limiting the spread of the virus to others. Similarly to the susceptible group, we can split the asymptomatic infected group into two subgroups: I_{A_n} and I_{A_a}. This allows us to represent the following relationship:

$$I_{A_n} + I_{A_a} = I_A,$$

where I_A denotes the total number of asymptomatic infected individuals. To capture the proportion of asymptomatic individuals behaving normally, we introduce the variable $y(t)$ defined as:

$$y(t) = \frac{I_{A_n}(t)}{I_{A_n}(t) + I_{A_a}(t)}.$$

In the expanded SEIR model, the compartments for susceptible individuals, S, and asymptomatic infected individuals, I_A, are composed of individuals who are indistinguishable from each other in the population, since individuals in I_A are asymptomatic. To address this, we assume that the initial ratios of susceptible individuals with normal behavior, $x(0)$, and asymptomatic individuals behaving normally, $y(0)$, are equal. This common ratio ensures that both groups start with the same proportion of individuals choosing normal behavior at the beginning of the simulation. However, it is also essential to allow for flexibility in the model. While we assume equal initial ratios by default, we can still consider scenarios where $x(0) \neq y(0)$ if necessary. This flexibility permits us to explore different initial conditions and observe how variations in the behavioral choices of susceptible and asymptomatic individuals impact the disease dynamics over time. These additional considerations can be readily incorporated into the

model:

$$\dot{S} = \Lambda - [\beta_n S x + \beta_a S(1-x)]\boxed{[I_S + I_A y + \kappa I_A(1-y)]} + \zeta R - \mu S$$
$$\dot{E} = [\beta_n S x + \beta_a S(1-x)]\boxed{[I_S + I_A y + \kappa I_A(1-y)]} - \Xi\sigma E - (1-\Xi)\sigma E - \mu E$$
$$\dot{I}_S = (1-\Xi)\sigma E - \gamma I_S - \mu I_S - \delta I_s$$
$$\dot{I}_A = \Xi\sigma E - \gamma I_A - \mu I_A$$
$$\dot{R} = \gamma[I_S + I_A] - \zeta R - \mu R.$$

This lays the foundation for further exploration of individuals switching between normal and altered behaviors, enriching the model with more dynamic scenarios. With the splits for those choosing b_n and b_a in place, we can move forward with building the replicator equations. Specifically, we will focus on the susceptible population and consider how individuals choose their behavior with respect to infection rates. Following along with Definition 2.4.16, we can build the replicator equation:

$$x_1 = x$$
$$x_2 = 1 - x$$
$$f_1 = -\beta_n I_S$$
$$f_2 = -\beta_a I_S$$

giving us

$$\begin{aligned}
\dot{x} &= x[-\beta_n I_S - (-x\beta_n I_S - (1-x)\beta_a I_S)] \\
&= -x\beta_n I_S - x(-x\beta_n I_S - (1-x)\beta_a I_S) \\
&= -x\beta_n I_S + x^2\beta_n I_S + x(1-x)\beta_a I_S \\
&= -x(1-x)\beta_n I_S + x(1-x)\beta_a I_S \\
&= x(1-x)(-\beta_n + \beta_a) I_S,
\end{aligned}$$

where we only look at I_S since the population cannot recognize asymptomatic individuals as infected. With this version of the replicator equation, all individuals would naturally

move towards choosing S_a since $\beta_a < \beta_n$. However, we need to provide a reason for individuals to consider choosing b_n instead. To achieve this, we introduce several parameters:

- k: This parameter represents the cost of choosing b_a, often associated with social costs. These costs could involve reduced interaction with loved ones, travel restrictions, and more.
- m_n: The perceived risk of developing symptoms for individuals choosing b_n.
- m_a: The perceived risk of developing symptoms for individuals choosing b_a.

We choose m_n and m_a in such a way that the perceived risk of developing symptoms is greater for those choosing b_n than for those choosing b_a, i.e.,

$$m_a < m_n.$$

With these values in place, we can determine the payoff values for choosing b_n and b_a as follows:

$$\begin{aligned} p_n(t) &= -m_n I_S(t), \\ p_a(t) &= -k - m_a I_S(t). \end{aligned}$$

These equations give us the payoffs associated with opting for b_n and b_a at time t, respectively. Furthermore, we can express the difference in payoffs as:

$$\begin{aligned} \Delta P(t) &= p_n(t) - p_a(t) \\ &= -m_n I_S(t) - [-k - m_a I_S(t)] \\ &= -m_n I_S(t) + k + m_a I_S(t) \\ &= k + (m_a - m_n) I_S(t). \end{aligned}$$

By examining $\Delta P(t)$, we can determine which option is more favorable at any given time t. Specifically:

- If $\Delta P(t) > 0$, then b_n is the more favorable option.
- If $\Delta P(t) < 0$, then b_a is the more favorable option.
- If $\Delta P(t) = 0$, then neither option is better than the other in terms of payoff.

Therefore, these values can fluctuate and after an individual chooses an initial strategy, they may want to swap after seeing theirs is no longer superior. Under real world circumstances, an individual can choose day by day, or week by week, whether or not they want to partake in protective measures, however when they have made a decision for the day, or week, we will be assuming they are stuck with their choice until the next day, or week. In order to incorporate this, we introduce new parameters τ and α. We define τ as the time unit of behavioral change, representing specific points in time when individuals can alter their behavior and α serves as the converting constant between regular time, t, and the behavioral change time unit with the following relationship:

$$\alpha > 0,$$
$$t = \alpha\tau.$$

By introducing τ and α, we can focus our attention on the payoff values at specific time points of behavioral change. Consequently, we narrow our lens to examine the payoff values of the form:

$$p_n(\tau) = -m_n I_S(\tau),$$
$$p_a(\tau) = -k - m_a I_S(\tau).$$

These equations provide us with the payoffs associated with choosing b_n and b_a at particular moments of behavioral change, allowing us to analyze the influence of the perceived risks of developing symptoms, m_n and m_a, and the cost of choosing b_a, k, on the decision-making process during these specific time intervals. With these in place we can

add a second part to the replicator equation with

$$\begin{aligned}
x_1 &= \frac{S_n}{S_n + S_a} = x(\tau), \\
x_2 &= \frac{S_a}{S_n + S_a} = 1 - \frac{S_n}{S_n + S_a} = 1 - x(\tau), \\
f_1 &= -m_n I_S(\tau), \\
f_2 &= -k - m_a I_S(\tau).
\end{aligned}$$

This results in the replicator equation:

$$\begin{aligned}
\frac{dx}{d\tau}(\tau) &= x(\tau)[-m_n I_S(\tau) - [x(\tau)(-m_n I_S(\tau)) + (1 - x(\tau))(-k - m_a I_S(\tau))]] \\
&= -m_n x(\tau) I_S(\tau) - x(\tau)[x(\tau)(-m_n I_S(\tau)) + (1 - x(\tau))(-k - m_a I_S(\tau))] \\
&= -m_n x(\tau) I_S(\tau) + m_n x(\tau)^2 I_S(\tau) - x(\tau)(1 - x(\tau))(-k - m_a I_S(\tau)) \\
&= x(\tau)[-m_n I_S(\tau) + x(\tau) m_n I_S(\tau)] - x(\tau)(1 - x(\tau))(-k - m_a I_S(\tau)) \\
&= x(\tau)(1 - x(\tau))(-m_n I(\tau)) - x(\tau)(1 - x(\tau))(-k - m_a I_S(\tau)) \\
&= x(\tau)(1 - x(\tau))[-m_n I(\tau) - (-k - m_a I_S(\tau))] \\
&= x(\tau)(1 - x(\tau))[\Delta P(\tau)] \\
&= x(\tau)(1 - x(\tau))[k + (m_a - m_n) I_S(\tau)].
\end{aligned}$$

We can change the time scale from τ to t by dividing by α and introducing the proportionality constant ρ, since $\frac{dx}{dt} = \frac{dx}{d\tau}\frac{d\tau}{dt} = \frac{dx}{d\tau}\frac{1}{\alpha}$ to get

$$\frac{dx}{dt}(t) = \frac{\rho}{\alpha} x(t)(1 - x(t))[k + (m_a - m_n) I_S(t)].$$

This gives the replicator equation of

$$\dot{x} = x(1 - x)(-\beta_n + \beta_a) I_S + \frac{\rho}{\alpha} x(1 - x)[k + (m_a - m_n) I_S].$$

Since asymptomatic individuals have the same choice and can actively change back and forth, we can follow the exact same process but replacing x with y to get

$$\dot{y} = y(1 - y)(-\beta_n + \beta_a) I_S + \frac{\rho}{\alpha} y(1 - y)[k + (m_a - m_n) I_S].$$

To address the fact that susceptible individuals can observe and copy the behavior of asymptomatic individuals, and vice versa, we need to modify the replicator equations accordingly. Instead of using the separate variables x and y, which represent the proportions of individuals choosing normal behavior in the susceptible and asymptomatic compartments, respectively, we will introduce a new variable, z, which represents the proportion of individuals choosing normal behavior across both groups. Introducing this variable will allow for individuals to emulate anyone they perceive to be susceptible, even if they may be an asymptomatic imposter. Therefore

$$\begin{aligned} z(t) &= \frac{S_n(t) + I_{A_n}(t)}{S_n(t) + S_a(t) + I_{A_n}(t) + I_{A_a}(t)} \\ &= \frac{S_n(t) + I_{A_n}(t)}{S(t) + I_A(t)} \\ &= \frac{x(t)S(t) + y(t)I_A(t)}{S(t) + I_A(t)}. \end{aligned}$$

The modified replicator equations become:

$$\begin{aligned} \dot{x} &= z(1-z)(-\beta_n + \beta_a)I_S + \frac{\rho}{\alpha} z(1-z)[k + (m_a - m_n)I_S], \\ \dot{y} &= z(1-z)(-\beta_n + \beta_a)I_S + \frac{\rho}{\alpha} z(1-z)[k + (m_a - m_n)I_S]. \end{aligned}$$

The similarity of these two equations is justified because, although we categorize individuals into two distinct groups, they perceive themselves as one collective. The transition from b_n to b_a, and vice versa, remains the same for both groups, reflecting their interconnectedness and shared decision-making process. Therefore, treating them with identical equations appropriately captures their unified behavior despite being recorded as separate subgroups. There is an important issue that requires addressing: when the variables x and y do not match up, specifically when $x_0 \neq y_0$, the elimination conditions, $z(1-z)$, no longer hold. In normal circumstances, if either b_n or b_a comprises the entire population, it should be impossible to switch back, leading to $\dot{x} = \dot{y} = 0$. This condition arises because the model is based on imitation dynamics, and if there is nobody to imitate, switching should not be allowed. However, we still want to account for the possibility of

switching if semi-dominance occurs. We define semi-dominance when either the entire susceptible population or the entire asymptomatic population has chosen a single behavior. In the semi-dominance situation in which all asymptomatic individuals are behaving in an altered manner, some may choose to imitate susceptible individuals who are behaving normally, thus causing them to switch and removing the semi-dominance. In order to address this scenario in the model, we need to introduce some additional restraints. These restraints will be added to the susceptible equation and will take the form of

$$\dot{S} = \Lambda - [\beta_n S \text{mid}(0, x, 1) + \beta_a S \text{mid}(0, (1-x), 1)][I_s + I_A \text{mid}(0, y, 1) + \kappa I_A \text{mid}(0, (1-y), 1)] + \zeta R - \mu S.$$

We have chosen to incorporate the mid function to ensure that the populations, when input into the model, remain within biologically and realistically plausible ranges. While adjusting $\dot{x}$ and $\dot{y}$ to simulate indistinguishable groups, a potential issue has become apparent. If $x_0 \neq y_0$ and a semi-dominance situation occurs, there is a possibility that the replicator equation may generate unrealistic values, representing a population either exceeding one hundred percent or falling below zero percent. An illustrative example of such a scenario is when $x_0 = 1$ and $y_0 = 0.5$, and the strategy with higher fitness is to act normally. In this case, our asymptomatic population, y, converges to one due to the strategy with higher fitness favoring normal behavior. Ideally, we would want our asymptomatic population to mimic the susceptible population, promoting a shift towards normal behavior. However, as $\dot{x} = \dot{y}$, when y increases and approaches one, x also increases. Given that $x_0 = 1$, this would cause x to exceed one, resulting in a population greater than one hundred percent. To address this potential flaw, when incorporating x and y back into $\dot{S}$, we use the mid function to constrain the values between zero and one. For the remainder of the thesis, we will set $x_0 = y_0$ which avoids this issue. However, to maintain flexibility in the model, we still allow for the possibility of $x_0 \neq y_0$.

Since the infection term is quite long and muddles the equation let,

$$\Psi(S, I_S, I_A, x, y) = [\beta_n S \text{mid}(0, x, 1) + \beta_a S \text{mid}(0, (1-x), 1)][I_s + I_A \text{mid}(0, y, 1) + \kappa I_A \text{mid}(0, (1-y), 1)],$$

making our model into

$$\begin{aligned}
\dot{S} &= \Lambda - \boxed{\Psi} + \zeta R - \mu S \\
\dot{E} &= \boxed{\Psi} - \Xi\sigma E - (1-\Xi)\sigma E - \mu E \\
\dot{I}_S &= (1-\Xi)\sigma E - \gamma I_S - \mu I_S - \delta I_S \\
\dot{I}_A &= \Xi\sigma E - \gamma I_A - \mu I_A \\
\dot{R} &= \gamma[I_S + I_A] - \zeta R - \mu R \\
\dot{x} &= \boxed{z(1-z)(-\beta_n + \beta_a)I_S + \frac{\rho}{\alpha} z(1-z)[k + (m_a - m_n)I_S]} \\
\dot{y} &= \boxed{z(1-z)(-\beta_n + \beta_a)I_S + \frac{\rho}{\alpha} z(1-z)[k + (m_a - m_n)I_S]}.
\end{aligned}$$

By introducing the replicator equation, we have enabled susceptible and asymptomatic infected individuals to make decisions that may help protect them from the virus. Now, let us incorporate the ability for infected symptomatic individuals to make a choice as well. Specifically, they can decide whether they want to quarantine or not. To do this, we will introduce a new state variable and a new parameter. Let I_Q represent the number of individuals who are quarantined, and let ϕ be the percentage of individuals who have the option to quarantine and choose to do so. Including these additions into the model will allow us to track the population of individuals who voluntarily decide to quarantine themselves, contributing to disease containment efforts. Since the individuals who choose to quarantine will not be able to transmit the virus to others, they will not be part of the infection term, Ψ. However, since they are still symptomatic and still perceivable by the population, they should be considered in the replicator equation. This consideration leads us to introduce a new variable, Υ, which represents the total population of symptomatic individuals and is defined as follows:

$$\Upsilon = I_S + I_Q.$$

Since individuals in quarantine are symptomatic, they will also have a disease induced death rate, δ, changing Λ to

$$\Lambda = \mu + \delta(I_S + I_Q).$$

This changes our expanded SEIR model to

$$\begin{aligned}
\dot{S} &= \Lambda - \Psi + \zeta R - \mu S \\
\dot{E} &= \Psi - \Xi\sigma E - (1-\Xi)\sigma E - \mu E \\
\dot{I}_S &= (1-\Xi)\sigma E - \boxed{\phi I_S} - \gamma I_S - \mu I_S - \delta I_S \\
\dot{I}_A &= \Xi\sigma E - \gamma I_A - \mu I_A \\
\dot{I}_Q &= \boxed{\phi I_S - \gamma I_Q - \mu I_Q - \delta I_Q} \\
\dot{R} &= \boxed{\gamma[I_S + I_A + I_Q]} - \zeta R - \mu R \\
\dot{x} &= z(1-z)(-\beta_n + \beta_a)\boxed{\Upsilon} + \frac{\rho}{\alpha} z(1-z)[k + (m_a - m_n)\Upsilon] \\
\dot{y} &= z(1-z)(-\beta_n + \beta_a)\boxed{\Upsilon} + \frac{\rho}{\alpha} z(1-z)[k + (m_a - m_n)\Upsilon].
\end{aligned} \tag{3.2}$$

To simulate this base model with behavioral components, we pull the parameter values used in the previous subsection and introduce the parameters utilized for the game theory and quarantine compartments. We can see the values and their sources in the table below:

Symbol	Source
$\beta_a = \beta_n(0.631) = 0.19397$	Wang et al. [44]
$\kappa = 0.631$	Wang et al. [44]
$\phi = 0.262$	Guillon and Kergall [19]
$x(0) = y(0) = 0.43$	Rab et al. [36]

Table 3.2: Behavior parameter values for Covid-19.

We will also be looking at the parameters α, m_n, m_a and k, but since they are unknown values corresponding to the sentiment of individuals at different times of the disease we will provide a few simulations with different scenarios.

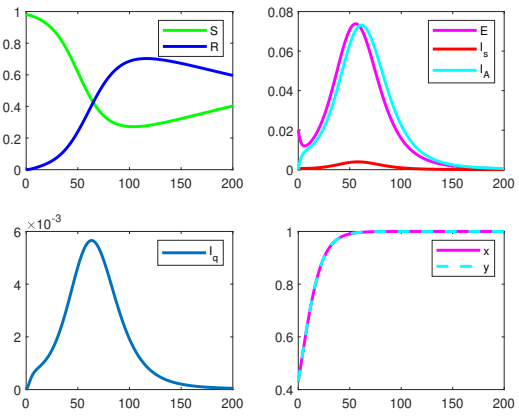

(a) Simulation of the state variables.

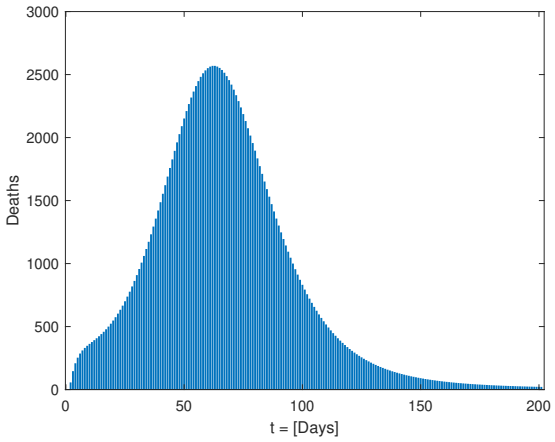

(b) Daily death toll.

Figure 3.2: Simulations of the model in equation (3.2) with parameters listed in the tables above and $\alpha = 7$ to signify a week before behavioral changes can occur, and $m_n = 0.8$, $m_a = 0.3$ and $k = 0.7$. For the death toll graph we assume an initial population of $N = 26446435$ [1].

It is important to provide an interpretation of m_n, m_a, and k, which represent the behavioral effects on a scale. For example, when we specify $k = 0.7$, it signifies a social cost of seven out of ten. In this context, a value of seven suggests a relatively significant social cost, but it still allows for the possibility of a more severe scenario.

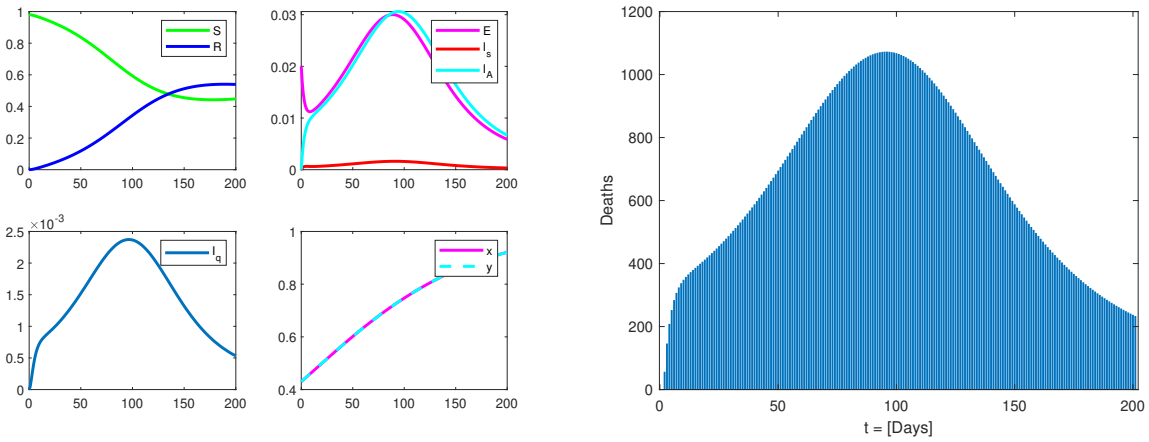

(a) Simulation of the state variables.

(b) Daily death toll.

Figure 3.3: Simulation of the model in equation (3.2) with the same parameters as previously in Figure 3.2a except with $k = 0.1$.

As illustrated, the population's perception of the social cost associated with a virus can exert a profound influence on the death toll. In Figure 3.2b, we observe a sharp spike in daily deaths, peaking at around 2500, and summing to 159530 when the social cost is perceived as a seven. However, in Figure 3.3b, the peak is significantly lower, reaching only 1100, and summing to 131920 when the social cost is perceived as a one out of ten. This stark contrast underscores the remarkable impact that a shift in social perception can have on outcomes. Notably, in the first simulation, more than half of the individuals who succumbed to the virus might have survived solely through a shift in societal perception. So far we have looked at game theory values, in which the population moves towards normal behavior, next we will look at a scenario in which they move towards altered.

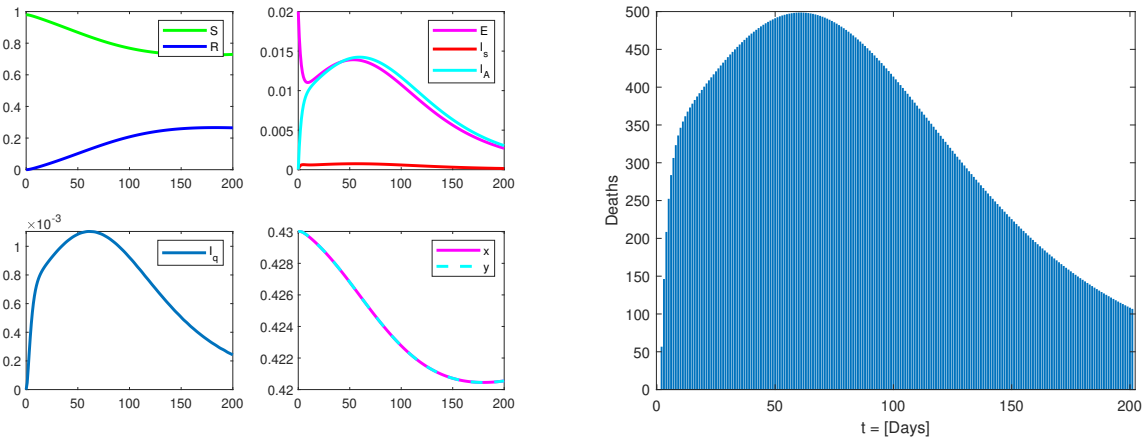

(a) Simulation of the state variables.

(b) Daily death toll.

Figure 3.4: Simulation of the model in equation (3.2) with the same parameters as previously in Figure 3.2a except $m_n = 0.9$, $m_a = 0.2$ and $k = 0.001$.

In Figure 3.4a we make the assumption that a person exhibiting normal behavior has immense perceived risk, someone using altered behavior is at low perceived risk and the social cost of altered behavior is incredibly small. Once again we have a decrease in peak daily death toll compared to Figures 3.2b and 3.3b. In Figure 3.4b we have a peak death toll of only 500 with total deaths at 67691. We can also see in Figure 3.4a that the overall infected population drops to a quarter of that in Figure 3.2a from individuals choosing to participate in disease avoidance strategies.

3.3 Adding Medical Intervention Component

In addition to the choices individuals can make regarding avoidance practices, we want to introduce medical intervention into the model. To account for this, we will add a new state variable, I_H, representing the population of individuals who require hospitalization. We will also introduce a few more parameters to capture the relevant dynamics. First, we introduce η as the ratio of individuals who become sick enough to require hospitalization. It is essential to note that while we refer to this compartment as "hospitalized," it

essentially represents a level of sickness that demands medical assistance. Next, we define δ_h as the death rate for individuals in the hospitalized compartment, where it is assumed that $\delta \leq \delta_h$ to represent the higher risk of mortality for those who are hospitalized. Additionally, we assume that individuals in the hospital will receive constant care and recover at a fixed rate, denoted as r [45]. This constant recovery rate is only active as long as there are hospitalized individuals. Therefore, we can represent the recovery rate for the hospitalized population, denoted $h(I_H)$, as follows:

$$h(I_H) = \min(rI_h, rH_c) = \begin{cases} rI_H & \text{for } I_H \leq H_c \\ rH_c & \text{for } I_H > H_c \end{cases}$$

where H_c is a maximal value representing the capacity of hospitals to handle patients. By incorporating the new state variable I_H and these additional parameters, we can account for the dynamics of hospitalization, recovery, and potentially increased mortality in the model. This extension allows us to analyze the effects of varying levels of sickness and the impact of hospital capacity on disease progression within the SEIR model framework, and results in

$$\begin{aligned}
\dot{S} &= \Lambda - \Psi + \zeta R - \mu S \\
\dot{E} &= \Psi - \Xi\sigma E - (1-\Xi)\sigma E - \mu E \\
\dot{I}_S &= (1-\Xi)\sigma E - \phi I_S - \boxed{\eta I_S} - \gamma I_S - \mu I_S - \delta I_S \\
\dot{I}_A &= \Xi\sigma E - \gamma I_A - \mu I_A \\
\dot{I}_H &= \boxed{\eta I_S - h(I_H) - \mu I_H - \delta_h I_H} \\
\dot{I}_Q &= \phi I_S - \gamma I_Q - \mu I_Q - \delta I_Q \\
\dot{R} &= \gamma[I_S + I_A + I_Q] + \boxed{h(I_H)} - \zeta R - \mu R \\
\dot{x} &= z(1-z)(-\beta_n + \beta_a)\Upsilon + \frac{\rho}{\alpha} z(1-z)[k + (m_a - m_n)\Upsilon], \\
\dot{y} &= z(1-z)(-\beta_n + \beta_a)\Upsilon + \frac{\rho}{\alpha} z(1-z)[k + (m_a - m_n)\Upsilon],
\end{aligned}$$

where $\Upsilon = I_S + I_H + I_Q$ and $\Lambda = \mu + \delta(I_S + I_Q) + \delta_h I_H$. As we consider the dynamics of the expanded SEIR model, it becomes evident that vaccination can play a crucial role in disease control and mitigation. While we have introduced a hospitalization compartment to account for the severity of sickness and medical assistance required, we must also explore the impact of vaccination on disease dynamics. Vaccines have proven to be powerful tools in reducing infection rates, minimizing mortality, and potentially leading to disease eradication. Let us now shift our focus to the incorporation of a vaccination compartment and explore how vaccination strategies can shape the trajectory of the disease within the model. To account for the impact of vaccination in the expanded SEIR model, we need to introduce a vaccination compartment and incorporate several new parameters. Considering this, we will add a new state variable, S_V, representing the population of individuals who have been vaccinated. Incorporating vaccination dynamics requires the introduction of additional parameters: the average rate at which the vaccine wears off, θ, and the infection rate for those who have received the vaccine, β_v. It's important to note that β_v should satisfy the condition $0 < \beta_v < \beta_a < \beta_n = \beta$. Next, we define $\Omega(S)$ to represent the vaccination rate, where the vaccination strategy is proportional to the number of susceptible individuals, S, as long as $S \leq S_c$, where S_c is a critical value based on maximum vaccine resources, and ω is a rate of vaccination [43]. This results in

$$\Omega(S) = \min(\omega S, \omega S_c) = \begin{cases} \omega S & \text{if } S \leq S_c \\ \omega S_c & \text{if } S > S_c \end{cases}$$

With vaccination considered, the infection term for vaccinated individuals becomes more complex. To handle this, and to follow the scheme for the non-vaccinated group, we introduce the variable ψ to represent this term concisely:

$$\psi = \beta_v S_v [I_S + I_A \text{mid}(0, y, 1) + \kappa I_A \text{mid}(0, (1-y), 1)].$$

By incorporating the vaccination compartment, along with these additional parameters and equations, we can analyze the effects of vaccination on disease dynamics within the

expanded SEIR model. This extension allows us to study the potential impact of vaccination strategies, vaccine coverage, and the wear-off rate on disease transmission and control. This will give us,

$$\begin{aligned}
\dot{S} &= \Lambda - \Psi + \zeta R - \boxed{\Omega(S) + \theta S_v} - \mu S \qquad (3.3)\\
\dot{S}_V &= \boxed{\Omega(S) - \theta S_v - \psi - \mu S_V}\\
\dot{E} &= \Psi + \boxed{\psi} - \Xi\sigma E - (1-\Xi)\sigma E + \psi - \mu E\\
\dot{I}_S &= (1-\Xi)\sigma E - \gamma I_S - \eta I_S - \phi I_S - \mu I_S - \delta I_S\\
\dot{I}_A &= \Xi\sigma E - \gamma I_A - \mu I_A\\
\dot{I}_H &= \eta I_S - h(I_H) - \mu I_H - \delta_h I_H\\
\dot{I}_Q &= \phi I_S - \gamma I_Q - \mu I_Q - \delta I_Q\\
\dot{R} &= \gamma(I_S + I_A + I_Q) + h(I_H) - \zeta R - \mu R\\
\dot{x} &= z(1-z)(-\beta_n + \beta_a)\Upsilon + \frac{\rho}{\alpha} z(1-z)[k + (m_a - m_n)\Upsilon]\\
\dot{y} &= z(1-z)(-\beta_n + \beta_a)\Upsilon + \frac{\rho}{\alpha} z(1-z)[k + (m_a - m_n)\Upsilon].
\end{aligned}$$

An important aspect of the vaccine that we need to account for is its ability to reduce the disease induced death rate. To represent this impact, we will introduce a parameter δ_v, such that $0 \leq \delta_v \leq \delta \leq \delta_h < 1$. This parameter quantifies the effectiveness of the vaccine in reducing mortality. To incorporate the vaccine's effect on mortality, we need to introduce new state variables: E_V, I_V, I_{QV}, I_{HV}, and D. These variables will represent the population of individuals in different states related to vaccination and disease progression. As a result of the new state variables, some of the previous equations will need adjustments:

$$\begin{aligned}
\Upsilon &= I_S + I_H + I_{HV} + I_Q + I_{QV} + I_V,\\
\Psi &= [\beta_n S\text{mid}(0, x, 1) + \beta_a S\text{mid}(0, (1-x), 1)][I_S + I_A\text{mid}(0, y, 1)\\
&\quad + \kappa I_A\text{mid}(0, (1-y), 1) + I_V],\\
\psi &= \beta_v S_v[I_S + I_A\text{mid}(0, y, 1) + \kappa I_A\text{mid}(0, (1-y), 1) + I_V].
\end{aligned}$$

Furthermore, we want the birth rate to be equal to the death rate to maintain a constant population. Hence, we define Λ as:

$$\begin{aligned}\Lambda = \mu[S + S_v + E + E_v + I_S + I_A + I_Q + I_{QV} + I_H + I_{HV} + I_V + R] \\ + \delta[I_S + I_Q] + \delta_h[I_H + \chi I_{HV}] + \delta_v[I_V + I_{QV}],\end{aligned}$$

where χ represents a reduction in the death rate for individuals sick enough to be hospitalized who also have the vaccine, resulting in $\chi\delta_h < \delta_h$.

Remark 3.3.1. *Before proceeding with the finalized model, we discuss an alternative methodology for dealing with differing death rates as a result of vaccination. In the above discussion, we described our chosen approach by splitting the exposed and infected terms into two nearly identical groups with only state variable changes and a death rate modification. However, we need to highlight an alternative option and explain why it was not selected for this model. Below, we present two SVIR models, each utilizing a different method:*

$$\begin{aligned}\dot{S} &= \Lambda - \beta SI - \omega S + \theta V + \zeta R - \mu S \\ \dot{V} &= -\beta_v VI + \omega S - \theta V - \mu V \\ \dot{I} &= \beta SI + \beta_v VI - \gamma I - \mu I - \delta I(1 - V) - \delta_v IV \\ \dot{R} &= \gamma I - \zeta R - \mu R\end{aligned} \tag{3.4}$$

$$\begin{aligned}\dot{S} &= \Lambda - \beta SI - \omega S + \theta V + \zeta R - \mu S \\ \dot{V} &= -\beta_v VI + \omega S - \theta V - \mu V \\ \dot{I}_S &= \beta SI - \gamma I_S - \mu I_S - \delta I_S \\ \dot{I}_V &= \beta_v VI - \gamma I_V - \mu I_V - \delta_v I_V \\ \dot{R} &= \gamma I_S + \gamma I_V - \zeta R - \mu R.\end{aligned} \tag{3.5}$$

In both sets of equations, Λ represents all the death terms being added back into the system. Additionally, in the second set of equations (3.5), we define $I = I_S + I_V$. As we can

observe, the first set of equations (3.4) *has one fewer state variable and handles differing infection death rates by making them proportional to the vaccinated population. However, the choice between the two options was influenced by the situation in which a vaccine is introduced in theof an epidemic. We assume in the initial stages of an epidemic, there is no vaccine available. When a vaccine is introduced, there will already be infected individuals present. The concern with using* (3.4) *arises when vaccinations are allowed. The death rate term* $\delta_v IV$ *is activated immediately, even though not enough time has passed for the newly vaccinated group to be infected. This issue becomes even more apparent when exposed terms are added to the model. Upon considering this issue with* (3.5)*, we find that once an individual is vaccinated, they must be infected and in state* I_V *before the term* δ_v *is activated. Therefore, it was decided that* (3.5)*, with its capability to handle this particular real-world scenario more accurately, was the option selected for this model.*

This will give us our finalized expanded SEIR model,

$$
\begin{aligned}
\dot{S} &= \Lambda - \Psi + \zeta R - \Omega(S) + \theta S_v - \mu S \\
\dot{S}_V &= \Omega(S) - \theta S_v - \psi - \mu S_v \\
\dot{E} &= \Psi - \Xi\sigma E - (1-\Xi)\sigma E - \mu E \\
\dot{E}_V &= \psi - \Xi\sigma E_V - (1-\Xi)\sigma E_V - \mu E_V \\
\dot{I}_S &= (1-\Xi)\sigma E - \gamma I_S - \eta I_S - \phi I_S - \mu I_S - \delta I_S \\
\dot{I}V &= (1-\Xi)\sigma E_V - \gamma I_V - \eta I_V - \phi I_V - \mu I_V - \delta_v I_V \\
\dot{I}_A &= \Xi\sigma[E + E_V] - \gamma I_A - \mu I_A \\
\dot{I}_H &= \eta I_S - h(I_H) - \mu I_H - \delta_h I_H \\
\dot{I}_{HV} &= \eta I_V - h(IHV) - \mu IHV - \chi\delta_h IHV \\
\dot{I}_Q &= \phi I_S - \gamma I_Q - \mu I_Q - \delta I_Q \\
\dot{I}_{QV} &= \phi I_V - \gamma I_{QV} - \mu I_{QV} - \delta_v I_{QV} \\
\dot{R} &= \gamma(I_S + I_A + I_Q + I_{QV} + I_V) + h(I_H) + h(I_{HV}) - \zeta R - \mu R \\
\dot{D} &= \Lambda \\
\dot{x} &= z(1-z)(-\beta_n + \beta_a)\Upsilon + \frac{\rho}{\alpha} z(1-z)[k + (m_a - m_n)\Upsilon] \\
\dot{y} &= z(1-z)(-\beta_n + \beta_a)\Upsilon + \frac{\rho}{\alpha} z(1-z)[k + (m_a - m_n)\Upsilon]
\end{aligned}
\tag{3.6}
$$

with secondary equations,

$$\Omega(S) = \min(\omega S, \omega S_c) = \begin{cases} \omega S & \text{if } S \leq S_c \\ \omega S_c & \text{if } S > S_c \end{cases}$$

$$h(I_H) = \min(rI_H, rH_c) = \begin{cases} rI_H & \text{for } I_H \leq H_c \\ rH_c & \text{for } I_H > H_c \end{cases}$$

$$z(t) = \frac{x(t)S(t) + y(t)I_A(t)}{S(t) + I_A(t)}$$

$$\Psi = [\beta_n S \text{mid}(0, x, 1) + \beta_a S \text{mid}(0, (1-x), 1)]$$

$$\times [I_s + I_A \text{mid}(0, y, 1) + \kappa I_A \text{mid}(0, (1-y), 1) + I_V]$$

$$\psi = \beta_v S_v [I_S + I_A \text{mid}(0, y, 1) + \kappa I_A \text{mid}(0, (1-y), 1) + I_V].$$

$$\Lambda = \mu[S + S_v + E + E_V + I_S + I_V + I_A + I_Q + I_{QV} + I_H + I_{HV} + R]$$

$$+ \delta[I_S + I_Q] + \delta_h[I_H + \chi I_{HV}] + \delta_v[I_V + I_{QV}]$$

$$\Upsilon = I_S + I_V + I_H + I_{HV} + I_Q + I_{QV}.$$

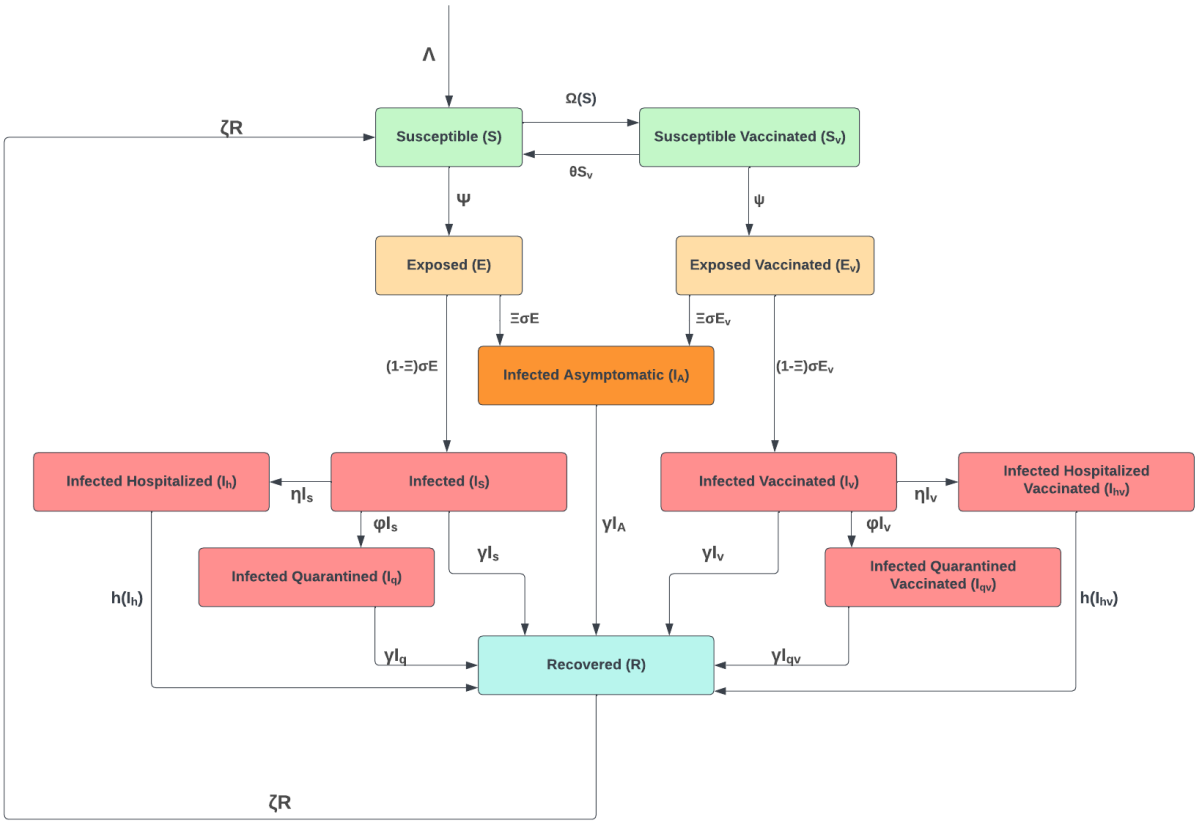

Figure 3.5: Flow Diagram of Be-SEIMR

We will call the expanded SEIR model, the Be-SEIMR model. Where Be stands for behavioral and M stands for medical intervention. In order to simulate the Be-SEIMR model, we will split the simulations into two parts. First we only introduce the hospitalization category, zeroing out any vaccination parameters, resulting in the following table of parameters:

Symbol	Source
$\eta = .00049$	CDC [15]
$r = \gamma = 0.167504$	
$H_c = 0.00152$	Block et al.[6]
$\delta_h = .2$	Dorjee et al. [12]

Table 3.3: Hospitalization parameter values for Covid-19.

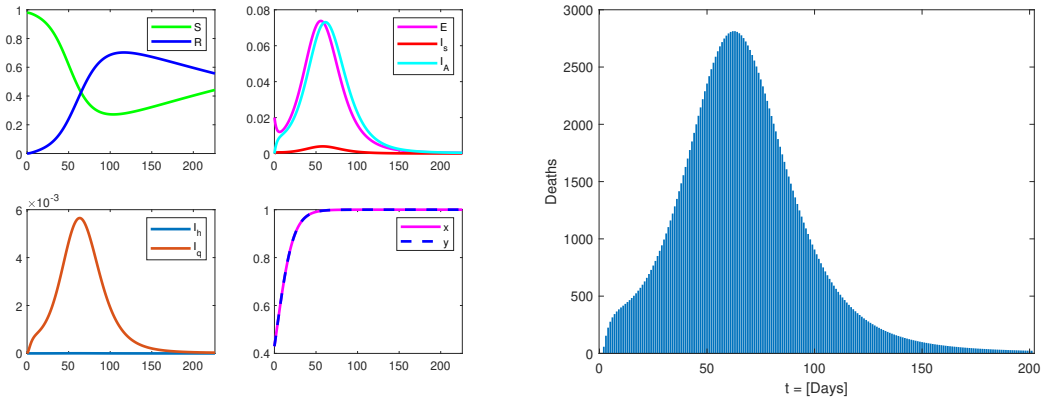

(a) Be-SEIMR model simulations. (b) Daily death toll with $N = 26446435$

Figure 3.6: Be-SEIMR simulations with $m_n = 0.8$, $m_a = 0.3$ and $k = 0.7$.

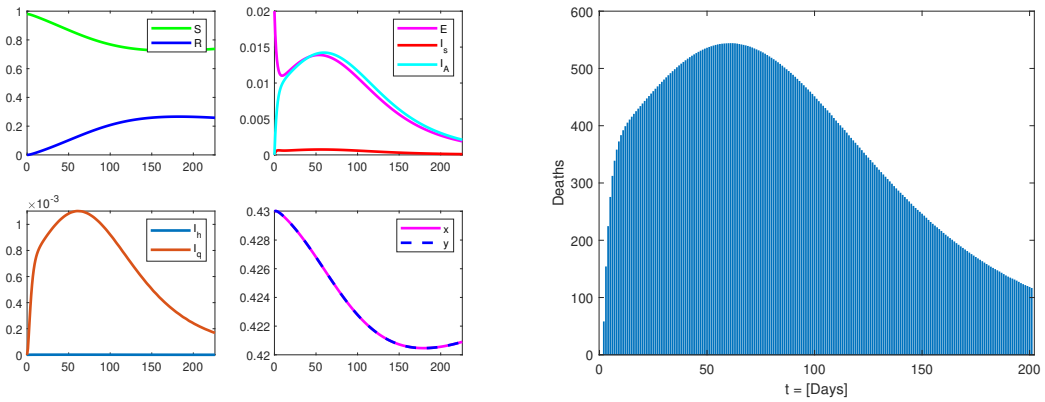

(a) Be-SEIMR model simulations. (b) Daily death toll with $N = 26446435$

Figure 3.7: Be-SEIMR simulations with $m_n = 0.9$, $m_a = 0.2$ and $k = 0.001$.

Finally we introduce vaccination into the model. We have the following parameters and their sources:

Symbol	Source
$\beta_v = \beta_n(1 - .635) = 0.13259793$	Braeye et al.[8]
$\theta = (\frac{1}{6})(\frac{1}{31}) = 0.0053763$	CDC [15]
$\omega = \frac{1698}{331900000} = 0.000005116$	CDC [15]
$S_c = \frac{2470}{331900000} = 0.00007442$	CDC [15]
$\chi = 1 - 0.896 = 0.104$	CDC [15]
$\delta_v = \chi(\delta_h) = 0.0208$	CDC [15]

Table 3.4: Vaccination parameter values for Covid-19.

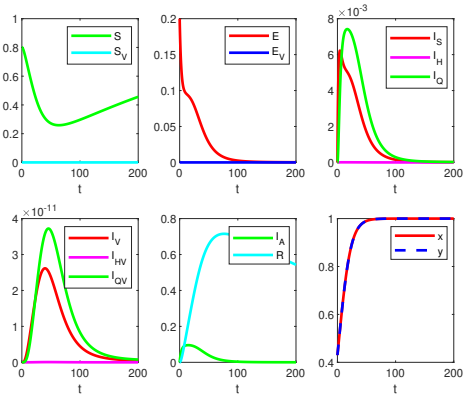

(a) Be-SEIMR model simulations.

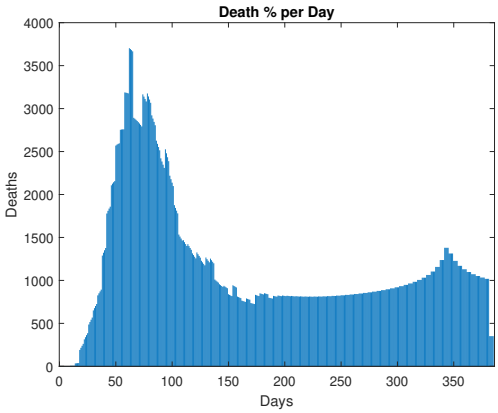

(b) Daily death toll with $N = 26446435$.

Figure 3.8: Be-SEIMR model simulations with $m_n = 0.8$, $m_a = 0.3$ and $k = 0.7$.

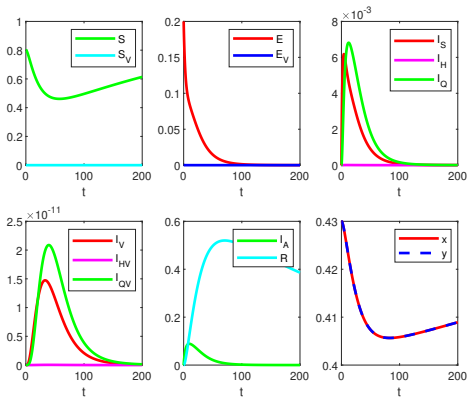

(a) Be-SEIMR model simulations.

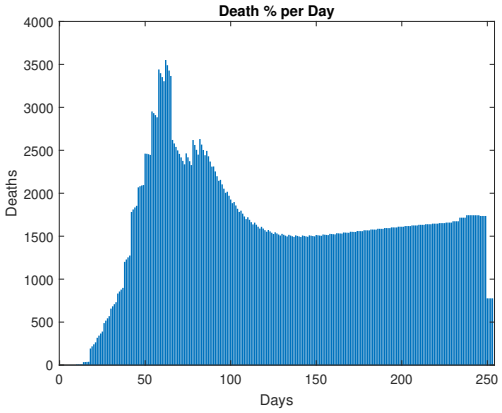

(b) Daily death toll with $N = 26446435$.

Figure 3.9: Be-SEIMR model simulations with $m_n = 0.9$, $m_a = 0.2$ and $k = 0.001$.

CHAPTER 4
ANALYSIS OF THE BE-SEIMR MODEL

4.1 Stability Analysis: Calculation of the Basic Reproduction Number

Here we will focus on determining the basic reproduction number for the Be-SEIMR model. A complication arises in determining the DFE for this model. Differing from the SEIR model and the other intermediate models found in the appendix, in this case, even when all infected compartments are set to zero, there remains the potential for individuals to transition between compartments S and S_V. The specific compartments in focus, following the removal of all infected compartments, are as follows:

$$\dot{S} = \Lambda - \Omega(S) + \theta S_V - \mu S$$
$$\dot{S}_V = \Omega(S) - \theta S_V - \mu S_V$$
$$\Omega(S) = \min(\omega S, \omega S_c)$$
$$\Lambda = \mu(S + S_V).$$

In order to find when these equations are in equilibrium, we need to find S, S_V such that

$$\Omega(S) - (\theta + \mu)S_V = 0$$
$$\Lambda - \Omega(S) + \theta S_V - \mu S = 0.$$

Since our total population is constant we can assume $S + S_V = 1$ and therefore we only have to solve when $\Omega(S) - (\theta + \mu)S_V = 0$ and then solve for S or S_V using the simpler equation $S + S_V = 1$. We substitute $S_V = 1 - S$ to give us the equation

$$\Omega(S) - (\theta + \mu)(1 - S) = 0 \Rightarrow \Omega(S) + (\theta + \mu)S = \mu + \theta.$$

Given the piecewise nature of $\Omega(S)$, we initially consider the scenario where $S \leq S_c$. In this context, we proceed to solve the equation for S, yielding:

$$\omega S + (\theta + \mu)S = \mu + \theta \Rightarrow (\omega + \theta + \mu)S = \mu + \theta \Rightarrow S = \frac{\mu + \theta}{\omega + \theta + \mu}$$

and therefore

$$1 - S = S_V = \frac{\omega}{\omega + \theta + \mu}.$$

So when $\frac{\mu+\theta}{\omega+\theta+\mu} = S \leq S_c$ we have a DFE of

$$\begin{aligned} x_l^* &= (E, E_v, I_S, I_V, I_A, I_H, I_{HV}, I_Q, I_{QV}, S, S_V, R, x, y) \\ &= \left(0, 0, 0, 0, 0, 0, 0, 0, 0, \frac{\mu + \theta}{\omega + \theta + \mu}, \frac{\omega}{\omega + \theta + \mu}, 0, 1, 1\right). \end{aligned}$$

Subsequently, let us proceed to the second case, where $S > S_c$. In this situation, $\Omega(S)$ takes on the value ωS_c. With this understanding, we can now proceed to solve the equation for V as follows:

$$\omega S_c - (\theta + \mu)S_V = 0 \Rightarrow -(\theta + \mu)S_V = -\omega S_c \Rightarrow S_V = \frac{\omega S_c}{\mu + \theta}$$

and therefore

$$1 - S_V = S = \frac{\mu + \theta - \omega S_c}{\mu + \theta}.$$

Then our DFE for when $\frac{\mu+\theta-\omega S_c}{\mu+\theta} = S > S_c$ is

$$\begin{aligned} x_g^* &= (E, E_v, I_S, I_V, I_A, I_H, I_{HV}, I_Q, I_{QV}, S, S_V, R, x, y) \\ &= \left(0, 0, 0, 0, 0, 0, 0, 0, 0, \frac{\mu + \theta - \omega S_c}{\mu + \theta}, \frac{\omega S_c}{\mu + \theta}, 0, 1, 1\right). \end{aligned}$$

Before advancing further in the process of determining $\mathcal{R}_0$, it is crucial to establish that these two cases are mutually exclusive and collectively exhaustive. In other words, there should be no possibility of overlap between these cases, nor can they both be false simultaneously. This ensures the consistency and validity of the subsequent analysis. We need to show that the two equilibrium cases

$$\frac{\mu + \theta}{\omega + \theta + \mu} = S \leq S_c, \tag{4.1}$$

$$\frac{\mu + \theta - \omega S_c}{\mu + \theta} = S > S_c \tag{4.2}$$

are mutually exclusive. First we will look at equation (4.1). Since $\omega, \theta \in \mathbb{R}^+ \cup \{0\}$ and $\mu \in \mathbb{R}^+$,

$$\frac{\mu + \theta}{\omega + \theta + \mu} \leq S_c \Rightarrow \mu + \theta \leq S_c(\omega + \theta + \mu).$$

Now if we take a look at equation (4.2), we have that

$$\frac{\mu + \theta - \omega S_c}{\mu + \theta} > S_c \Rightarrow \mu + \theta - \omega S_c > S_c(\mu + \theta) \Rightarrow \mu + \theta > S_c(\omega + \theta + \mu).$$

Hence, it can be concluded that equation (4.1) and equation (4.2) are mutually exclusive and furthermore, at least one of these equations must always hold true. The DFEs represented by x_l^* and x_g^* correspond to distinct real-world scenarios. The equilibrium x_l^* is relevant when the initial susceptible population $S_0 \leq S_c$. This circumstance arises when a vaccine has been present in a population for an extended period. Notably, due to the relationship $1 - S_0 = S_{V0}$, this configuration implies a larger proportion of the population has been vaccinated. Conversely, the equilibrium x_g^* is relevant when a vaccine is relatively new to a population or when vaccination has not been widespread. In the period immediately preceding the vaccine's release or during the introduction of the vaccine to a new region, x_g^* becomes the more plausible option to consider. This is due to the fact that the majority of individuals would not have been vaccinated yet. On the other hand, x_l^* becomes more significant in a region that has remained unaffected by the virus, and where preemptive vaccination has taken place. In such a scenario, allowing more time for people to receive the vaccine results in a higher proportion of the population being vaccinated, making x_l^* the more realistic equilibrium. Ultimately, the distinction between x_l^* and x_g^* allows for a nuanced understanding of various vaccination scenarios within the context of diseases like Covid-19. With the equilibrium points established for each scenario, we can now progress to calculate $\mathcal{R}_0$.

Before proceeding with the calculation of $\mathcal{R}_0$, it is imperative to acknowledge the inherent nonsmooth characteristics of the Be-SEIMR model. In calculating $\mathcal{R}_0$ for a compartmental epidemic model according to the methods by van den Driessche and

Watmough [39], the equations governing all state variables are expected to be at least twice continuous differentiable. In this context, the involvement of non-smooth mid and min functions in the equations for S, S_V, I_H, I_{HV}, and R renders them unsuitable for straightforward analysis. However, the nonsmooth min functions appearing in the vaccination and hospitalization compartments are locally smooth at the DFEs found above, since the DFEs are away from the nonsmooth points of these functions, and so remain smooth under perturbations from the DFEs, which is a requirement for a stability analysis. On the other hand, the mid functions present within Ψ and ψ, which are associated with the behavioral compartments, do experience nonsmoothness at the DFEs. Because of this, we proceed by setting $x = y = 1$, so that $\dot{x} = \dot{y} = 0$ and x and y are constants, for the remainder of this section, indicating that all individuals are opting for normal behavior. This corresponds to considering the SEIMR submodel of the full Be-SEIMR model, with game theory components from the model removed. In this scenario, the right-hand side functions of the submodel are all locally smooth (at least twice continuously differentiable) at the DFEs. Hence, we consider perturbations to all state variables except for x and y, which will remain constant and we may use the theory from van den Driessche and Watmough [39].

$$\mathcal{F} = \begin{bmatrix} \Psi \\ \psi \\ 0 \\ 0 \\ 0 \\ 0 \\ 0 \\ 0 \\ 0 \\ 0 \end{bmatrix}, \mathcal{V}^- = \begin{bmatrix} (\sigma+\mu)E \\ (\sigma+\mu)E_V \\ (\gamma+\eta+\phi+\mu+\delta)I_S \\ (\gamma++\eta+\phi+\mu+\delta_v)I_V \\ (\gamma+\mu)I_A \\ \min(rI_H,rH_c)+(\mu+\delta_h)I_H \\ \min(rI_{HV},rH_c)+(\mu+\chi\delta_h)I_{HV} \\ (\gamma+\mu+\delta)I_Q \\ (\gamma+\mu+\delta_v)I_{QV} \\ \min(\omega S,\omega S_c)+\mu S \\ (\theta+\mu)S_V \\ (\zeta+\mu)R \end{bmatrix}, \mathcal{V}^+ = \begin{bmatrix} 0 \\ 0 \\ (1-\Xi)\sigma E \\ (1-\Xi)\sigma E_V \\ \Xi\sigma[E+E_V] \\ \eta I_S \\ \eta I_V \\ \phi I_S \\ \phi I_V \\ \Lambda+\zeta R+\theta S_V \\ \min(\omega S,\omega S_c) \\ \gamma(I_S+I_A+I_Q+I_{QV}+I_V)+\min(rI_H,rH_c)+\min(rI_{HV},rH_c) \end{bmatrix}.$$

This results in

$$\mathcal{V} = \mathcal{V}^- - \mathcal{V}^+ = \begin{bmatrix} (\sigma+\mu)E \\ (\sigma+\mu)E_V \\ (\gamma+\eta+\phi+\mu+\delta)I_S-(1-\Xi)\sigma E \\ (\gamma+\eta+\phi+\mu+\delta_v)I_V-(1-\Xi)\sigma E_V \\ (\gamma+\mu)I_A-\Xi\sigma[E+E_V] \\ \min(rI_H,rH_c)+(\mu+\delta_h)I_H-\eta I_S \\ \min(rI_{HV},rH_c)+(\mu+\chi\delta_h)I_{HV}-\eta I_V \\ (\gamma+\mu+\delta)I_Q-\phi I_S \\ (\gamma+\mu+\delta_v)I_{QV}-\phi I_V \\ \min(\omega S,\omega S_c)+\mu S-\Lambda-\zeta R-\theta S_V \\ (\theta+\mu)S_V-\min(\omega S,\omega S_c) \\ (\zeta+\mu)R-\gamma(I_S+I_A+I_Q+I_{QV}+I_V)-\min(rI_H,rH_c)-\min(rI_{HV},rH_c) \end{bmatrix}.$$

Upon obtaining these results, the subsequent step involves calculating the Jacobians, evaluating them at the DFE, and subsequently deriving F and V. Since we are fixing $x = y = 1$, $\dot{x}$ and $\dot{y}$ will be set to 0, thus keeping their values in equilibrium. Similar to previous steps, our approach involves calculating the Jacobian matrices for both $\mathcal{F}$ and $\mathcal{V}$.

$\mathbf{J_x}\mathcal{F}$

$$= \begin{bmatrix} 0 & 0 & \beta_n S & \beta_n S & \beta_n S & \mathbf{0}_{1,9} \\ 0 & 0 & \beta_v S_v & \beta_v S_v & \beta_v S_v & \mathbf{0}_{1,9} \\ \mathbf{0}_{8,1} & \mathbf{0}_{8,1} & \mathbf{0}_{8,1} & \mathbf{0}_{8,1} & \mathbf{0}_{8,1} & \mathbf{0}_{8,9} \end{bmatrix}$$

$\mathbf{J_x}\mathcal{V}$

$$= \begin{bmatrix} \sigma+\mu & 0 & 0 & 0 & 0 & 0 & 0 & 0 & 0 & 0 & 0 & 0 & 0 & 0 \\ 0 & \sigma+\mu & 0 & 0 & 0 & 0 & 0 & 0 & 0 & 0 & 0 & 0 & 0 & 0 \\ -(1-\Xi)\sigma & 0 & \gamma+\eta+\phi+\mu+\delta & 0 & 0 & 0 & 0 & 0 & 0 & 0 & 0 & 0 & 0 & 0 \\ 0 & -(1-\Xi)\sigma & 0 & \gamma+\eta+\phi+\mu+\delta_v & 0 & 0 & 0 & 0 & 0 & 0 & 0 & 0 & 0 & 0 \\ -\Xi\sigma & -\Xi\sigma & 0 & 0 & \gamma+\mu & 0 & 0 & 0 & 0 & 0 & 0 & 0 & 0 & 0 \\ 0 & 0 & -\eta & 0 & 0 & \mu+\delta_h+r & 0 & 0 & 0 & 0 & 0 & 0 & 0 & 0 \\ 0 & 0 & 0 & -\eta & 0 & 0 & \mu+\chi\delta_h+r & 0 & 0 & 0 & 0 & 0 & 0 & 0 \\ 0 & 0 & -\phi & 0 & 0 & 0 & 0 & \gamma+\mu+\delta & 0 & 0 & 0 & 0 & 0 & 0 \\ 0 & 0 & 0 & -\phi & 0 & 0 & 0 & 0 & \gamma+\mu+\delta_v & 0 & 0 & 0 & 0 & 0 \\ -\mu & -\mu & -\mu-\delta & -\mu-\delta_v & -\mu & -\mu-\delta_h & -\mu-\chi\delta_h & -\mu-\delta & -\mu-\delta_v & \omega & -\theta & -\zeta & 0 & 0 \\ 0 & 0 & 0 & 0 & 0 & 0 & 0 & 0 & 0 & -\omega & \mu+\theta & 0 & 0 & 0 \\ 0 & 0 & -\gamma & -\gamma & -\gamma & -r & -r & -\gamma & -\gamma & 0 & 0 & \zeta+\mu & 0 & 0 \end{bmatrix}$$

Then we can plug in both equilibrium and reduce the Jacobians down to the 9×9 top left corner to obtain:

$$F(x_l^*) = \begin{bmatrix} 0 & 0 & \frac{\beta_n(\mu+\theta)}{\omega+\theta+\mu} & \frac{\beta_n(\mu+\theta)}{\omega+\theta+\mu} & \frac{\beta_n(\mu+\theta)}{\omega+\theta+\mu} & 0 & 0 & 0 & 0 \\ 0 & 0 & \frac{\beta_v\omega}{\omega+\theta+\mu} & \frac{\beta_v\omega}{\omega+\theta+\mu} & \frac{\beta_v\omega}{\omega+\theta+\mu} & 0 & 0 & 0 & 0 \\ 0 & 0 & 0 & 0 & 0 & 0 & 0 & 0 & 0 \\ 0 & 0 & 0 & 0 & 0 & 0 & 0 & 0 & 0 \\ 0 & 0 & 0 & 0 & 0 & 0 & 0 & 0 & 0 \\ 0 & 0 & 0 & 0 & 0 & 0 & 0 & 0 & 0 \\ 0 & 0 & 0 & 0 & 0 & 0 & 0 & 0 & 0 \\ 0 & 0 & 0 & 0 & 0 & 0 & 0 & 0 & 0 \\ 0 & 0 & 0 & 0 & 0 & 0 & 0 & 0 & 0 \end{bmatrix}, F(x_g^*) = \begin{bmatrix} 0 & 0 & \frac{\beta_n(\mu+\theta-\omega S_c)}{\mu+\theta} & \frac{\beta_n(\mu+\theta-\omega S_c)}{\mu+\theta} & \frac{\beta_n(\mu+\theta-\omega S_c)}{\mu+\theta} & 0 & 0 & 0 & 0 \\ 0 & 0 & \frac{\beta_v\omega S_c}{\mu+\theta} & \frac{\beta_v\omega S_c}{\mu+\theta} & \frac{\beta_v\omega S_c}{\mu+\theta} & 0 & 0 & 0 & 0 \\ 0 & 0 & 0 & 0 & 0 & 0 & 0 & 0 & 0 \\ 0 & 0 & 0 & 0 & 0 & 0 & 0 & 0 & 0 \\ 0 & 0 & 0 & 0 & 0 & 0 & 0 & 0 & 0 \\ 0 & 0 & 0 & 0 & 0 & 0 & 0 & 0 & 0 \\ 0 & 0 & 0 & 0 & 0 & 0 & 0 & 0 & 0 \\ 0 & 0 & 0 & 0 & 0 & 0 & 0 & 0 & 0 \\ 0 & 0 & 0 & 0 & 0 & 0 & 0 & 0 & 0 \end{bmatrix}$$

$$V(x_l^*) = V(x_g^*)$$

$$= \begin{bmatrix} \sigma+\mu & 0 & 0 & 0 & 0 & 0 & 0 & 0 & 0 \\ 0 & \sigma+\mu & 0 & 0 & 0 & 0 & 0 & 0 & 0 \\ -(1-\Xi)\sigma & 0 & \gamma+\eta+\phi+\mu+\delta & 0 & 0 & 0 & 0 & 0 & 0 \\ 0 & -(1-\Xi)\sigma & 0 & \gamma+\eta+\phi+\mu+\delta_v & 0 & 0 & 0 & 0 & 0 \\ -\Xi\sigma & -\Xi\sigma & 0 & 0 & \gamma+\mu & 0 & 0 & 0 & 0 \\ 0 & 0 & -\eta & 0 & 0 & \mu+\delta_h+r & 0 & 0 & 0 \\ 0 & 0 & 0 & -\eta & 0 & 0 & \mu+\chi\delta_h+r & 0 & 0 \\ 0 & 0 & -\phi & 0 & 0 & 0 & 0 & \gamma+\mu+\delta & 0 \\ 0 & 0 & 0 & -\phi & 0 & 0 & 0 & 0 & \gamma+\mu+\delta_v \end{bmatrix}.$$

Then we also can find V^{-1},

$$V^{-1}(x_l^*) = V^{-1}(x_g^*) = \begin{bmatrix} \frac{1}{a} & 0 & 0 & 0 & 0 & 0 & 0 & 0 & 0 \\ 0 & \frac{1}{a} & 0 & 0 & 0 & 0 & 0 & 0 & 0 \\ \frac{(1-\Xi)\sigma}{ab} & 0 & \frac{1}{b} & 0 & 0 & 0 & 0 & 0 & 0 \\ 0 & \frac{(1-\Xi)\sigma}{ac} & 0 & \frac{1}{c} & 0 & 0 & 0 & 0 & 0 \\ \frac{\Xi\sigma}{a(\gamma+\mu)} & \frac{\Xi\sigma}{a(\gamma+\mu)} & 0 & 0 & \frac{1}{\gamma+\mu} & 0 & 0 & 0 & 0 \\ \frac{(1-\Xi)\sigma\eta}{ab(\mu+\delta_h+r)} & 0 & \frac{\eta}{b(\mu+\delta_h+r)} & 0 & 0 & \frac{1}{\mu+\delta_h+r} & 0 & 0 & 0 \\ 0 & \frac{(1-\Xi)\sigma\eta}{ac(\mu+\chi\delta_h+r)} & 0 & \frac{\eta}{c(\mu+\chi\delta_h+r)} & 0 & 0 & \frac{1}{\mu+\chi\delta_h+r} & 0 & 0 \\ \frac{(1-\Xi)\sigma\phi}{ab(\gamma+\mu+\delta)} & 0 & \frac{\phi}{b(\gamma+\mu+\delta)} & 0 & 0 & 0 & 0 & \frac{1}{\gamma+\mu+\delta} & 0 \\ 0 & \frac{(1-\Xi)\sigma\phi}{ac(\gamma+\mu+\delta_v)} & 0 & \frac{\phi}{c(\gamma+\mu+\delta_v)} & 0 & 0 & 0 & 0 & \frac{1}{\gamma+\mu+\delta_v} \end{bmatrix}$$

with the following,

$$a = \sigma + \mu, \qquad b = \gamma + \eta + \phi + \mu + \delta, \qquad c = \gamma + \eta + \phi + \mu + \delta_v.$$

We can also find,

$$FV^{-1}(x_l^*)$$

$$= \frac{1}{\omega+\theta+\mu} \begin{bmatrix} \frac{\beta_n d(1-\Xi)\sigma}{(\sigma+\mu)b} + \frac{\beta_n d\Xi\sigma}{(\sigma+\mu)(\gamma+\mu)} & \frac{\beta_n d(1-\Xi)\sigma}{(\sigma+\mu)(\gamma+\eta+\phi+\mu+\delta_v)} + \frac{\beta_n d\Xi\sigma}{(\sigma+\mu)(\gamma+\mu)} & \frac{\beta_n d}{\gamma+\eta+\phi+\mu+\delta} & \frac{\beta_n d}{\gamma+\eta+\phi+\mu+\delta_v} & \frac{\beta_n d}{\gamma+\mu} & \mathbf{0}_{1,4} \\ \frac{\beta_v\omega(1-\Xi)\sigma}{(\sigma+\mu)b} + \frac{\beta_v\omega\Xi\sigma}{(\sigma+\mu)(\gamma+\mu)} & \frac{\beta_v\omega(1-\Xi)\sigma}{(\sigma+\mu)(\gamma+\eta+\phi+\mu+\delta_v)} + \frac{\beta_v\omega\Xi\sigma}{(\sigma+\mu)(\gamma+\mu)} & \frac{\beta_v\omega}{\gamma+\eta+\phi+\mu+\delta} & \frac{\beta_v\omega}{\gamma+\eta+\phi+\mu+\delta_v} & \frac{\beta_v\omega}{\gamma+\mu} & \mathbf{0}_{1,4} \\ \mathbf{0}_{7,1} & \mathbf{0}_{7,1} & \mathbf{0}_{7,1} & \mathbf{0}_{7,1} & \mathbf{0}_{7,1} & \mathbf{0}_{7,4} \end{bmatrix}$$

with the following,

$$b = \gamma + \eta + \phi + \mu + \delta, \qquad d = \mu + \theta.$$

We can also find,

$$FV^{-1}(x_g^*)$$
$$= \frac{1}{\mu+\theta}\begin{bmatrix} \frac{\beta_n g(1-\Xi)\sigma}{(\sigma+\mu)b} + \frac{\beta_n g \Xi \sigma}{(\sigma+\mu)(\gamma+\mu)} & \frac{\beta_n g(1-\Xi)\sigma}{(\sigma+\mu)c} + \frac{\beta_n g \Xi \sigma}{(\sigma+\mu)(\gamma+\mu)} & \frac{\beta_n g}{\gamma+\eta+\phi+\mu+\delta} & \frac{\beta_n g}{c} & \frac{\beta_n g}{\gamma+\mu} & \mathbf{0}_{1,4} \\ \frac{\beta_v \omega S_c(1-\Xi)\sigma}{(\sigma+\mu)b} + \frac{\beta_v \omega S_c \Xi \sigma}{(\sigma+\mu)(\gamma+\mu)} & \frac{\beta_v \omega S_c(1-\Xi)\sigma}{(\sigma+\mu)c} + \frac{\beta_v \omega S_c \Xi \sigma}{(\sigma+\mu)(\gamma+\mu)} & \frac{\beta_v \omega S_c}{\gamma+\eta+\phi+\mu+\delta} & \frac{\beta_v \omega S_c}{c} & \frac{\beta_v \omega S_c}{\gamma+\mu} & \mathbf{0}_{1,4} \\ \mathbf{0}_{7,1} & \mathbf{0}_{7,1} & \mathbf{0}_{7,1} & \mathbf{0}_{7,1} & \mathbf{0}_{7,1} & \mathbf{0}_{7,4} \end{bmatrix}$$

with the following,

$$b = \gamma + \eta + \phi + \mu + \delta, \qquad c = \gamma + \eta + \phi + \mu + \delta_v, \qquad g = \mu + \theta - \omega S_c$$

Since $FV^{-1}(x_l^*)$ and $FV^{-1}(x_g^*)$ are not upper triangular we need to find the eigenvalues. To make things easier we will generalize both $FV^{-1}(x_l^*)$ and $FV^{-1}(x_g^*)$ as

$$\begin{bmatrix} a & b & c & d & e & 0 & 0 & 0 & 0 \\ f & g & h & i & j & 0 & 0 & 0 & 0 \\ 0 & 0 & 0 & 0 & 0 & 0 & 0 & 0 & 0 \\ \vdots & \vdots & \vdots & \vdots & \vdots & \vdots & \vdots & \vdots & \vdots \\ 0 & 0 & 0 & 0 & 0 & 0 & 0 & 0 & 0 \end{bmatrix}$$

where a through j are placeholders. Utilizing the placeholder values we get the characteristic polynomial:

$$-\lambda^7(ag - a\lambda - bf - g\lambda + \lambda^2).$$

We can see that when we set this to zero, we have that $\lambda = 0$, with algebraic multiplicity seven, or

$$ag - a\lambda - bf - g\lambda + \lambda^2 = 0 \Rightarrow \lambda^2 - (g+a)\lambda + (ag - bf) = 0.$$

From here we can solve with the quadratic equation, giving us

$$\begin{aligned}\lambda &= \frac{(g+a) \pm \sqrt{(g+a)^2 - 4(ag-bf)}}{2} \\ &= \frac{a+g \pm \sqrt{g^2+2ag+a^2-4ag+4bf}}{2} \\ &= \frac{a+g \pm \sqrt{g^2+a^2-2ag+4bf}}{2} \\ &= \frac{a+g \pm \sqrt{(g-a)^2+4bf}}{2}.\end{aligned}$$

We can then take the spectral radius

$$\begin{aligned}\rho(FV^{-1}(x_l^*)) &= \frac{a+g+\sqrt{(g-a)^2+4bf}}{2} \\ \rho(FV^{-1}(x_g^*)) &= \frac{a+g+\sqrt{(g-a)^2+4bf}}{2},\end{aligned}$$

where for x_l^* we have that

$$\begin{aligned}a &= \frac{\beta_n(\mu+\theta)(1-\Xi)\sigma}{(\sigma+\mu)(\gamma+\eta+\phi+\mu+\delta)} + \frac{\beta_n(\mu+\theta)\Xi\sigma}{(\sigma+\mu)(\gamma+\mu)} \\ b &= \frac{\beta_n(\mu+\theta)(1-\Xi)\sigma}{(\sigma+\mu)(\gamma+\eta+\phi+\mu+\delta_v)} + \frac{\beta_n(\mu+\theta)\Xi\sigma}{(\sigma+\mu)(\gamma+\mu)} \\ f &= \frac{\beta_v\omega(1-\Xi)\sigma}{(\sigma+\mu)(\gamma+\eta+\phi+\mu+\delta)} + \frac{\beta_v\omega\Xi\sigma}{(\sigma+\mu)(\gamma+\mu)} \\ g &= \frac{\beta_v\omega(1-\Xi)\sigma}{(\sigma+\mu)(\gamma+\eta+\phi+\mu+\delta_v)} + \frac{\beta_v\omega\Xi\sigma}{(\sigma+\mu)(\gamma+\mu)},\end{aligned}$$

and for x_g^* the placeholders as,

$$\begin{aligned}a &= \frac{\beta_n(\mu+\theta-\omega S_c)(1-\Xi)\sigma}{(\sigma+\mu)(\gamma+\eta+\phi+\mu+\delta)} + \frac{\beta_n(\mu+\theta-\omega S_c)\Xi\sigma}{(\sigma+\mu)(\gamma+\mu)} \\ b &= \frac{\beta_n(\mu+\theta-\omega S_c)(1-\Xi)\sigma}{(\sigma+\mu)(\gamma+\eta+\phi+\mu+\delta_v)} + \frac{\beta_n(\mu+\theta-\omega S_c)\Xi\sigma}{(\sigma+\mu)(\gamma+\mu)} \\ f &= \frac{\beta_v\omega S_c(1-\Xi)\sigma}{(\sigma+\mu)(\gamma+\eta+\phi+\mu+\delta)} + \frac{\beta_v\omega S_c\Xi\sigma}{(\sigma+\mu)(\gamma+\mu)} \\ g &= \frac{\beta_v\omega S_c(1-\Xi)\sigma}{(\sigma+\mu)(\gamma+\eta+\phi+\mu+\delta_v)} + \frac{\beta_v\omega S_c\Xi\sigma}{(\sigma+\mu)(\gamma+\mu)}.\end{aligned}$$

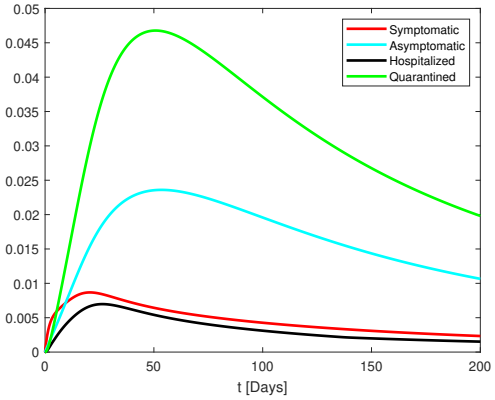

(a) In this figure $\mathcal{R}_0 = 5.8290$.

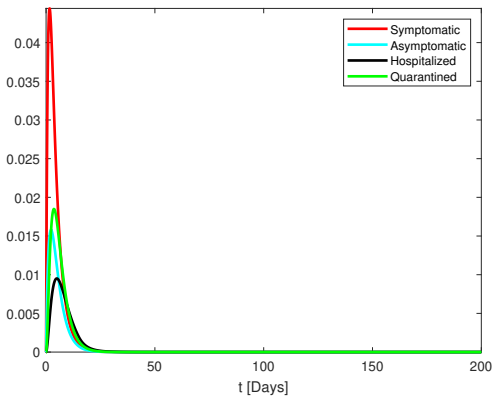

(b) In this figure $\mathcal{R}_0 = 0.2432$.

Figure 4.1: Simulations of the SEIMR model with varying $\mathcal{R}_0$ given x_l^*.

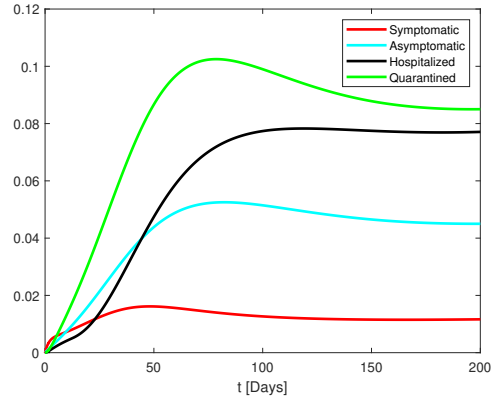

(a) In this figure $\mathcal{R}_0 = 5.2976$.

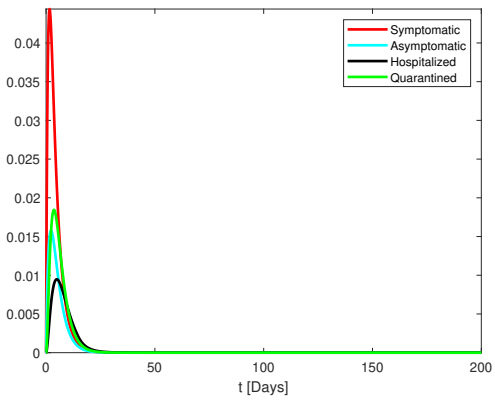

(b) In this figure $\mathcal{R}_0 = 0.4217$.

Figure 4.2: Simulations of the SEIMR model with varying $\mathcal{R}_0$ given x_g^*.

In Figures 4.1a and 4.1b, $\frac{\mu+\theta-\omega S_c}{\mu+\theta} > S_c$ and in Figures 4.2a and 4.2b, $\frac{\mu+\theta-\omega S_c}{\mu+\theta} \leq S_c$. Further in Figure 4.1a, we have that $\beta_n = 5$, $\beta_v = 2$, $\mu = 0.005$, $\theta = 0.2$, $\Xi = 0.2$, $\sigma = 0.02$, $\gamma = 0.03$, $\eta = 0.2$, $\phi = 0.3$, $\delta = 0.006$, $\omega = 0.4$ and $S_c = 0.1$. In Figure 4.1b, we have that $\beta_n = 0.5$, $\beta_v = 0.2$, $\mu = 0.001$, $\theta = 0.5$, $\Xi = 0.2$, $\sigma = 0.5$, $\gamma = 0.5$, $\eta = 0.1$, $\phi = 0.3$, $\delta = 0.005$, $\omega = 0.4$ and $S_c = 0.5$. In Figure 4.2a, we have that $\beta_n = 5$, $\beta_v = 2$, $\mu = 0.005$, $\theta = 0.02$, $\Xi = 0.2$, $\sigma = 0.02$, $\gamma = 0.03$, $\eta = 0.2$, $\phi = 0.3$, $\delta = 0.006$, $\omega = 0.4$ and $S_c = 0.5$. In Figure 4.2b, $\beta_n = 0.5$, $\beta_v = 0.2$, $\mu = 0.001$, $\theta = 0.5$, $\Xi = 0.2$, $\sigma = 0.5$, $\gamma = 0.5$, $\eta = 0.1$,

$\phi = 0.3$, $\delta = 0.005$, $\omega = 0.4$ and $S_c = 0.7$. As expected the disease dies out when $\mathcal{R}_0 < 1$ and persists when $\mathcal{R}_0 > 1$.

4.2 Sensitivity Analysis: Derivation of the Sensitivity Equations

We will now embark on the sensitivity analysis to ascertain the parameters that wield the greatest influence within the Be-SEIMR model in equation (3.6). We will designate the reference parameters as follows:

$$\mathbf{p}^* = (\beta_n^*, \beta_a^*, \beta_v^*, \theta^*, \sigma^*, \Xi^*, \eta^*, \phi^*, \gamma^*, \zeta^*, \omega^*, r^*, k^*, m_a^*, m_n^*, S_0^*, E_0^*, x_0^*, y_0^*). \tag{4.3}$$

Additionally, we will consider the following to be constants:

$$\mathbf{C} = (\kappa, \mu, \delta, \delta_h, \delta_v, \chi, \rho, \alpha, H_c, S_c, S_{V0}, E_{V0}, I_{S0}, I_{V0}, I_{A0}, I_{H0}, I_{HV0}, I_{Q0}, I_{QV0}, R_0). \tag{4.4}$$

We also define,

$$\mathbf{x} = (S, S_V, E, E_V, I_S, I_V, I_A, I_H, I_{HV}, I_Q, I_{QV}, R, x, y),$$
$$\mathbf{f} = (f_1, f_2, f_3, \ldots, f_{13}, f_{14}).$$

Where $\mathbf{f}$ is the right-hand side. We also choose directions matrix

$$\mathbf{M} = \begin{bmatrix} m_{1,1} & \cdots & m_{1,19} \\ \vdots & \ddots & \vdots \\ m_{19,1} & \cdots & m_{19,19} \end{bmatrix} \in \mathbb{R}^{19\times 19}.$$

Given the presence of a total of 14 compartments in the Be-SEIMR model, we highlight the derivation of sensitivity equations associated with five. The remaining nine compartments require similar calculations; however, their details will be provided in the appendix. Let us commence by examining the susceptibility compartment, denoted as S. We will choose

$$\dot{S} = O_S(\mathbf{p}, \mathbf{x}) + W_S(\mathbf{p}, \mathbf{x})$$
$$O_S(\mathbf{p}, \mathbf{x}) = \Lambda + \theta S_V + \zeta R - \mu S,$$
$$W_S(\mathbf{p}, \mathbf{x}) = -\Omega - \Psi$$

Here, O_S represents the collection of smooth functions in the compartment S, while W_S represents the non-differentiable, nonsmooth functions. Given the smooth nature of O_S, the calculation of directional derivatives becomes straightforward:

$$
\begin{aligned}
O'_S(\mathbf{p}^*, \mathbf{x}^*; (M, \mathbf{S_x})) &= JO_S(\mathbf{p}^*, \mathbf{x}^*) \begin{bmatrix} M \\ \mathbf{S_x} \end{bmatrix} \\
&= \begin{bmatrix} J_{\mathbf{p}} O_S(\mathbf{p}^*, \mathbf{x}^*) & | & J_{\mathbf{x}} O(\mathbf{p}^*, \mathbf{x}^*) \end{bmatrix} \begin{bmatrix} M \\ \mathbf{S_x} \end{bmatrix} \\
&= \begin{bmatrix} \mathbf{0}_{1,3} & S_V^* & \mathbf{0}_{1,5} & R^* & \mathbf{0}_{1,9} & | & 0 & \mu+\theta^* & \mu & \mu & \mu+\delta & \mu+\delta_v & \mu & \mu+\delta_h & \mu+\delta_h\chi & \mu+\delta & \mu+\delta_v & \mu+\zeta^* & 0 & 0 \end{bmatrix} \begin{bmatrix} \mathbf{M} \\ \mathbf{S_x} \end{bmatrix} \\
&= \begin{bmatrix} S_V^* m_{4,1} + R^* m_{10,1} + (\mu+\theta^*) S_{S_V}^{\beta_n} + \mu(S_E^{\beta_n} + S_{E_V}^{\beta_n} + S_{I_A}^{\beta_n}) + (\mu+\delta)(S_{I_S}^{\beta_n} + S_{I_Q}^{\beta_n}) \\ S_V^* m_{4,2} + R^* m_{10,2} + (\mu+\theta^*) S_{S_V}^{\beta_a} + \mu(S_E^{\beta_a} + S_{E_V}^{\beta_a} + S_{I_A}^{\beta_a}) + (\mu+\delta)(S_{I_S}^{\beta_a} + S_{I_Q}^{\beta_a}) \\ \vdots \\ S_V^* m_{4,19} + R^* m_{10,19} + (\mu+\theta^*) S_{S_V}^{y_0} + \mu(S_E^{y_0} + S_{E_V}^{y_0} + S_{I_A}^{y_0}) + (\mu+\delta)(S_{I_S}^{y_0} + S_{I_Q}^{y_0}) \end{bmatrix}^T \\
&+ \begin{bmatrix} (\mu+\delta_v)(S_{I_V}^{\beta_n} + S_{I_{QV}}^{\beta_n}) + (\mu+\delta_h)(S_{I_H}^{\beta_n} + \chi S_{I_{HV}}^{\beta_n}) + (\mu+\zeta^*) S_R^{\beta_n} \\ (\mu+\delta_v)(S_{I_V}^{\beta_a} + S_{I_{QV}}^{\beta_a}) + (\mu+\delta_h)(S_{I_H}^{\beta_a} + \chi S_{I_{HV}}^{\beta_a}) + (\mu+\zeta^*) S_R^{\beta_a} \\ \vdots \\ (\mu+\delta_v)(S_{I_V}^{y_0} + S_{I_{QV}}^{y_0}) + (\mu+\delta_h)(S_{I_H}^{y_0} + \chi S_{I_{HV}}^{y_0}) + (\mu+\zeta^*) S_R^{y_0} \end{bmatrix}^T .
\end{aligned}
$$

In the case of W_S, our approach involves deriving LD-derivatives of Ω and Ψ individually and, subsequently combining them to yield the final result for the nonsmooth sensitivity equation. Let us initiate by examining the LD-derivative of Ω.

$$
\begin{aligned}
\Omega'(\mathbf{p}^*, \mathbf{x}^*; (M, \mathbf{S_x})) &= \mathrm{slmin}([\omega^* \mathrm{S}^* \ \mathrm{J}_{\mathbf{p}} \omega^* \mathrm{S}^* \mathrm{M} + \mathrm{J}_{\mathbf{x}} \omega^* \mathrm{S}^* \mathbf{S_x}], [\omega^* \mathrm{S_c} \ \mathrm{J}_{\mathbf{p}} \omega^* \mathrm{S_c} \mathrm{M} + \mathrm{J}_{\mathbf{x}} \omega^* \mathrm{S_c} \mathbf{S_x}]) \\
&= \mathrm{slmin}([\omega^* \mathrm{S}^* \ \mathrm{SM}_\omega + \omega^* \mathrm{S_S}], [\omega^* \mathrm{S_c} \ \mathrm{S_c M}_\omega]) \\
&= \mathrm{slmin} \left(\begin{bmatrix} \omega^* S^* \\ S^* m_{11,1} + \omega^* S_S^\beta \\ \vdots \\ S m_{11,19} + \omega^* S_S^{y_0} \end{bmatrix}^{\mathrm{T}}, \begin{bmatrix} \omega^* S_c \\ S_c m_{11,1} \\ \vdots \\ S_c m_{11,19} \end{bmatrix}^{\mathrm{T}} \right)
\end{aligned}
$$

As Ψ involves a substantial sum of terms, we break it down into the following components:

$$\Psi = I_S\beta_n SM_x + I_A M_y \beta_n SM_x + \kappa I_A M_{1-y}\beta_n SM_x + I_V \beta_n SM_x$$
$$+ I_S\beta_a SM_{1-x} + I_A M_y \beta_a SM_{1-x} + \kappa I_A M_{1-y}\beta_a SM_{1-x} + I_V \beta_a SM_{1-x} = \sum_{i=1}^{8} \Psi_i.$$

where

$$\Psi_1 = I_S\beta_n SM_x$$
$$\Psi_2 = I_A M_y \beta_n SM_x$$
$$\Psi_3 = \kappa I_A M_{1-y}\beta_n SM_x$$
$$\Psi_4 = I_V \beta_n SM_x$$
$$\Psi_5 = I_S\beta_a SM_{1-x}$$
$$\Psi_6 = I_A M_y \beta_a SM_{1-x}$$
$$\Psi_7 = \kappa I_A M_{1-y}\beta_a SM_{1-x}$$
$$\Psi_8 = I_V \beta_a SM_{1-x}$$

To simplify things, we will utilize shorthand notation, where $\Psi_i' = \Psi_i'(\mathbf{p}, \mathbf{x}; (M, \mathbf{S_x}))$.

$$\Psi_1 = I_S^*\beta_n^* S^* M_x$$
$$\Rightarrow \Psi_1' = I_S^{*\prime}\beta_n^* S^* M_x + I_S^*\beta_n^{*\prime} S^* M_x + I_S^*\beta_n^* S^{*\prime} M_x + I_S^*\beta_n^* S^* M_x'$$
$$= \begin{bmatrix} \mathbf{0}_{23,1} \\ \beta_n^* S^* M_x \\ \mathbf{0}_{9,1} \end{bmatrix} \mathbf{S_x} + \begin{bmatrix} I_S^* S^* M_x \\ \mathbf{0}_{32,1} \end{bmatrix} M + \begin{bmatrix} \mathbf{0}_{19,1} \\ I_S^*\beta_n^* M_x \\ \mathbf{0}_{13,1} \end{bmatrix} S_S +$$
$$I_S^*\beta_n^* S^* \text{slmid}([\mathbf{0}_{1,20}], [\text{x}^*, \text{S}_\text{x}], [1, \mathbf{0}_{1,19}])$$
$$= \begin{bmatrix} \beta_n^* S^* M_x S_{I_S}^{\beta_n} + I_S^* S^* M_x m_{1,1} + I_S^*\beta_n^* M_x S_S^{\beta_n} \\ \vdots \\ \beta_n^* S^* M_x S_{I_S}^{y_0} + I_S^* S^* M_x m_{1,19} + I_S^*\beta_n^* M_x S_S^{y_0} \end{bmatrix}^T +$$
$$I_S^*\beta_n^* S^* \text{slmid}([\mathbf{0}_{1,20}], [\text{x}^*, \text{S}_\text{x}], [1, \mathbf{0}_{1,19}])$$

We also have that

$$
\begin{aligned}
&\Psi_2 = I_A^* M_y \beta_n^* S^* M_x \\
\Rightarrow\ &\Psi_2' = I_A^{*\prime} M_y \beta_n^* S^* M_x + I_A^* M_y' \beta_n^* S^* M_x + I_A^* M_y \beta_n^{*\prime} S^* M_x + I_A^* M_y \beta_n^* S^{*\prime} M_x + I_A^* M_y \beta_n^* S^* M_x' \\
&= \begin{bmatrix} \mathbf{0}_{25,1} \\ M_y \beta_n^* S^* M_x \\ \mathbf{0}_{7,1} \end{bmatrix} \mathbf{S_x} + I_A^* \beta_n^* S^* M_x \text{slmid}([\mathbf{0}_{1,20}], [\text{y}^*, \text{S}_\text{y}], [1, \mathbf{0}_{1,19}]) + \\
&\begin{bmatrix} I_A^* M_y S^* M_x \\ \mathbf{0}_{32,1} \end{bmatrix} M + \begin{bmatrix} \mathbf{0}_{19,1} \\ I_A^* M_y \beta_n^* M_x \\ \mathbf{0}_{13,1} \end{bmatrix} \mathbf{S_x} + I_A^* M_y \beta_n^* S^* \text{slmid}([\mathbf{0}_{1,20}], [\text{x}^*, \text{S}_\text{x}], [1, \mathbf{0}_{1,19}]) \\
&= \begin{bmatrix} I_A^* M_y S^* M_x m_{1,1} + I_A^* M_y \beta_n^* M_x S_S^{\beta_n} + M_y \beta_n^* S^* M_x S_{I_A}^{\beta_n} \\ \vdots \\ I_A^* M_y S^* M_x m_{1,19} + I_A^* M_y \beta_n^* M_x S_S^{y_0} + M_y \beta_n^* S^* M_x S_{I_A}^{y_0} \end{bmatrix}^T + \\
&I_A^* M_y \beta_n^* S^* \text{slmid}([\mathbf{0}_{1,20}], [\text{x}^*, \text{S}_\text{x}], [1, \mathbf{0}_{1,19}]) + \text{I}_\text{A}^* \beta_\text{n}^* \text{S}^* \text{M}_\text{x} \text{slmid}([\mathbf{0}_{1,20}], [\text{y}^*, \text{S}_\text{y}], [1, \mathbf{0}_{1,19}]).
\end{aligned}
$$

We also have that

$$
\begin{aligned}
&\Psi_3 = \kappa I_A^* M_{1-y} \beta_n^* S^* M_x \\
&\quad \Rightarrow \Psi_3' \\
&\quad = \kappa I_A^{*\prime} M_{1-y} \beta_n^* S^* M_x + \kappa I_A^* M_{1-y}' \beta_n^* S^* M_x + \kappa I_A^* M_{1-y} \beta_n^{*\prime} S^* M_x + \kappa I_A^* M_{1-y} \beta_n^* S^{*\prime} M_x + \\
&\kappa I_A^* M_{1-y} \beta_n^* S^* M_x' \\
&\quad = \begin{bmatrix} \mathbf{0}_{25,1} \\ \kappa M_{1-y} \beta_n^* S^* M_x \\ \mathbf{0}_{7,1} \end{bmatrix} \mathbf{S_x} + \kappa I_A^* \beta_n^* S^* M_x \text{slmid}([\mathbf{0}_{1,20}], [1 - \text{y}^*, -\text{S}_\text{y}], [1, \mathbf{0}_{1,19}]) + \\
&\begin{bmatrix} \kappa I_A^* M_{1-y} S^* M_x \\ \mathbf{0}_{32,1} \end{bmatrix} \mathbf{M} + \begin{bmatrix} \mathbf{0}_{19,1} \\ \kappa I_A^* M_{1-y} \beta_n^* M_x \\ \mathbf{0}_{13,1} \end{bmatrix} S_S + \kappa I_A^* M_{1-y} \beta_n^* S \text{slmid}([\mathbf{0}_{1,20}], [\text{x}^*, \text{S}_\text{x}], [1, \mathbf{0}_{1,19}]) \\
&\quad = \begin{bmatrix} \kappa I_A^* M_{1-y} S^* M_x m_{1,1} + \kappa I_A^* M_{1-y} \beta_n^* M_x S_S^\beta + \kappa M_{1-y} \beta_n^* S^* M_x S_{I_A}^\beta \\ \vdots \\ \kappa I_A^* M_{1-y} S^* M_x m_{1,19} + \kappa I_A^* M_{1-y} \beta_n^* M_x S_S^{y_0} + \kappa M_{1-y} \beta_n^* S^* M_x S_{I_A}^{y_0} \end{bmatrix}^T + \\
&\kappa I_A^* \beta_n^* S^* M_x \text{slmid}([\mathbf{0}_{1,20}], [1 - \text{y}^*, -\text{S}_\text{y}], [1, \mathbf{0}_{1,19}]) + \\
&\kappa I_A^* M_{1-y} \beta_n^* S^* \text{slmid}([\mathbf{0}_{1,20}], [\text{x}^*, \text{S}_\text{x}], [1, \mathbf{0}_{1,19}])
\end{aligned}
$$

Following the illustration of the process for the initial three Ψ_i terms, we will streamline the presentation by omitting the intermediary steps and proceeding directly to the

conclusions. The outcome is as follows:

$$\Psi_4' = \begin{bmatrix} I_V^* S^* M_x m_{1,1} + I_V^* \beta_n^* M_x S_S^{\beta} + \beta_n^* S^* M_x S_{I_V}^{\beta} \\ \vdots \\ I_V^* S^* M_x m_{1,19} + I_V^* \beta_n^* M_x S_S^{y_0} + \beta_n^* S^* M_x S_{I_V}^{y_0} \end{bmatrix}^T + I_V^* \beta_n^* S^* \text{slmid}([\mathbf{0}_{1,20}], [\text{x}^*, \text{S}_\text{x}], [1, \mathbf{0}_{1,19}])$$

$$\Psi_5' = \begin{bmatrix} I_S^* S^* M_{1-x} m_{2,1} + I_S^* \beta_a^* M_{1-x} S_S^{\beta_n} + \beta_a^* S^* M_{1-x} S_{I_S}^{\beta} \\ \vdots \\ I_S^* S^* M_{1-x} m_{2,19} + I_S^* \beta_a^* M_{1-x} S_S^{y_0} + \beta_a^* S^* M_{1-x} S_{I_S}^{y_0} \end{bmatrix}^T +$$

$$I_S^* \beta_a^* S^* \text{slmid}([\mathbf{0}_{1,20}], [1 - \text{x}^*, -\text{S}_\text{x}], [1, \mathbf{0}_{1,19}])$$

and

$$\Psi_6' = \begin{bmatrix} I_A^* M_y S^* M_{1-x} m_{2,1} + I_A^* M_y \beta_a^* M_{1-x} S_S^{\beta_n} + M_y \beta_a^* S^* M_{1-x} S_{I_A}^{\beta_n} \\ \vdots \\ I_A^* M_y S^* M_{1-x} m_{2,19} + I_A^* M_y \beta_a^* M_{1-x} S_S^{y_0} + M_y \beta_a^* S^* M_{1-x} S_{I_A}^{y_0} \end{bmatrix}^T +$$

$$I_A^* \beta_a^* S^* M_{1-x} \text{slmid}([\mathbf{0}^{20}], [\text{y}^*, \text{S}_\text{y}], [1, \mathbf{0}_{1,19}]) + \text{I}_\text{A}^* \text{M}_\text{y} \beta_\text{a}^* \text{S}^* \text{slmid}([\mathbf{0}_{1,20}], [1 - \text{x}^*, -\text{S}_\text{x}], [1, \mathbf{0}_{1,19}])$$

$$\Psi_7' = \begin{bmatrix} \kappa I_A^* M_{1-y} S^* M_{1-x} m_{2,1} + \kappa I_A^* M_{1-y} \beta_a^* M_{1-x} S_S^{\beta_n} + \kappa M_{1-y} \beta_a^* S^* M_{1-x} S_{I_A}^{\beta_n} \\ \vdots \\ \kappa I_A^* M_{1-y} S^* M_{1-x} m_{2,19} + \kappa I_A^* M_{1-y} \beta_a^* M_{1-x} S_S^{y_0} + \kappa M_{1-y} \beta_a^* S^* M_{1-x} S_{I_A}^{y_0} \end{bmatrix}^T +$$

$$\kappa I_A^* \beta_a^* S^* M_{1-x} \text{slmid}([\mathbf{0}_{1,20}], [1 - \text{y}^*, -\text{S}_\text{y}], [1, \mathbf{0}_{1,19}]) +$$

$$\kappa I_A^* M_{1-y} \beta_a^* S^* \text{slmid}([\mathbf{0}_{1,20}], [1 - \text{x}^*, -\text{S}_\text{x}], [1, \mathbf{0}_{1,19}])$$

$$\Psi_8' = \begin{bmatrix} I_V^* S^* M_{1-x} m_{2,1} + I_V^* \beta_a^* M_{1-x} S_S^{\beta_n} + \beta_a^* S^* M_{1-x} S_{IV}^{\beta_n} \\ \vdots \\ I_V^* S^* M_{1-x} m_{2,19} + I_V^* \beta_a^* M_{1-x} S_S^{y_0} + \beta_a^* S^* M_{1-x} S_{IV}^{y_0} \end{bmatrix}^T +$$

$$I_V^* \beta_a^* S^* \text{slmid}([\mathbf{0}_{1,20}], [1 - \text{x}^*, -\text{S}_\text{x}], [1, \mathbf{0}_{1,19}]).$$

Hence, with the LD-derivatives for all the Ψ_i' terms completed, we can consolidate them by summing them together to obtain:

$$\Psi' = \Psi_1' + \Psi_2' + \Psi_3' + \Psi_4' + \Psi_5' + \Psi_6' + \Psi_7' + \Psi_8'.$$

With that we can now write

$$\dot{S}_{\mathbf{S}} = O_S' + W_S' = O_S' - \Omega' - \Psi'.$$

Moving forward, our focus shifts to examining the compartment I_S. Notably, the right hand side function is smooth:

$$\dot{I}_S = (1-\Xi)\sigma E - \gamma I_S - \eta I_S - \phi I_S - \mu I_S - \delta I_S,$$

Given its smooth nature, the LD-derivative for this compartment can be readily derived as follows:

$$\begin{aligned}
&I_S'(\mathbf{p}^*, \mathbf{x}^*; (\mathbf{M}, \mathbf{S_x})) \\
&= \begin{bmatrix} J_{\mathbf{p}} I_S(\mathbf{p}^*, \mathbf{x}^*) & | & J_{\mathbf{x}} I_S(\mathbf{p}^*, \mathbf{x}^*) \end{bmatrix} \begin{bmatrix} \mathbf{M} \\ \mathbf{S_x} \end{bmatrix} \\
&= \begin{bmatrix} \mathbf{0}_{4,1} \\ (1-\Xi^*)E^* \\ -\sigma^* E^* \\ -I_S^* \\ -I_S^* \\ -I_S^* \\ \mathbf{0}_{10,1} \\ \hline 0 \\ 0 \\ (1-\Xi^*)\sigma^* \\ 0 \\ -(\gamma^*+\eta^*+\phi^*+\mu+\delta) \\ \mathbf{0}_{9,1} \end{bmatrix}^T \begin{bmatrix} \mathbf{M} \\ \mathbf{S_x} \end{bmatrix} \\
&= \begin{bmatrix} (1-\Xi^*)E^* m_{5,1} - \sigma^* E^* m_{6,1} - I_S(m_{7,1}+m_{8,1}+m_{9,1}) + (1-\Xi^*)\sigma^* S_E^{\beta} - (\gamma^*+\eta^*+\phi^*+\mu+\delta) S_{I_S}^{\beta} \\ \vdots \\ (1-\Xi^*)E^* m_{5,19} - \sigma^* E^* m_{6,19} - I_S(m_{7,19}+m_{8,19}+m_{9,19}) + (1-\Xi^*)\sigma^* S_E^{y_0} - (\gamma^*+\eta^*+\phi^*+\mu+\delta) S_{I_S}^{y_0}. \end{bmatrix}^T.
\end{aligned}$$

Continuing our analysis, we now delve into the recovered category:

$$\dot{R} = \gamma(I_S + I_A + I_Q + I_{QV} + I_V) + h(I_H) + h(I_{HV}) - \zeta R - \mu R = O_R(\mathbf{p}, \mathbf{x}) + W_R(\mathbf{p}, \mathbf{x}).$$

Similarly, we proceed to express this as a sum of a smooth and a nonsmooth function:

$$O_R(\mathbf{p}, \mathbf{x}) = \gamma(I_S + I_A + I_Q + I_{QV} + I_V) - \zeta R - \mu R$$
$$W_R(\mathbf{p}, \mathbf{x}) = h(I_H) + h(I_{HV}).$$

Regarding the smooth portion, we find the following:

$$\begin{aligned}
&O'_R(\mathbf{p}^*, \mathbf{x}^*; (\mathbf{M}, \mathbf{S_x})) \\
&= \left[J_{\mathbf{p}} O_R(\mathbf{p}^*, \mathbf{x}^*) \quad | \quad J_{\mathbf{x}} O(\mathbf{p}^*, \mathbf{x}^*) \right] \begin{bmatrix} \mathbf{M} \\ \mathbf{S_x} \end{bmatrix} \\
&= \left[\mathbf{0}_{1,8} \; I_S^*{+}I_A^*{+}I_Q^*{+}I_{QV}^*{+}I_V^* \; {-}R^* \; \mathbf{0}_{9,1} \mid \mathbf{0}_{4,1} \; \gamma^* \; \gamma^* \; \gamma^* \; 0 \; 0 \; \gamma^* \; \gamma^* \; {-}\zeta^*{-}\mu \; 0 \; 0 \right] \begin{bmatrix} \mathbf{M} \\ \mathbf{S_x} \end{bmatrix} \\
&= \begin{bmatrix} (I_S^*{+}I_A^*{+}I_Q^*{+}I_{QV}^*{+}I_V^*)m_{9,1}{-}R^*m_{10,1}{+}\gamma^*(S_{I_S}^{\beta}{+}S_{I_V}^{\beta}{+}S_{I_A}^{\beta}{+}S_{I_Q}^{\beta}{+}S_{I_{QV}}^{\beta}){+}(-\zeta^*{-}\mu)S_R^{\beta} \\ \vdots \\ (I_S^*{+}I_A^*{+}I_Q^*{+}I_{QV}^*{+}I_V^*)m_{9,19}{-}R^*m_{10,19}{+}\gamma^*(S_{I_S}^{y0}{+}S_{I_V}^{y0}{+}S_{I_A}^{y0}{+}S_{I_Q}^{y0}{+}S_{I_{QV}}^{y0}){+}(-\zeta^*{-}\mu)S_R^{y0} \end{bmatrix}.
\end{aligned}$$

As for the first nonsmooth part, specifically $h(I_H)$, the expression is as follows:

$$\begin{aligned}
h(I_H)' &= \mathrm{slmin}([\mathrm{r}^*\mathrm{I}_{\mathrm{H}}^* \; \mathrm{J}_{\mathbf{p}}\mathrm{r}^*\mathrm{I}_{\mathrm{H}}^*\mathrm{M} + \mathrm{J}_{\mathbf{x}}\mathrm{r}^*\mathrm{I}_{\mathrm{H}}^*\mathbf{S_x}], [\mathrm{r}^*\mathrm{H_c} \; \mathrm{J}_{\mathbf{p}}\mathrm{r}^*\mathrm{H_c}\mathrm{M} + \mathrm{J}_{\mathbf{x}}\mathrm{r}^*\mathrm{H_c}\mathbf{S_x}]) \\
&= \mathrm{slmin}([\mathrm{r}^*\mathrm{I}_{\mathrm{H}}^* \; [\mathbf{0}_{1,11}, \mathrm{I}_{\mathrm{H}}^*, \mathbf{0}_{1,7}]\mathrm{M} + [\mathbf{0}_{1,7}, \mathrm{r}^*, \mathbf{0}_{1,6}]\mathbf{S_x}], [\mathrm{r}^*\mathrm{H_c} \; [\mathbf{0}_{1,11}, \mathrm{H_c}, \mathbf{0}_{1,7}]\mathrm{M} + \mathbf{0}\mathbf{S_x}]) \\
&= \mathrm{slmin}([\mathrm{r}^*\mathrm{I}_{\mathrm{H}}^* \; \mathrm{I}_{\mathrm{H}}^*\mathrm{m}_{12,1} + \mathrm{r}^*\mathrm{S}_{\mathrm{I_H}}^{\beta} \; \cdots \; \mathrm{I}_{\mathrm{H}}^*\mathrm{m}_{12,1} + \mathrm{r}^*\mathrm{S}_{\mathrm{I_H}}^{\mathrm{y0}}]^{\mathrm{T}}, [\mathrm{r}^*\mathrm{H_c} \; \mathrm{H_c}\mathrm{m}_{12,1} \; \cdots \; \mathrm{H_c}\mathrm{m}_{12,19}]^{\mathrm{T}}).
\end{aligned}$$

Moving on to the second nonsmooth component, namely $h(I_{HV})$, the expression is as follows:

$$\begin{aligned}
&h(I_{HV})' \\
&= \mathrm{slmin}([\mathrm{r}^*\mathrm{I}_{\mathrm{HV}}^* \; \mathrm{J}_{\mathbf{p}}\mathrm{r}^*\mathrm{I}_{\mathrm{V}}^*\mathrm{M} + \mathrm{J}_{\mathbf{x}}\mathrm{r}^*\mathrm{I}_{\mathrm{V}}^*\mathbf{S_x}], [\mathrm{r}^*\mathrm{H_c} \; \mathrm{J}_{\mathbf{p}}\mathrm{r}^*\mathrm{H_c}\mathrm{M} + \mathrm{J}_{\mathbf{x}}\mathrm{r}^*\mathrm{H_c}\mathbf{S_x}]) \\
&= \mathrm{slmin}([\mathrm{r}^*\mathrm{I}_{\mathrm{HV}}^* \; [\mathbf{0}_{1,11}, \mathrm{I}_{\mathrm{HV}}^*, \mathbf{0}_{1,7}]\mathrm{M} + [\mathbf{0}_{1,8}, \mathrm{r}^*, \mathbf{0}_{1,5}]\mathbf{S_x}], [\mathrm{r}^*\mathrm{H_c} \; [\mathbf{0}_{1,11}, \mathrm{H_c}, \mathbf{0}_{1,7}]\mathrm{M} + \mathbf{0}\mathbf{S_x}]) \\
&= \mathrm{slmin}([\mathrm{r}^*\mathrm{I}_{\mathrm{HV}}^* \; \mathrm{I}_{\mathrm{HV}}^*\mathrm{m}_{12,1} + \mathrm{r}^*\mathrm{S}_{\mathrm{I_{HV}}}^{\beta} \; \cdots \; \mathrm{I}_{\mathrm{HV}}^*\mathrm{m}_{12,1} + \mathrm{r}^*\mathrm{S}_{\mathrm{I_{HV}}}^{\mathrm{y_0}}]^{\mathrm{T}}, [\mathrm{r}^*\mathrm{H_c} \; \mathrm{H_c}\mathrm{m}_{12,1} \; \cdots \; \mathrm{H_c}\mathrm{m}_{12,19}]^{\mathrm{T}}).
\end{aligned}$$

In conclusion, we can express the sensitivity equation for the nonsmooth part of R as follows:

$$W'_R(\mathbf{p}^*, \mathbf{x}^*; (\mathbf{M}, \mathbf{S_x})) = h(I_H)' + h(I_{HV})'.$$

Upon combining the smooth and nonsmooth components, the resultant equation becomes:

$$
\begin{aligned}
S_R = {} & \operatorname{slmin}([\mathrm{r}^*\mathrm{I}_{\mathrm{H}}^* \; \mathrm{I}_{\mathrm{H}}^*\mathrm{m}_{12,1} + \mathrm{r}^*\mathrm{S}_{\mathrm{I_H}}^{\beta} \; \cdots \; \mathrm{I}_{\mathrm{H}}^*\mathrm{m}_{12,1} + \mathrm{r}^*\mathrm{S}_{\mathrm{I_H}}^{\mathrm{y0}}]^{\mathrm{T}}, [\mathrm{r}^*\mathrm{H_c} \; \mathrm{H_c}\mathrm{m}_{12,1} \; \cdots \; \mathrm{H_c}\mathrm{m}_{12,19}]^{\mathrm{T}}) \\
& + \operatorname{slmin}([\mathrm{r}^*\mathrm{I}_{\mathrm{H}}^* \; \mathrm{I}_{\mathrm{HV}}^*\mathrm{m}_{12,1} + \mathrm{r}^*\mathrm{S}_{\mathrm{I_{HV}}}^{\beta} \; \cdots \; \mathrm{I}_{\mathrm{HV}}^*\mathrm{m}_{12,1} + \mathrm{r}^*\mathrm{S}_{\mathrm{I_{HV}}}^{\mathrm{y0}}]^{\mathrm{T}}, [\mathrm{r}^*\mathrm{H_c} \; \mathrm{H_c}\mathrm{m}_{12,1} \; \cdots \; \mathrm{H_c}\mathrm{m}_{12,19}]^{\mathrm{T}}) \\
& + \begin{bmatrix} (I_S^*+I_A^*+I_Q^*+I_{QV}^*+I_V^*)m_{9,1} - R^* m_{10,1} + \gamma^*(S_{I_S}^{\beta}+S_{I_V}^{\beta}+S_{I_A}^{\beta}+S_{I_Q}^{\beta}+S_{I_{QV}}^{\beta}) + (-\zeta^*-\mu)S_R^{\beta} \\ \vdots \\ (I_S^*+I_A^*+I_Q^*+I_{QV}^*+I_V^*)m_{9,19} - R^* m_{10,19} + \gamma^*(S_{I_S}^{y_0}+S_{I_V}^{y_0}+S_{I_A}^{y_0}+S_{I_Q}^{y_0}+S_{I_{QV}}^{y_0}) + (-\zeta^*-\mu)S_R^{y_0} \end{bmatrix}
\end{aligned}
$$

Proceeding further, we turn our attention to the sensitivities for x and y. Given the relationship $\dot{x} = \dot{y}$, we are afforded the opportunity to derive the sensitivity equations for these variables concurrently. Recall

$$\dot{x} = z(1-z)(-\beta_n + \beta_a)\Upsilon + \frac{\rho}{\alpha} z(1-z)[k + (m_a - m_n)\Upsilon]$$

where

$$\Upsilon = I_S + I_V + I_H + I_{HV} + I_Q + I_{QV}, z(t) = \frac{x(t)S(t) + y(t)I_A(t)}{S(t) + I_A(t)}.$$

Fortunately, the smooth right hand side function simplifies the solving process:

$$
\begin{aligned}
& f'_{13}(\mathbf{p}^*, \mathbf{x}^*; (M, \mathbf{S_x})) \\
& = \begin{bmatrix} J_{\mathbf{p}} f_{13}(\mathbf{p}^*, \mathbf{x}^*) & | & J_{\mathbf{x}} f_{13}(\mathbf{p}^*, \mathbf{x}^*) \end{bmatrix} \begin{bmatrix} \mathbf{M} \\ \mathbf{S_x} \end{bmatrix} \\
& = \begin{bmatrix}
\Upsilon^*(z^*)(1-z^*) \\
\Upsilon^*(z^*)(1-z^*) \\
\mathbf{0}_{10,1} \\
\frac{\rho}{\alpha}(z^*)(1-z^*) \\
\frac{\rho}{\alpha}\Upsilon^*(z^*)(1-z^*) \\
\frac{\rho}{\alpha}\Upsilon^*(z^*)(1-z^*) \\
\mathbf{0}_{[4,1]} \\
\frac{(\frac{\rho}{\alpha}(\Upsilon^*(m_a^*-m_n^*)+k^*)+\Upsilon^*(\beta_a^*-\beta_n^*))(\frac{2(x^*S^*+I_A^*y^*)^2}{(S^*+I_A^*)^3}+\frac{x^*}{S^*+I_A^*}-\frac{2x^*(x^*S^*+I_A^*y^*)-x^*S^*-I_A^*y^*}{(S^*+I_A^*)^2}}{} \\
\mathbf{0}_{3,1} \\
(\frac{\rho}{\alpha}(m_a^*-m_n^*)-\beta_n^*+\beta_a^*)(z^*)(1-z^*) \\
(\frac{\rho}{\alpha}(m_a^*-m_n^*)-\beta_n^*+\beta_a^*)(z^*)(1-z^*) \\
(\frac{\rho}{\alpha}(\Upsilon^*(m_a^*-m_n^*)+k^*)+\Upsilon^*(\beta_a^*-\beta_n^*))(\frac{2(x^*S^*+I_A^*y^*)^2}{(S^*+I_A^*)^3}+\frac{y^*}{S^*+I_A^*}-\frac{2y^*(x^*S^*+I_A^*y^*)-x^*S^*-I_A^*y^*}{(S+I_A)^2} \\
(\frac{\rho}{\alpha}(m_a^*-m_n^*)-\beta_n^*+\beta_A^*)(z^*)(1-z^*) \\
(\frac{\rho}{\alpha}(m_a^*-m_n^*)-\beta_n^*+\beta_A^*)(z^*)(1-z^*) \\
(\frac{\rho}{\alpha}(m_a^*-m_n^*)-\beta_n^*+\beta_A^*)(z^*)(1-z^*) \\
(\frac{\rho}{\alpha}(m_a^*-m_n^*)-\beta_n^*+\beta_A^*)(z^*)(1-z^*) \\
0 \\
(\frac{\rho}{\alpha}(\Upsilon^*(m_a^*-m_a^*)+k^*)+\Upsilon^*(\beta_a^*-\beta_n^*))(\frac{S^*}{S^*+I_A^*})(\frac{2S^*(S^*x+I_A^*y^*)}{(S^*+I_A^*)^2}) \\
(\frac{\rho}{\alpha}(\Upsilon^*(m_a^*-m_a^*)+k^*)+\Upsilon^*(\beta_a^*-\beta_n^*))(\frac{I_A^*}{S^*+I_A^*})(\frac{2I_A^*(S^*x+I_A^*y^*)}{(S^*+I_A^*)^2})
\end{bmatrix}^T \begin{bmatrix} \mathbf{M} \\ \mathbf{S_x} \end{bmatrix}
\end{aligned}
$$

Concerning the initial values of the sensitivity system, $\mathbf{S_x}(0)$, the initial function of the Be-SEIMR model is:

$$\mathbf{f}_0(\mathbf{p}) = (S_0, 0, E_0, 0, 0, 0, 0, 0, 0, 0, 0, 0, x_0, y_0).$$

Hence, it follows that:

$$\mathbf{f}_0'(\mathbf{p}^*; \mathbf{M}) = \mathbf{Jf}_0(\mathbf{p}^*)\mathbf{M} = \begin{bmatrix} 0&0&0&0&0&0&0&0&0&0&0&0&0&0&0&1&0&0&0 \\ 0&0&0&0&0&0&0&0&0&0&0&0&0&0&0&0&1&0&0 \\ 0&0&0&0&0&0&0&0&0&0&0&0&0&0&0&0&0&0&0 \\ 0&0&0&0&0&0&0&0&0&0&0&0&0&0&0&0&0&0&0 \\ 0&0&0&0&0&0&0&0&0&0&0&0&0&0&0&0&0&0&0 \\ 0&0&0&0&0&0&0&0&0&0&0&0&0&0&0&0&0&0&0 \\ 0&0&0&0&0&0&0&0&0&0&0&0&0&0&0&0&0&0&0 \\ 0&0&0&0&0&0&0&0&0&0&0&0&0&0&0&0&0&0&0 \\ 0&0&0&0&0&0&0&0&0&0&0&0&0&0&0&0&0&0&0 \\ 0&0&0&0&0&0&0&0&0&0&0&0&0&0&0&0&0&0&0 \\ 0&0&0&0&0&0&0&0&0&0&0&0&0&0&0&0&0&0&0 \\ 0&0&0&0&0&0&0&0&0&0&0&0&0&0&0&0&0&0&0 \\ 0&0&0&0&0&0&0&0&0&0&0&0&0&0&0&0&0&1&0 \\ 0&0&0&0&0&0&0&0&0&0&0&0&0&0&0&0&0&0&1 \end{bmatrix} \mathbf{M} = \begin{bmatrix} m_{16,1} & \cdots & m_{16,19} \\ m_{17,1} & \cdots & m_{17,19} \\ 0 & \cdots & 0 \\ 0 & \cdots & 0 \\ 0 & \cdots & 0 \\ 0 & \cdots & 0 \\ 0 & \cdots & 0 \\ 0 & \cdots & 0 \\ 0 & \cdots & 0 \\ 0 & \cdots & 0 \\ 0 & \cdots & 0 \\ 0 & \cdots & 0 \\ m_{18,1} & \cdots & m_{18,19} \\ m_{19,1} & \cdots & m_{19,19} \end{bmatrix}.$$

4.3 Local Sensitivity Analysis

In order to implement the sensitivity system and produce simulations, we used Matlab's ode45 to simulate the model and coded the necessary nonsmooth functions, slmin and slmid. As seen in equation (4.3), we have β_n,β_a,β_v, θ, σ, Ξ, η, ϕ, γ, ζ, ω, r, k, m_a, m_n, S_0, E_0, x_0 and y_0 as parameters and in equation (4.4) we have κ, μ, δ, δ_h, δ_v, χ, ρ, α, H_c, S_c, S_{V0}, E_{V0}, I_{S0}, I_{V0}, I_{A0}, I_{H0}, I_{HV0}, I_{Q0}, I_{QV0} and R_0 as constants. Our simulations utilized the reference parameters

$$\mathbf{p}^* = (\beta_n^*, \beta_a^*, \beta_v^*, \theta^*, \sigma^*, \Xi^*, \eta^*, \phi^*, \gamma^*, \zeta^*, \omega^*, r^*, k^*, m_a^*, m_n^*, S_0^*, E_0^*, x_0^*, y_0^*)$$

where

$$\beta_n^* = 0.363282 \qquad \beta_a^* = 0.19397$$

$$\beta_v^* = 0.13259793 \qquad \theta^* = 0.0053763$$

$$\sigma^* = 0.196078 \qquad \Xi^* = 0.8787$$

$$\eta^* = 0.0049 \qquad \phi^* = 0.262$$

$$\gamma^* = 0.167504 \qquad \zeta^* = 0.00273973$$

$$\omega^* = 0.000005116 \qquad r^* = 0.167504$$

$$m_n^* = 0.9 \qquad m_a^* = 0.2$$

$$k^* = 0.001 \qquad S_0^* = 0.8$$

$$E_0^* = 0.2 \qquad x_0^* = 0.43$$

$$y_0^* = 0.43$$

We also used the directions matrix $\mathbf{M} = \mathbf{I}_{19}$ as well as constant values:

$$\delta = 0.01017576 \qquad \delta_v = 0.0208$$

$$\delta_h = 0.2 \qquad \chi = 0.104$$

$$\rho = 1 \qquad \alpha = 7$$

$$H_c = 0.00152 \qquad \kappa = 0.631$$

$$S_c = 0.00007442 \qquad \mu = 0.0000391389$$

We conduct simulations to assess the sensitivities of the fourteen state variables, considering the specified $\mathbf{p}^*$ and constant values. The total area under each curve provides the primary measure of the sensitivity of the state variables to the reference parameter.

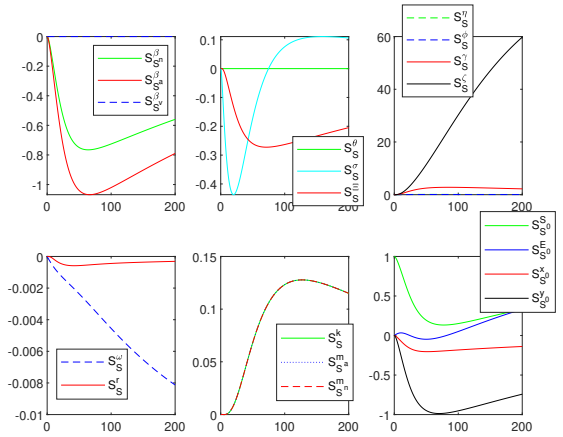

(a) Simulations of $\mathbf{S}_S$.

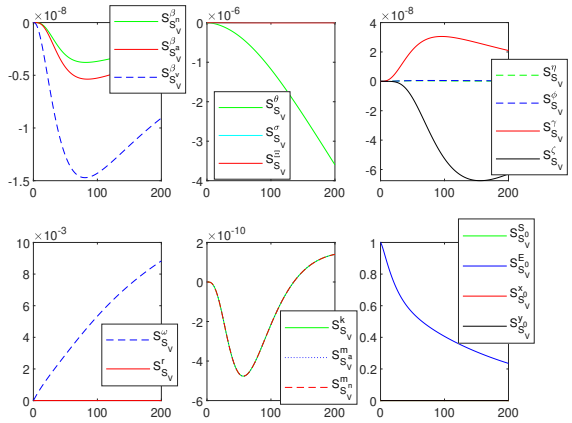

(b) Simulations of $\mathbf{S}_{S_V}$.

Figure 4.3: Simulations of the lexicographic sensitivity functions for the susceptible compartments.

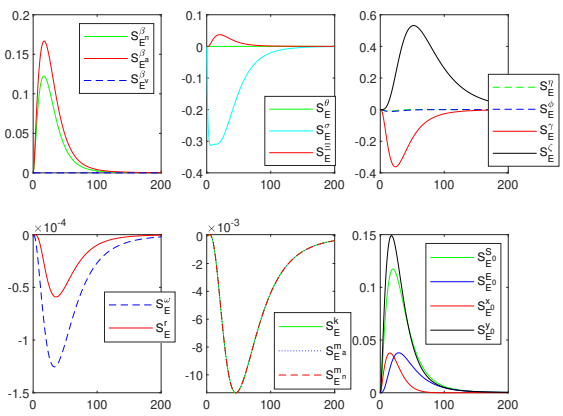

(a) Simulations of $\mathbf{S}_E$.

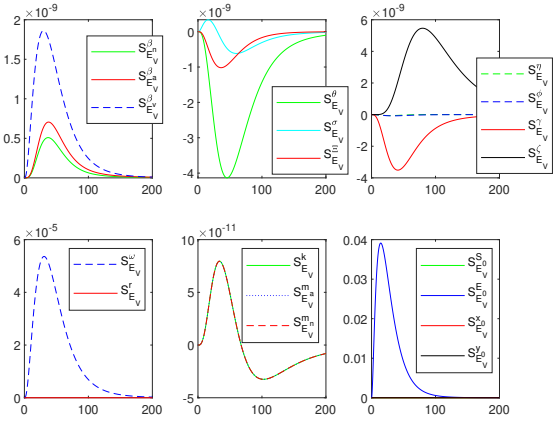

(b) Simulations of $\mathbf{S}_{E_V}$.

Figure 4.4: Simulations of the lexicographic sensitivity functions for the exposed compartments.

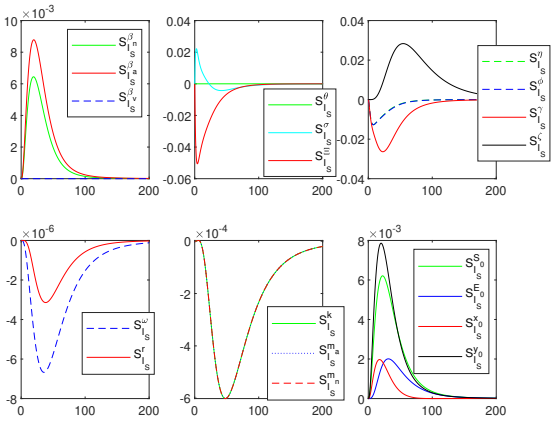

(a) Simulations of $\mathbf{S}_{I_S}$.

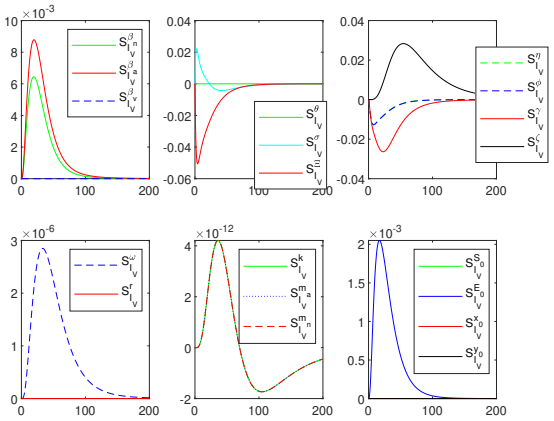

(b) Simulations of $\mathbf{S}_{I_V}$.

Figure 4.5: Simulations of the lexicographic sensitivity functions for the symptomatic infected compartments.

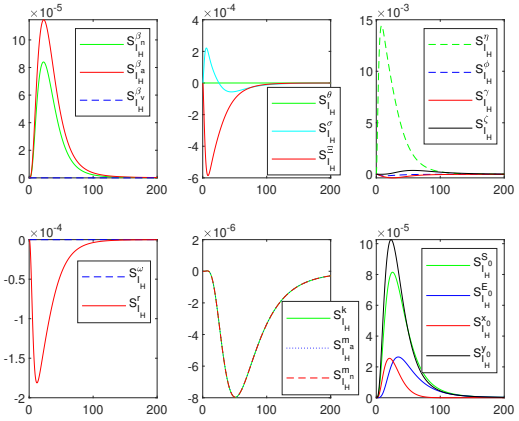

(a) Simulations of $\mathbf{S}_{I_H}$.

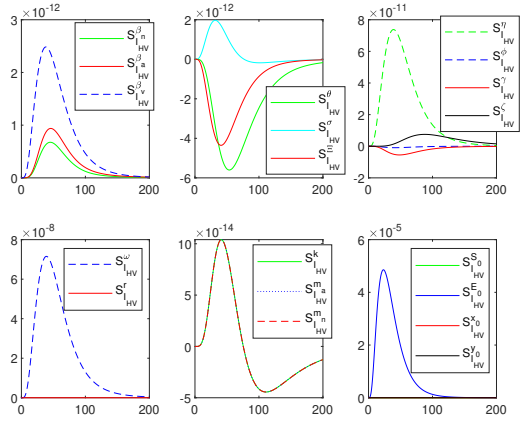

(b) Simulations of $\mathbf{S}_{I_{HV}}$.

Figure 4.6: Simulations of the lexicographic sensitivity functions for the hospitalized infected compartments.

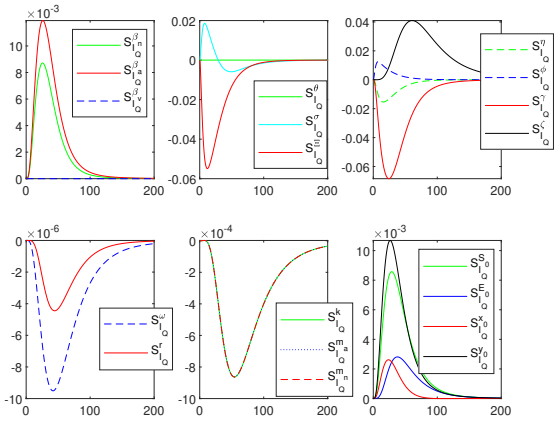

(a) Simulations of $\mathbf{S}_{I_Q}$.

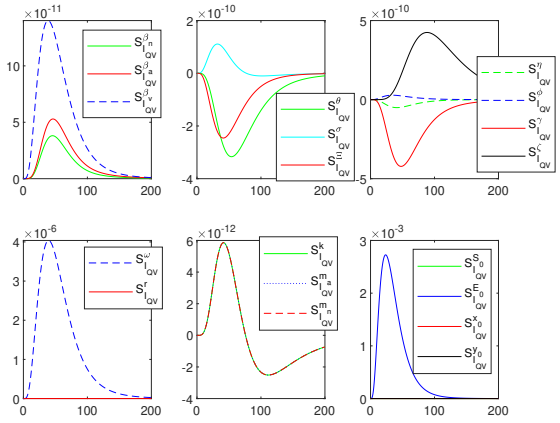

(b) Simulations of $\mathbf{S}_{I_{QV}}$.

Figure 4.7: Simulations of the lexicographic sensitivity functions for the quarantined infected compartments.

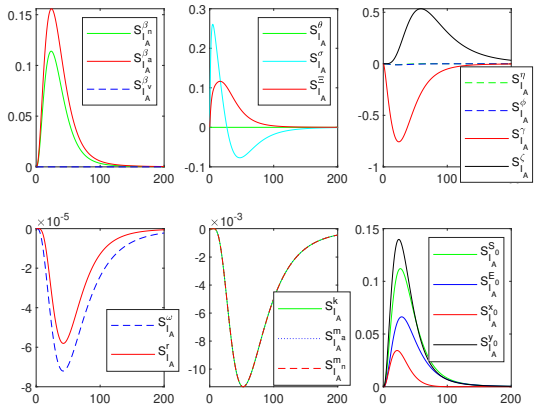

(a) Simulations of $\mathbf{S}_{I_A}$.

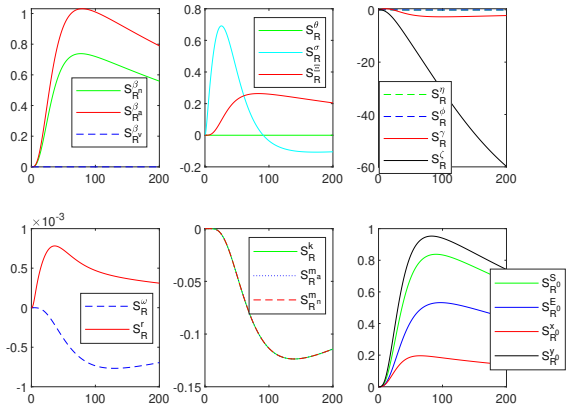

(b) Simulations of $\mathbf{S}_R$.

Figure 4.8: Simulations of the lexicographic sensitivity functions for the asymptomatic infected compartment and the recovered compartment.

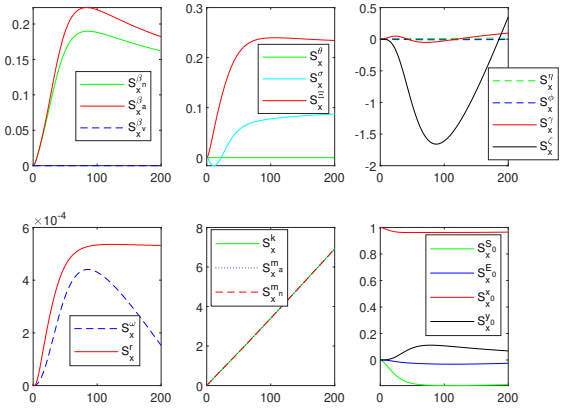

(a) Simulations of $\mathbf{S}_x$.

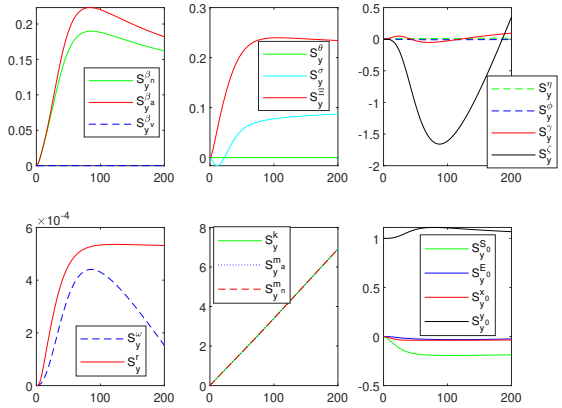

(b) Simulations of $\mathbf{S}_y$.

Figure 4.9: Simulations of the lexicographic sensitivity functions for the game theory compartments.

We further employed bar graphs to provide a succinct and easily interpretable representation of the overall sensitivity. In these bar graphs, the height of each bar, denoted as h, is determined by the integral $h(p,k) = \int_{t_0}^{t_f} |S_k^p(t)|dt$, where p corresponds to a chosen parameter for analysis, k represents a state variable, and $t_0 = 0$ and $t_f = 200$ are the time limits, all with respect to the reference parameter p^*.

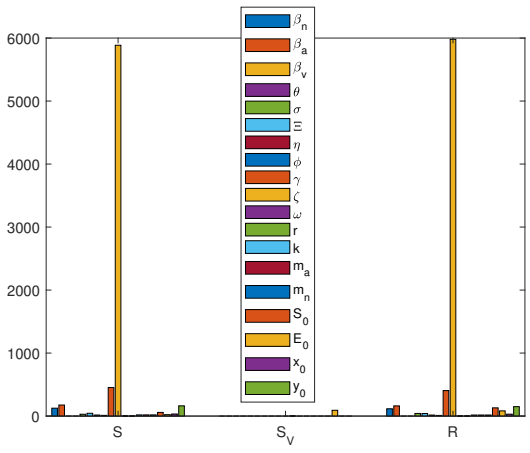

(a) Graphs of h for S, S_V, and R.

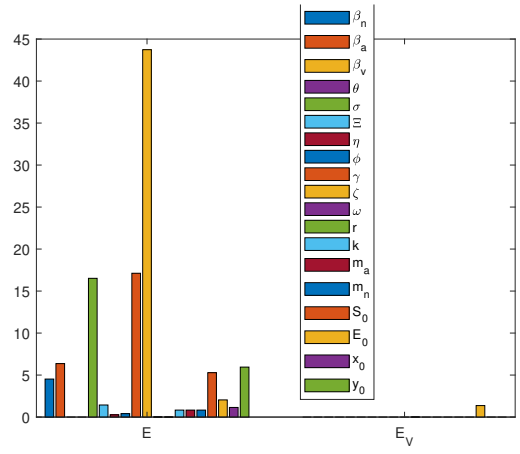

(b) Graphs of h for E and E_V.

Figure 4.10: Graphs of $h(p,k)$ for different variables and all parameters.

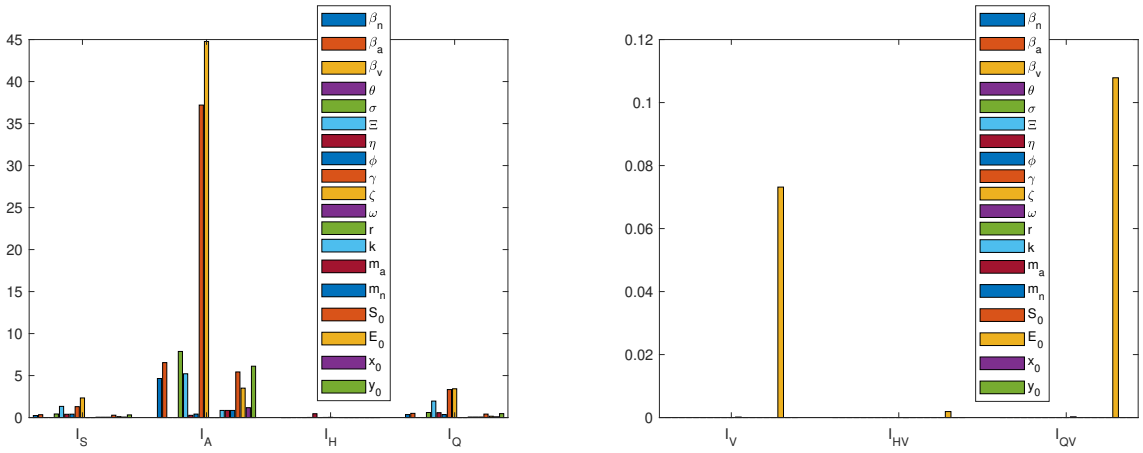

(a) Graphs of h for I_S, I_A, I_H and I_Q.

(b) Graphs of h for I_V, I_{HV} and I_{QV}.

Figure 4.11: Graphs of $h(p, k)$ for different variables and all parameters.

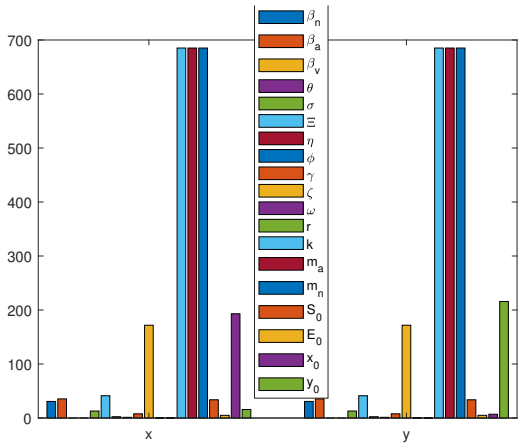

(a) Graphs of h for x and y.

Figure 4.12: Graphs of $h(p, k)$ for different variables.

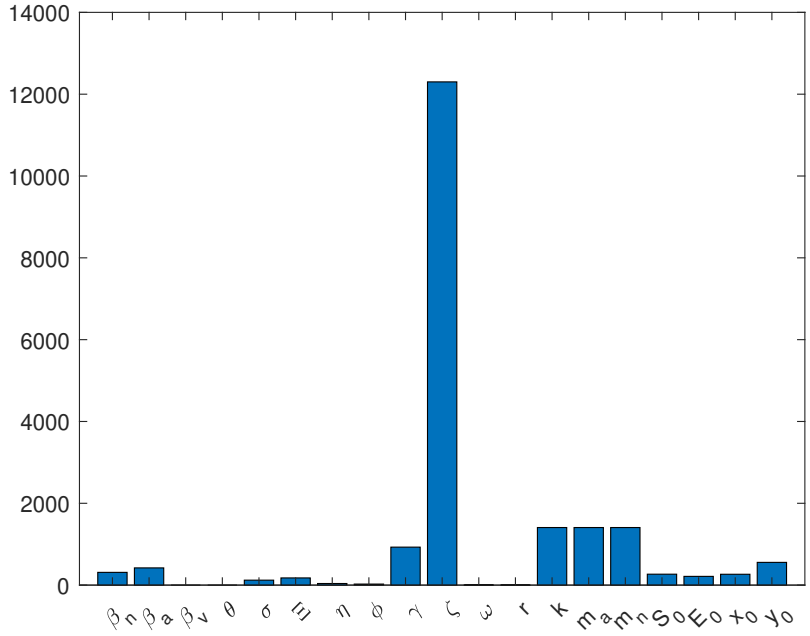

Figure 4.13: Graph of $\tilde{h}(p) = \sum_{k=1}^{n_x} \int_{t_0}^{t_f} |S_k^p(t)|dt$ for all parameters.

We can see from Figure 4.13 that ζ is by far the most influential parameter. As seen in figures 3.8a and 3.9a, the disease appears to die out due to the population remaining in the recovered compartment for a lengthy period of time. Since ζ is the reciprocal of the average waning immunity period, or the average length of time that individuals are naturally immune, it makes sense that altering that value would potentially cause dramatic changes. However, due to a low $\mathcal{R}_0$ it could still die out after an extended period of time.

4.4 Semi-Local Sensitivity Analysis: Exploring Different Behavioral and Medical Intervention Scenarios

Even though we pulled from real world values, as seen with reference parameters (4.3), to simulate the parameter sensitivities of the Be-SEIMR model, we want to explore alternative situations to see how the sensitivities may change.

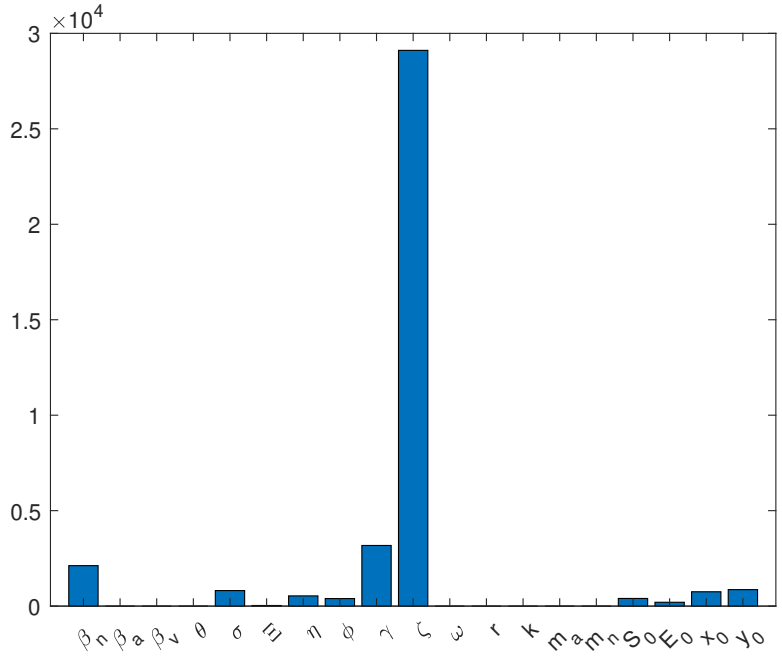

Figure 4.14: Parameter influence levels given the reference parameters from Acuña-Zegarra [1]. These parameters are $\beta_n^* = 0.363282$, $\sigma^* = 0.196078$, $\gamma^* = 0.167504$, $\zeta^* = 0.00273973$ and $\Xi^* = 0.8787$. We also have two additional reference parameters $S_0^* = 0.8$ and $E_0^* = 0.2$ and constants $\delta = 0.01017576$ and $\mu = 0.0000391389$.

All other reference parameters are set to zero to "turn them off" in the simulation but to still allow us to see how sensitive they are at zero. As we progress further and add back in other parameters, we will assume all other reference parameters are zero unless stated otherwise. Once again, ζ is by far the most influential parameter. As depicted in Figure 4.15, the majority of the population transitions to the recovered category, conferring immunity on the majority.

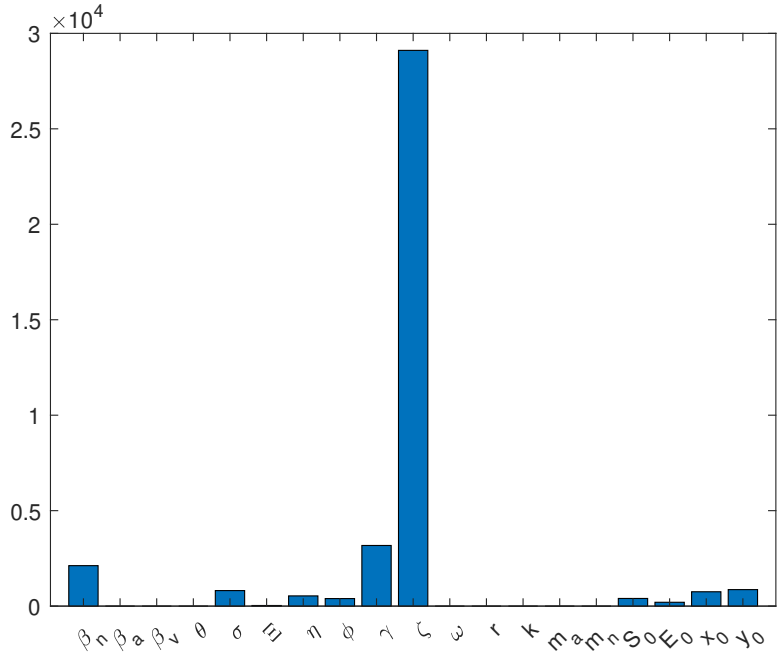

Figure 4.15: Graphs of $\tilde{h}(p) = \sum_{k=1}^{n_x} \int_{t_0}^{t_f} |S_k^p(t)|dt$ with the parameters given in Figure 4.14.

Since $\zeta^* = 0.00273973$ means that the average waning immunity period is a year, $\frac{1}{0.00273973} = 365$, individuals remain in the compartment for a relatively long period of time. If we were to change ζ to a shorter period of time, we may find the sensitivities to be different. Changing ζ from a year to a month, $\zeta^* = \frac{1}{30} = 0.333333$, we see some drastic changes in the sensitivity bar graphs, as seen in figure 4.16.

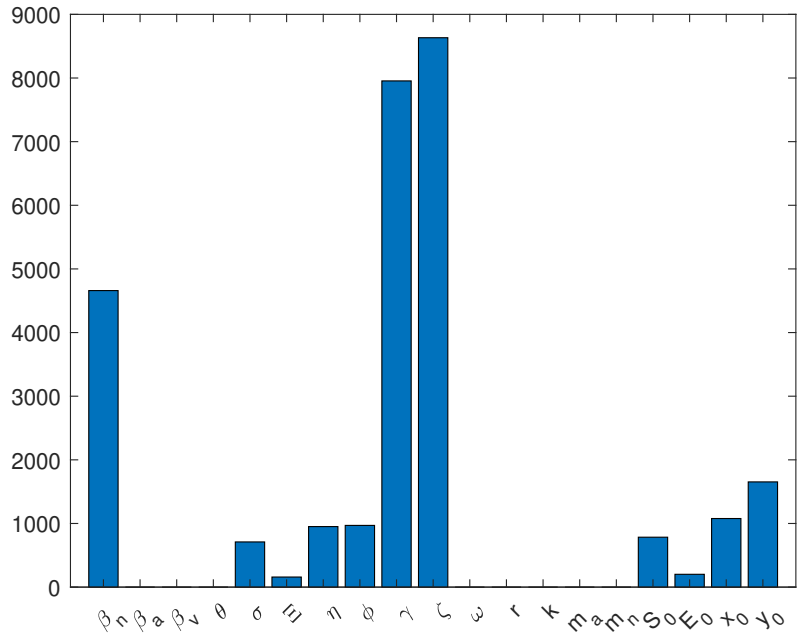

Figure 4.16: Parameter influence levels given by $\tilde{h}(p)$, with the same reference parameters as Figure 4.14 but with an increased ζ value.

We can easily see in figure 4.16 that even though ζ is still is the most influential, the differences between ζ and the other parameters is much smaller than in Figure 4.14, where ζ went from 30000 to 9000. This change can also be seen in Figure 4.17, where the recovered compartment no longer consists of the majority of the population.

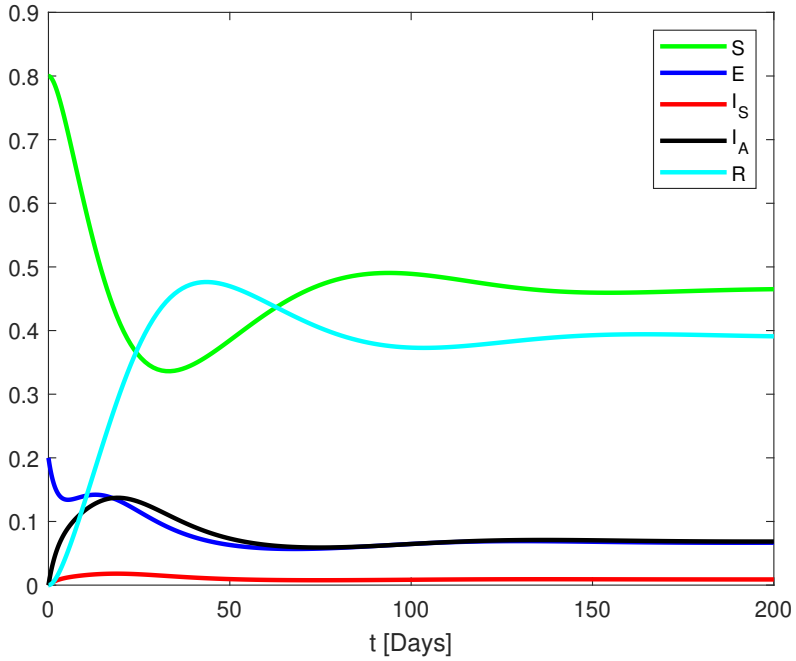

Figure 4.17: Be-SEIMR simulations to accompany Figure 4.16.

For more comprehensive comparisons, we will adopt the modified one-month ζ as it facilitates a clearer range of values. In Figure 4.13, we identify the following parameters as the next most influential after ζ: k, m_a, and m_n. To further investigate their impact, we will incorporate these parameters, along with β_a, α and ρ, into our model. In addition, we will initialize the state variables x_0 and y_0 with values of 0.43. We also will set $\beta_a^* = 0.19397$, $\kappa = 0.631$, $\alpha = 7$ and $\rho = 1$, while allowing us to vary m_a^*, m_n^*, and k^*. This variation will enable us to explore how changes in these parameters affect the sensitivity graphs.

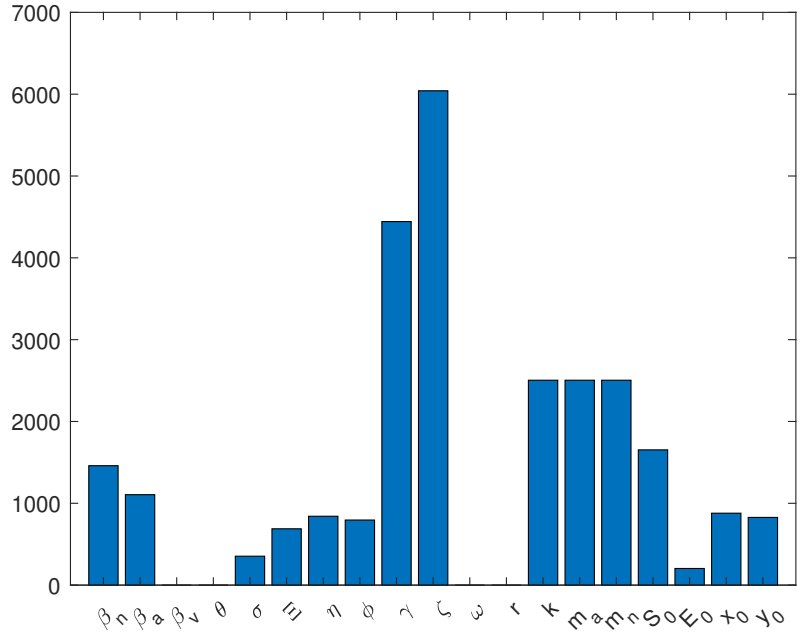

Figure 4.18: Parameter influence levels given by $\tilde{h}(p)$, with $m_n = 0.7$, $m_a = 0.3$ and $k = 0.1$.

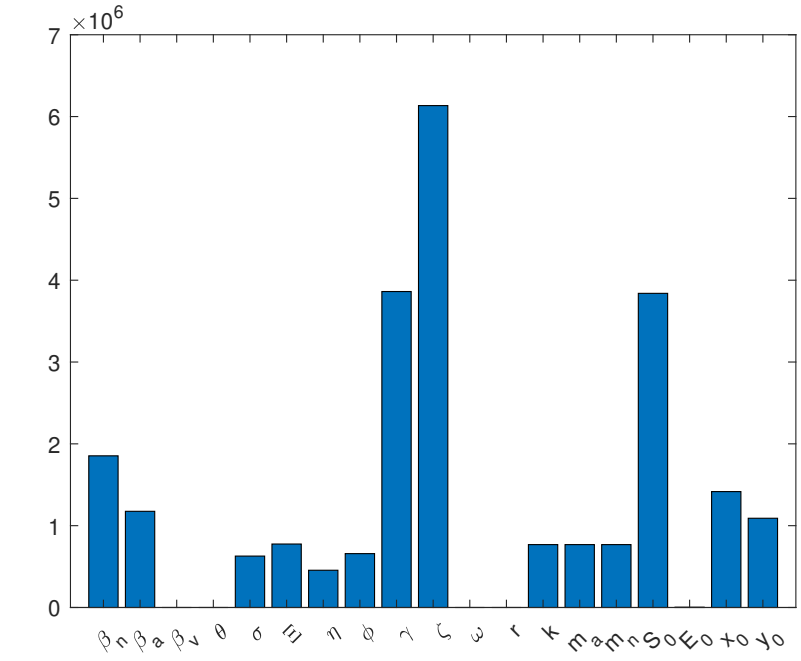

Figure 4.19: Parameter influence levels given by $\tilde{h}(p)$, with $m_n = 0.7$, $m_a = 0.3$ and $k = 0.5$.

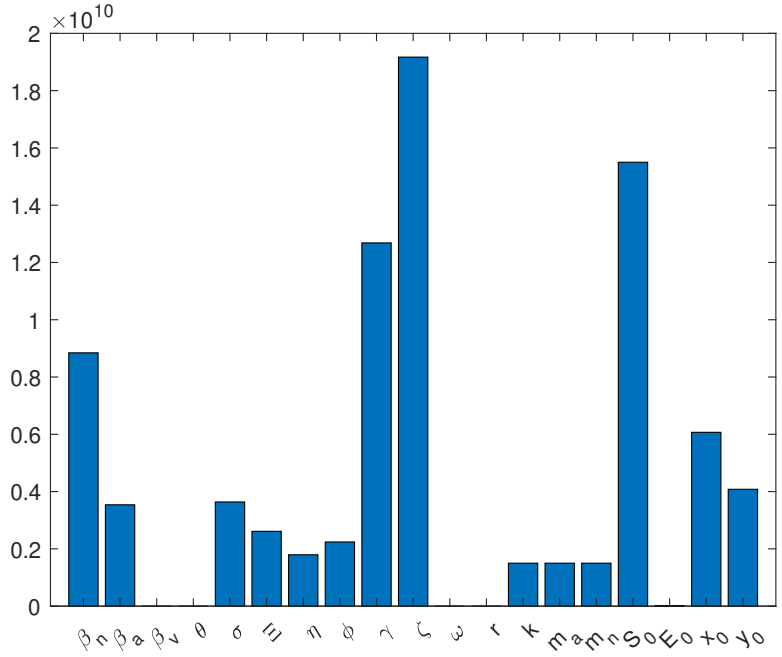

Figure 4.20: Parameter influence levels given by $\tilde{h}(p)$, with $m_n = 0.7$, $m_a = 0.3$ and $k = 0.9$.

Comparing Figure 4.18, Figure 4.19, and Figure 4.20, we observe striking differences among them. When k is set to a lower value, ζ remains the most influential parameter, albeit with a reduced sensitivity magnitude, dropping to approximately 6000. In this scenario, k, m_n, and m_a exhibit significant influence compared to other parameters. However, as we increase the value of k, all parameters experience a substantial increase in magnitude. In relative terms, when k reaches 0.9, as shown in Figure 4.20, the parameters spike dramatically. The parametric sensitivity of ζ reaches nearly 2×10^{10}, and interestingly, k, m_n, and m_a become the least influential among the nonzero parameters in this particular context. Now if we lock $k = 0.5$ and modify m_n and m_a, we can get different results. If we change m_n or m_a, the bar graphs look nearly identical to Figure 4.19. As seen in Figure 4.21, Figure 4.22, and Figure 4.23, I_S and I_A are incredibly small. Therefore since the difference of m_n and m_a is multiplied by Υ, their impact on the overall model is much smaller than k and the sensitivities will change much more due to k than m_a or m_n.

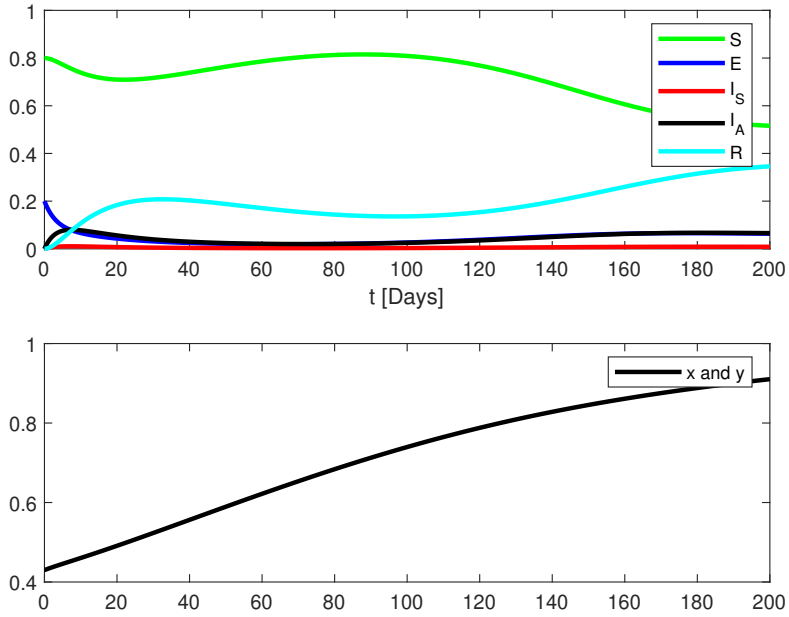

Figure 4.21: Be-SEIMR simulations with $m_n = 0.7$, $m_a = 0.3$ and $k = 0.1$.

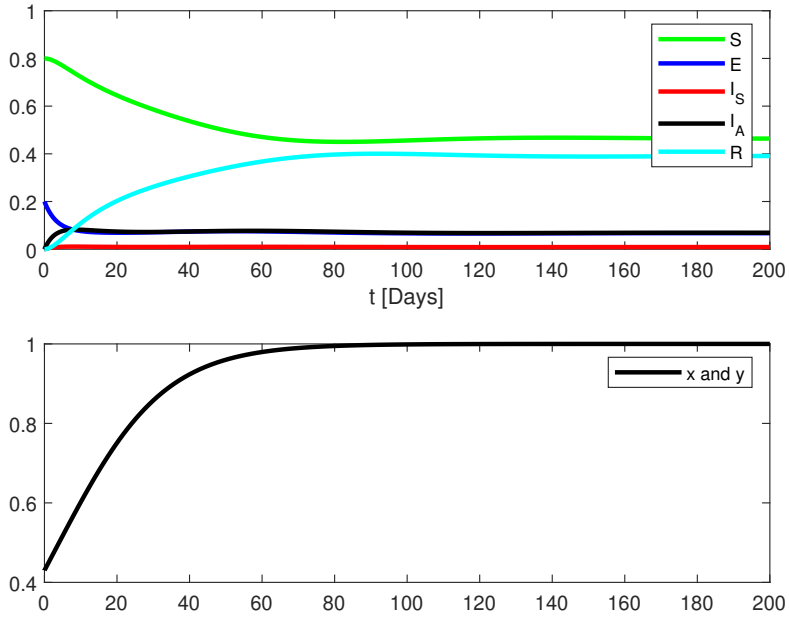

Figure 4.22: Be-SEIMR simulations with $m_n = 0.7$, $m_a = 0.3$ and $k = 0.5$.

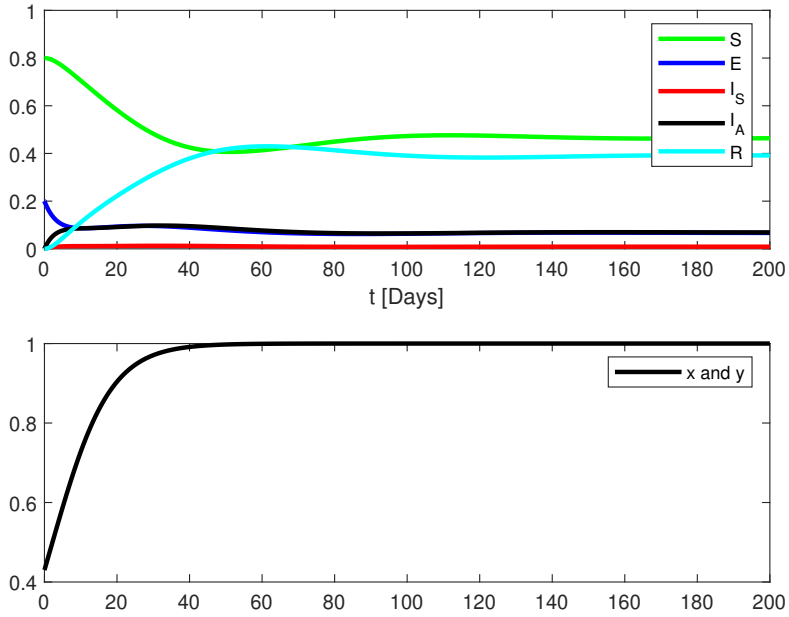

Figure 4.23: Be-SEIMR simulations with $m_n = 0.7$, $m_a = 0.3$ and $k = 0.9$.

Going forward we will be assuming $k^* = 0.1$, $m_n^* = 0.7$ and $m_a^* = 0.3$. Now we would like to reintroduce the rest of the parameters, as they deal with some form of medical intervention. We let $\beta_v^* = 0.13259793$, $\chi = 0.104$, $\delta_v = 0.0208$, $\delta_h = 0.2$, $\phi^* = 0.262$ and $r^* = 0.167504$. We also change $\eta^* = 0.1$ for a more populated hospitalized population. This leaves us with H_c, S_c, θ^* and ω^* as parameters to alter and see the results.

First we look towards a situation with low medical intervention. We have a max hospitalization capacity and vaccine distribution of 0.001, or 0.1% of the population, a vaccination rate of $\omega^* = 0.01$, 100 people per day, and a vaccine waning immunity rate of $\theta^* = 0.01667$, 60 days. Once again we see a large spike in sensitivity values, Figure 4.24, where the most influential parameter, ζ, is nearly at 7×10^6. For the most part, the sensitivities look similar to previous simulations qualitatively.

When we increase medical interventions, as exemplified in Figure 4.25, a significant transformation becomes evident in the other sensitivity simulations. With the specific values of $\omega^* = 0.1$, $\theta^* = 0.0083$, $S_c = 0.1$, and $H_c = 0.1$, not only does the scale of influence

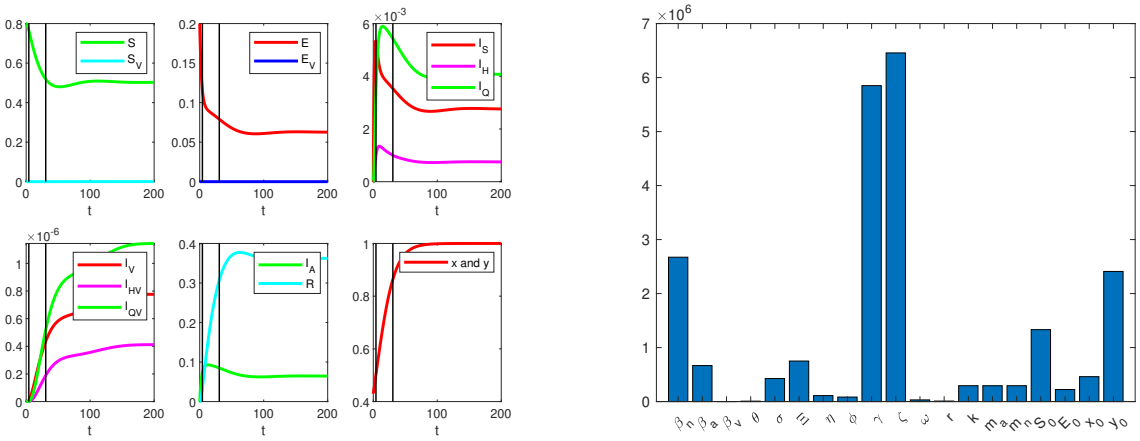

(a) Model simulations. (b) Parameter influence levels.

Figure 4.24: Parameter influence levels $\tilde{h}(p)$, with low medical intervention values where $\omega = 0.01$, $\theta = 0.01667$, $S_c = 0.001$, $H_c = 0.001$.

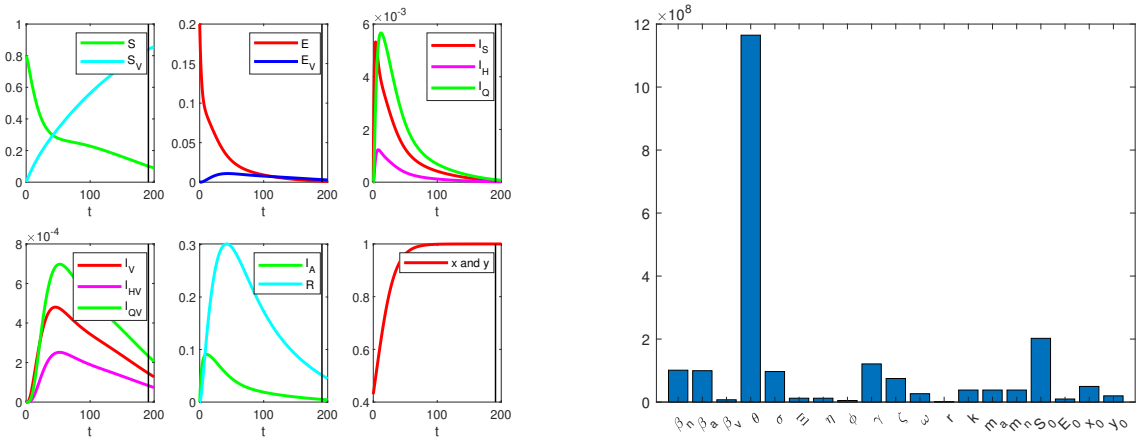

(a) Model simulations. (b) Parameter influence levels.

Figure 4.25: Parameter influence levels $\tilde{h}(p)$, with low medical intervention values where $\omega = 0.1$, $\theta = 0.0083$, $S_c = 0.1$, $H_c = 0.1$.

increase once more, with the most influential parameter surging to 12×10^8 sensitivity value, but the ranking of influential parameters also undergoes a noteworthy shift. In this context, θ emerges as the overwhelmingly predominant parameter, with S_0 trailing behind at approximately one-sixth of θ's magnitude. We now reduce θ back to the previous value of 0.01667 and further raise S_c, H_c and ω to see if that reduces the significance of θ.

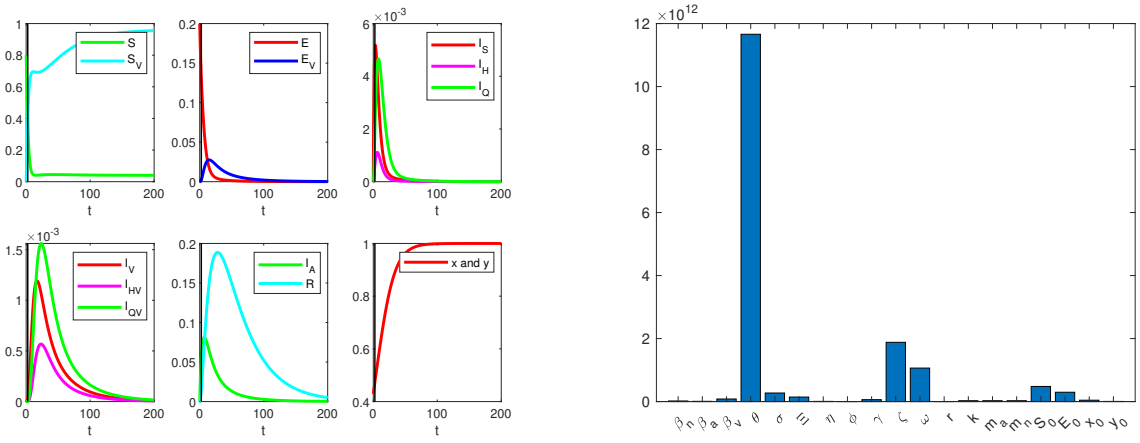

(a) Model simulations.

(b) Parameter influence levels.

Figure 4.26: Parameter influence levels $\tilde{h}(p)$, with high medical intervention values where $\omega = 0.4$, $\theta = 0.01667$, $S_c = 0.4$, $H_c = 0.4$.

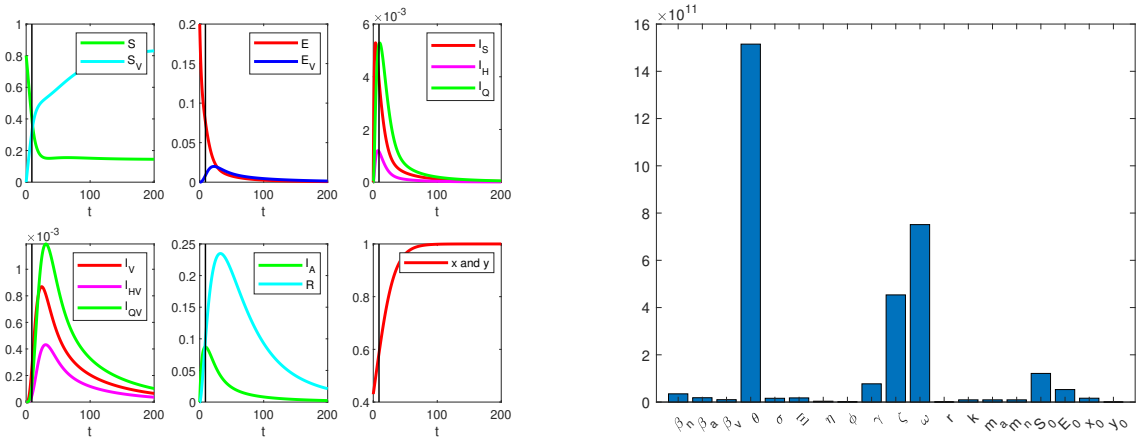

(a) Model simulations.

(b) Parameter influence levels.

Figure 4.27: Parameter influence levels $\tilde{h}(p)$, with high medical intervention values where $\omega = 0.1$, $\theta = 0.01667$, $S_c = 0.4$, $H_c = 0.4$.

When we opt to increase the parameters $\omega^* = 0.4$, $S_c = 0.4$, and $H_c = 0.4$, as seen in Figure 4.26, while simultaneously reducing $\theta^* = 0.01667$, an interesting pattern emerges. The dominance of θ persists, maintaining its position as the most influential parameter. However, the influence of nearly all other parameters experiences a significant reduction, with only ζ and ω standing out as exceptions, both nearly doubling in magnitude. If we choose to reduce ω back to its previous value of 0.1 we find some interesting results.

In Figure 4.27, a noteworthy shift in parameter influence becomes evident. The most influential parameter, θ, has its sensitivity rating decrease to approximately 15×10^{11}. However, the more substantial change lies in the significant growth of ω and ζ. The parameter ω ascends to become the second most influential, approaching roughly half the influence of θ, while ζ nearly triples its previous magnitude observed in the context of medical intervention sensitivity simulations.

4.5 Discussion

While conducting simulations in Section 4.3 and the simulations considering real-world parameters drawn from Acuña-Zegarra [1] in Subsection 4.4, we consistently observed that the most influential parameter was unquestionably ζ, the average waning immunity period, which represents the duration of an individual's natural immunity to the disease. The second most influential parameter, when excluding the game theory sensitivities, was γ—the reciprocal of the average infected period. With the real-world values in play, we can interpret these findings as indicating that γ and ζ hold paramount significance in determining the persistence or eradication of the disease. In scenarios without medical interventions or the capability for individuals to engage in disease avoidance strategies, the fate of the disease largely hinges on these inherent disease parameters. This implies that in the absence of medical solutions, individuals may find themselves with limited options to evade illness, relying largely on chance when dealing with a sufficiently dangerous disease. When we introduced disease avoidance practices into the simulations, ζ remained the most influential parameter, although its dominance was less pronounced, resulting in a more equitable balance among the parameters. Instead of rendering other parameters virtually irrelevant in comparison, they all assumed more comparable levels of influence. Moreover, we noticed that changes in the value of k, the social cost associated with altered behavior, exerted the most significant influence on m_n, m_a, k, and S_0. When k was set to a high value, indicating that people perceived disease avoidance strategies as highly costly to their

social lives, S_0 became notably influential. In this scenario, the disease transmission itself remained relatively unaffected, but the initial pool of susceptibles, S_0, assumed greater importance in determining whether the disease would persist or not. However, when k was set to a low value, a contrasting dynamic emerged. Suddenly, m_a, m_n, and k took on heightened significance in the disease dynamics. While ζ and γ remained the most influential parameters, the choices individuals made in response to the perceived social cost of disease avoidance had a more substantial impact on the disease's survival under these conditions. Upon the introduction of medical interventions, a striking shift in parameter influence occurs. The parameter θ, the average vaccination rate, emerges as the single most influential parameter, towering six times above the influence of the next most important parameter. This pronounced dominance of θ underscores its pivotal role. As θ correlates with the rate of vaccination and other medical intervention strategies, it surpasses the intrinsic dangers and characteristics of the virus itself. This leads us to a significant conclusion, when resources are available, the wide distribution and easy accessibility of a vaccine can have the most profound impact on the disease's longevity and containment. In essence, the availability and efficient deployment of vaccines can override the inherent properties of the virus, establishing them as the primary determinant of the disease's outcome.

CHAPTER 5
CONCLUSION

In this thesis, our aim was to harness the power of game theory and nonsmooth functions to enhance the realism of disease spread simulations within populations. Nonsmooth functions introduce a unique challenge, as standard theory falters when dealing with points of nondifferentiability. However, leveraging recent advancements in nonsmooth analysis, we have successfully adapted sensitivity analysis techniques to accommodate these intricate functions.

We extended the standard SEIR model by introducing additional complexities in the form of mortality rates, asymptomatic infections, alterations in behavior, and medical interventions. This extended model, which we called the Be-SEIMR model, became the focal point of this thesis. We provided simulations of the model using parameter values from the literature [1]. Subsequently, we performed a stability analysis, a fundamental endeavor that allowed us to determine a basic reproduction number, $\mathcal{R}_0$, for the SEIMR submodel where behavioral changes were turned off. This insight provided critical information about the model's potential for disease transmission. Next, we conducted a sensitivity analysis, a pivotal step in identifying the most influential parameters within our Be-SEIMR model. This analysis unveiled key insights into which parameters exerted the greatest impact on the model's outcomes and dynamics.

While conducting simulations, we observed the following key points regarding the influence of parameters on disease dynamics:

- The most influential parameter is ζ, representing the average waning immunity period, indicating its crucial role in determining disease persistence.
- The second most influential parameter, excluding game theory considerations, is γ (average infected period), showing its importance in disease dynamics.

- Real-world values highlight the significance of γ and ζ in determining disease persistence in scenarios without medical interventions or disease avoidance strategies.
- In the absence of medical solutions, individuals may have limited options to evade illness, relying largely on chance when dealing with a sufficiently dangerous disease.
- Introduction of disease avoidance practices reduces the dominance of ζ, resulting in a more balanced influence of parameters.
- Changes in the social cost parameter (k) significantly impacts m_n, m_a, k, and S_0, with high k making S_0 more influential and low k increasing the importance of m_a, m_n, and k in disease dynamics.
- While ζ and γ remain the most influential parameters, the choices individuals make in response to the perceived social cost of disease avoidance have a more substantial impact on disease survival under these conditions.
- Upon the introduction of medical interventions, a striking shift in parameter influence occurs. The parameter θ, representing the average vaccination rate, emerges as the single most influential parameter, towering six times above the influence of the next most important parameter. This dominance of θ underscores its pivotal role, surpassing the intrinsic dangers and characteristics of the virus itself.

In summary, the analysis reveals that the influence of parameters on disease dynamics varies depending on the presence of disease avoidance practices and medical interventions. The parameters ζ and γ are paramount in scenarios without interventions, while θ takes precedence when resources for medical interventions are available. The availability and efficient deployment of vaccines can override the inherent properties of the virus, establishing them as the primary determinant of the disease's outcome, ultimately resulting in the eradication of the disease.

The development of the Be-SEIMR model involved an expansion of the conventional SEIR model, aiming to create a framework that closely mimics the dynamics of COVID-19 while maintaining the versatility to simulate other diseases. This approach opens up multiple avenues for future research and exploration. Firstly, the Be-SEIMR model offers opportunities for further expansion and refinement to address scenarios not covered in this thesis. Future work could involve incorporating factors like viral mutations, considering how a virus might evolve to counteract vaccines, and allowing for changes in vaccine effectiveness over time. Additionally, the model could be extended to account for disease spread across different regions, encompassing cities, states, or even countries, offering a more comprehensive perspective on disease dynamics. Another avenue for future research could involve shifting the focus away from COVID-19 and applying the model to study other diseases, such as the common cold or influenza. This would serve as a rigorous test of the model's adaptability and open doors for researchers to tailor it to better simulate specific diseases, just as we have expanded upon the SEIR model in this thesis. Finally, a more in depth exploration into the calculation of $\mathcal{R}_0$ could be done. This would either allow us to find the formula for the full Be-SEIMR model with behavior components or looking into connecting the analysis of the SEIMR submodel to the concept of partial stability [42]. This approach would provide a more comprehensive understanding of a given disease's risk factors and enable a more precise determination of whether an epidemic will occur.

REFERENCES

[1] Manuel Adrian Acuña-Zegarra, Saúl Díaz-Infante, David Baca-Carrasco, and Daniel Olmos-Liceaga. Covid-19 optimal vaccination policies: A modeling study on efficacy, natural and vaccine-induced immunity responses. *Mathematical Biosciences*, 337:108614, 2021.

[2] Paul I Barton, Kamil A Khan, Peter Stechlinski, and Harry AJ Watson. Computationally relevant generalized derivatives: theory, evaluation and applications. *Optimization Methods and Software*, 33(4-6):1030–1072, 2018.

[3] Chris T Bauch. Imitation dynamics predict vaccinating behaviour. *Proceedings of the Royal Society B: Biological Sciences*, 272(1573):1669–1675, 2005.

[4] Chris T Bauch and Samit Bhattacharyya. Evolutionary game theory and social learning can determine how vaccine scares unfold. *PLoS Computational Biology*, 8(4):e1002452, 2012.

[5] R Alexander Bentley and Paul Ormerod. Social versus independent interest in'bird flu'and'swine flu'. *PLoS Currents*, 1, 2009.

[6] Miguel Á González Block, Hortensia Reyes Morales, Lucero Cahuana Hurtado, Alejandra Balandrán, Edna Méndez, World Health Organization, et al. Mexico: health system review. 2020.

[7] Martin CJ Bootsma and Neil M Ferguson. The effect of public health measures on the 1918 influenza pandemic in us cities. *Proceedings of the National Academy of Sciences*, 104(18):7588–7593, 2007.

[8] Toon Braeye, Lucy Catteau, Ruben Brondeel, Joris AF van Loenhout, Kristiaan Proesmans, Laura Cornelissen, Herman Van Oyen, Veerle Stouten, Pierre Hubin, Matthieu Billuart, et al. Vaccine effectiveness against transmission of alpha, delta and omicron sars-cov-2-infection, belgian contact tracing, 2021–2022. *Vaccine*, 41(20):3292–3300, 2023.

[9] Fred Brauer and Carlos Castillo-Chavez. *Mathematical Models for Communicable Diseases*. SIAM, 2012.

[10] Chao-Ran Cai, Zhi-Xi Wu, and Jian-Yue Guan. Behavior of susceptible-vaccinated–infected–recovered epidemics with diversity in the infection rate of individuals. *Physical Review E*, 88(6):062805, 2013.

[11] Frank H Clarke. *Optimization and Nonsmooth Analysis*. SIAM, 1990.

[12] Kunchok Dorjee, Hyunju Kim, Elizabeth Bonomo, and Rinchen Dolma. Prevalence and predictors of death and severe disease in patients hospitalized due to covid-19: A comprehensive systematic review and meta-analysis of 77 studies and 38,000 patients. *PloS One*, 15(12):e0243191, 2020.

[13] John Duffy. Smallpox and the indians in the american colonies. *Bulletin of the History of Medicine*, 25(4):324–341, 1951.

[14] Darren Flynn-Primrose, Steven C Walker, Michael Li, Benjamin M Bolker, David JD Earn, and Jonathan Dushoff. Toward a comprehensive system for constructing compartmental epidemic models. *arXiv preprint arXiv:2307.10308*, 2023.

[15] Centers for Disease Control and Prevention. Covid data tracker, 2023.

[16] Zhiru Gao, Yinghui Xu, Chao Sun, Xu Wang, Ye Guo, Shi Qiu, and Kewei Ma. A systematic review of asymptomatic infections with covid-19. *Journal of Microbiology, Immunology and Infection*, 54(1):12–16, 2021.

[17] Shikha Garg, Lindsay Kim, Michael Whitaker, Alissa O'Halloran, Charisse Cummings, Rachel Holstein, Mila Prill, Shua J Chai, Pam D Kirley, Nisha B Alden, et al. Hospitalization rates and characteristics of patients hospitalized with laboratory-confirmed coronavirus disease 2019—covid-net, 14 states, march 1–30, 2020. *Morbidity and mortality weekly report*, 69(15):458, 2020.

[18] Robert Gibbons. *A Primer in Game Theory*. Pearson Academic, 1992.

[19] Marlène Guillon and Pauline Kergall. Attitudes and opinions on quarantine and support for a contact-tracing application in france during the covid-19 outbreak. *Public health*, 188:21–31, 2020.

[20] Herbert W Hethcote. A thousand and one epidemic models. In *Frontiers in Mathematical Biology*, pages 504–515. Springer, 1994.

[21] Herbert W Hethcote. The mathematics of infectious diseases. *SIAM Review*, 42(4):599–653, 2000.

[22] Josef Hofbauer and Karl Sigmund. *Evolutionary games and population dynamics*. Cambridge University Press, 1998.

[23] Rosemary Horrox. The black death. In *The Black Death*. Manchester University Press, 2013.

[24] Arno Karlen. *Man and microbes: disease and plagues in history and modern times*. Simon and Schuster, 1996.

[25] Kamil A Khan and Paul I Barton. Generalized derivatives for solutions of parametric ordinary differential equations with non-differentiable right-hand sides. *Journal of Optimization Theory and Applications*, 163:355–386, 2014.

[26] Kamil A Khan and Paul I Barton. A vector forward mode of automatic differentiation for generalized derivative evaluation. *Optimization Methods and Software*, 30(6):1185–1212, 2015.

[27] Li-Lin Liang, Hsu-Sung Kuo, Hsiu J Ho, and Chun-Ying Wu. Covid-19 vaccinations are associated with reduced fatality rates: Evidence from cross-county quasi-experiments. *Journal of Global Health*, 11, 2021.

[28] Shaoying Liu, Yongzhen Pei, Changguo Li, and Lansun Chen. Three kinds of tvs in a sir epidemic model with saturated infectious force and vertical transmission. *Applied Mathematical Modelling*, 33(4):1923–1932, 2009.

[29] Zaibunnisa Memon, Sania Qureshi, and Bisharat Rasool Memon. Assessing the role of quarantine and isolation as control strategies for covid-19 outbreak: a case study. *Chaos, Solitons & Fractals*, 144:110655, 2021.

[30] James Dickson Murray. *Mathematical Biology: II: Spatial Models and Biomedical Applications*, volume 3. Springer, 2003.

[31] Yu Nesterov. Lexicographic differentiation of nonsmooth functions. *Mathematical Programming*, 104:669–700, 2005.

[32] Martin J Osborne. *An introduction to game theory*, volume 3. Oxford university press New York, 2004.

[33] Todd L Parsons and David JD Earn. Analytical approximations for the phase plane trajectories of the sir model with vital dynamics. *HAL Open Science*, 2023.

[34] Lawrence Perko. *Differential equations and dynamical systems*, volume 7. Springer Science & Business Media, 2013.

[35] Piero Poletti, Bruno Caprile, Marco Ajelli, Andrea Pugliese, and Stefano Merler. Spontaneous behavioural changes in response to epidemics. *Journal of theoretical biology*, 260(1):31–40, 2009.

[36] Shanay Rab, Mohd Javaid, Abid Haleem, and Raju Vaishya. Face masks are new normal after covid-19 pandemic. *Diabetes & Metabolic Syndrome: Clinical Research & Reviews*, 14(6):1617–1619, 2020.

[37] Stephen Schecter. Geometric singular perturbation theory analysis of an epidemic model with spontaneous human behavioral change. *Journal of Mathematical Biology*, 82(6):54, 2021.

[38] Stefan Scholtes. *Introduction to piecewise differentiable equations*. Springer, 2012.

[39] Pauline Van den Driessche and James Watmough. Reproduction numbers and sub-threshold endemic equilibria for compartmental models of disease transmission. *Mathematical Biosciences*, 180(1-2):29–48, 2002.

[40] Raffaele Vardavas, Romulus Breban, and Sally Blower. Can influenza epidemics be prevented by voluntary vaccination? *PLoS Computational Biology*, 3(5):e85, 2007.

[41] John Von Neumann and Oskar Morgenstern. Theory of games and economic behavior. In *Theory of games and economic behavior*. Princeton university press, 2007.

[42] Vladimir Ilich Vorotnikov. *Partial stability and control*. Springer, 1998.

[43] Aili Wang, Yanni Xiao, and Robert Smith. Multiple equilibria in a non-smooth epidemic model with medical-resource constraints. *Bulletin of Mathematical Biology*, 81:963–994, 2019.

[44] Qiangping Wang, Xing Huang, Yansen Bai, Xuan Wang, Haijun Wang, Xuebin Hu, Feng Wang, Xianke Wang, Jincao Chen, Qianxue Chen, et al. Epidemiological characteristics of covid-19 in medical staff members of neurosurgery departments in hubei province: a multicentre descriptive study. *MedRxiv*, pages 2020–04, 2020.

[45] Wendi Wang and Shigui Ruan. Bifurcations in an epidemic model with constant removal rate of the infectives. *Journal of Mathematical Analysis and Applications*, 291(2):775–793, 2004.

[46] Mengbin Ye, Lorenzo Zino, Alessandro Rizzo, and Ming Cao. Game-theoretic modeling of collective decision making during epidemics. *Physical Review E*, 104(2):024314, 2021.

[47] Nazar Zaki and Elfadil A Mohamed. The estimations of the covid-19 incubation period: A scoping reviews of the literature. *Journal of Infection and Public Health*, 14(5):638–646, 2021.

Appendices

APPENDIX A
$\mathcal{R}_0$ FOR INTERMEDIATE MODELS

A.1 SEIR Model $\mathcal{R}_0$ Formulation

In this appendix we will be finding the $\mathcal{R}_0$ for a few of the intermediate SEIR models that were used to build the final Be-SEIMR model. First we start with a epidemic model containing the quarantined and asymptomatic compartments.

$$\begin{aligned}
\dot{E} &= \Psi - \Xi\sigma E - (1-\Xi)\sigma E - \mu E \\
\dot{I}_S &= (1-\Xi)\sigma E - \gamma I_S - \phi I_S - \mu I_S - \delta I_S \\
\dot{I}_A &= \Xi\sigma E - \gamma I_A - \mu I_A \\
\dot{I}_Q &= \phi I_S - \gamma I_Q - \mu I_Q - \delta I_Q \\
\dot{S} &= \Lambda - \Psi + \zeta R - \mu S \\
\dot{R} &= \gamma(I_S + I_A + I_Q) - \zeta R - \mu R
\end{aligned}$$

with secondary equations

$$\begin{aligned}
\Lambda &= \mu(S + E + I_S + I_A + I_Q + R) + \delta(I_S + I_Q) \\
\Psi &= \beta_n S(I_s + I_A) \\
\Upsilon &= I_S + I_Q
\end{aligned}$$

Once again we have to solve for $\mathcal{R}_0$. First we find $\mathcal{F}$, $\mathcal{V}^-$ and $\mathcal{V}^+$,

$$\mathcal{F} = \begin{bmatrix} \Psi \\ 0 \\ 0 \\ 0 \\ 0 \\ 0 \end{bmatrix}, \mathcal{V}^- = \begin{bmatrix} (\sigma+\mu)E \\ (\gamma+\phi+\mu+\delta)I_S \\ (\gamma+\mu)I_A \\ (\gamma+\mu+\delta)I_Q \\ \mu S \\ (\zeta+\mu)R \end{bmatrix}, \mathcal{V}^+ = \begin{bmatrix} 0 \\ (1-\Xi)\sigma E \\ \Xi\sigma E \\ \phi I_S \\ \Lambda + \zeta R \\ \gamma(I_S + I_A + I_Q) \end{bmatrix}$$

then we have that

$$\mathcal{V} = \begin{bmatrix} (\sigma+\mu)E \\ (\gamma+\phi+\mu+\delta)I_S - (1-\Xi)\sigma E \\ (\gamma+\mu)I_A - \Xi\sigma E \\ (\gamma+\mu+\delta)I_Q - \phi I_S \\ \mu S - \Lambda - \zeta R \\ (\zeta+\mu)R - \gamma(I_S + I_A + I_Q) \end{bmatrix}.$$

Now that we have $\mathcal{F}$ and $\mathcal{V}$ we need to identify the disease free equilibrium. For this model we have

$$x^* = (E, I_S, I_A, I_Q, S, R) = (0, 0, 0, 0, 1, 0)$$

which corresponds to all people being susceptible and all individuals acting with normal behavior. With these pieces we can find the Jacobians, however we only need the top

quadrant leaving us with 4×4 matrices,

$$F(x^*) = \begin{bmatrix} 0 & \beta_n & \beta_n & 0 \\ 0 & 0 & 0 & 0 \\ 0 & 0 & 0 & 0 \\ 0 & 0 & 0 & 0 \end{bmatrix}$$

$$V(x^*) = \begin{bmatrix} \sigma+\mu & 0 & 0 & 0 \\ (\Xi-1)\sigma & \gamma+\phi+\mu+\delta & 0 & 0 \\ -\Xi\sigma & 0 & \gamma+\mu & 0 \\ 0 & -\phi & 0 & \gamma+\mu+\delta \end{bmatrix}$$

$$V^{-1}(x^*) = \begin{bmatrix} \frac{1}{\sigma+\mu} & 0 & 0 & 0 \\ \frac{(1-\Xi)\sigma}{(\sigma+\mu)(\gamma+\phi+\mu+\delta)} & \frac{1}{\gamma+\phi+\mu+\delta} & 0 & 0 \\ \frac{\Xi\sigma}{(\sigma+\mu)(\gamma+\mu)} & 0 & \frac{1}{\gamma+\mu} & 0 \\ \frac{((1-\Xi)\sigma)(\phi)}{(\sigma+\mu)(\gamma+\phi+\mu+\delta)(\gamma+\mu+\delta)} & \frac{\phi}{(\gamma+\phi+\mu+\delta)(\gamma+\mu+\delta)} & 0 & \frac{1}{\gamma+\mu+\delta} \end{bmatrix}.$$

Then we have that

$$FV^{-1} = \begin{bmatrix} \frac{\beta_n(1-\Xi)\sigma}{(\sigma+\mu)(\gamma+\phi+\mu+\delta)} & \frac{\beta_n}{\gamma+\phi+\mu+\delta} & \frac{\beta_a}{\gamma+\mu} & 0 \\ 0 & 0 & 0 & 0 \\ 0 & 0 & 0 & 0 \\ 0 & 0 & 0 & 0 \end{bmatrix}.$$

Once again, since FV^{-1} is upper triangular and has only one non zero entry along the diagonal, we can easily see that

$$\rho(FV^{-1}) = \mathcal{R}_0 = \frac{\beta_n(1-\Xi)\sigma}{(\sigma+\mu)(\gamma+\phi+\mu+\delta)}.$$

A.2 Be-SEIMR Model Without Vaccination $\mathcal{R}_0$ Formulation

Here we look at another intermediate SEIR model. This time we add in minimal medical intervention with hospitalization. This model serves as the Be-SEIMR model without vaccination and behavioral components.

$$\begin{aligned} \dot{E} &= \Psi - \Xi\sigma E - (1-\Xi)\sigma E - \mu E \\ \dot{I}_S &= (1-\Xi)\sigma E - \gamma I_S - \eta I_S - \phi I_S - \mu I_S - \delta I_S \\ \dot{I}_A &= \Xi\sigma E - \gamma I_A - \mu I_A \\ \dot{I}_H &= \eta I_S - h(I_H) - \mu I_H - \delta_h I_H \\ \dot{I}_Q &= \phi I_S - \gamma I_Q - \mu I_Q - \delta I_Q \\ \dot{S} &= \Lambda - \Psi + \zeta R - \mu S \\ \dot{R} &= \gamma(I_S + I_A + I_Q) + h(I_H) - \zeta R - \mu R \end{aligned}$$

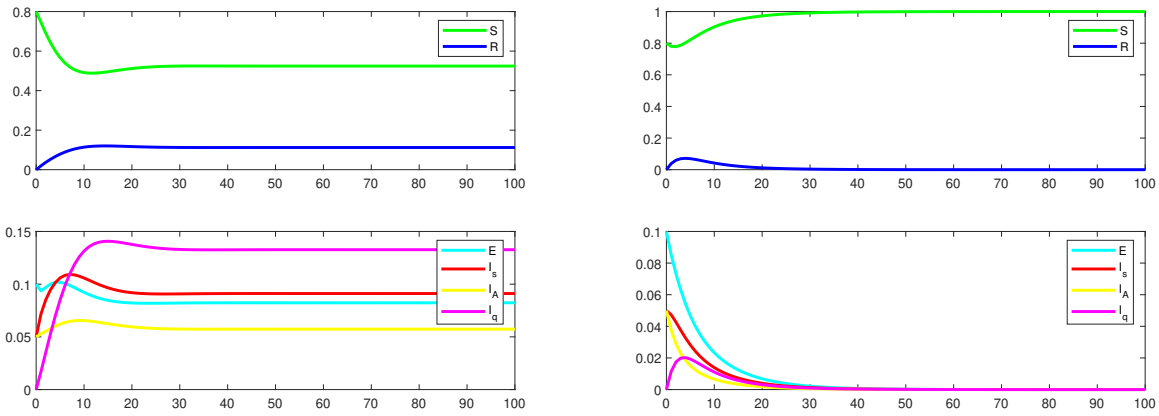

(a) $\mathcal{R}_0 > 1$ (b) $\mathcal{R}_0 < 1$

Figure A.1: For figure (a) we have $\mathcal{R}_0 = 1.263$ with $\beta_n = 0.8$, $\mu = 0.001$, $\Xi = 0.2$, $\sigma = 0.7$, $\gamma = 0.2$, $\phi = 0.3$ and $\delta = 0.005$. For figure (b) we have $\mathcal{R}_0 = 0.4953$ with $\beta_n = 0.5$, $\mu = 0.001$, $\Xi = 0.2$, $\sigma = 0.5$, $\gamma = 0.5$, $\phi = 0.3$ and $\delta = 0.005$.

with secondary equations

$$\begin{aligned}
\Lambda &= \mu(S + E + I_S + I_A + I_H + I_Q + R) + \delta(I_S + I_Q) + \delta_h I_H \\
\Psi &= \beta_n S(I_S + I_A) \\
\Upsilon &= I_S + I_Q + I_H \\
h(I_H) &= \min(rI_H, rH_c).
\end{aligned}$$

For this version of the model we have that

$$\mathcal{F} = \begin{bmatrix} \Psi \\ 0 \\ 0 \\ 0 \\ 0 \\ 0 \\ 0 \end{bmatrix}, \mathcal{V}^- = \begin{bmatrix} (\sigma + \mu)E \\ (\gamma + \eta + \phi + \mu + \delta)I_S \\ (\gamma + \mu)I_A \\ (\mu + \delta_h)I_H + min(rI_h, rH_c) \\ (\gamma + \mu + \delta)I_Q \\ \mu S \\ (\zeta + \mu)R \end{bmatrix}, \mathcal{V}^+ = \begin{bmatrix} 0 \\ (1 - \Xi)\sigma E \\ \Xi\sigma E \\ \eta I_S \\ \phi I_S \\ \Lambda + \zeta R \\ \gamma(I_S + I_A + I_Q) + min(rI_h, rH_c) \end{bmatrix}$$

and therefore

$$\mathcal{V} = \begin{bmatrix} (\sigma + \mu)E \\ (\gamma + \eta + \phi + \mu + \delta)I_S - (1 - \Xi)\sigma E \\ (\gamma + \mu)I_A - \Xi\sigma E \\ (\mu + \delta_h)I_H + min(rI_H, rH_c) - \eta I_S \\ (\gamma + \mu + \delta)I_Q - \phi I_S \\ \mu S - \Lambda - \zeta R \\ (\zeta + \mu)R - \gamma(I_S + I_A + I_Q) - min(rI_H, rH_c) \end{bmatrix}.$$

With these found we once again need to find the Jacobian for $\mathcal{F}$ and $\mathcal{V}$, but we only need to worry about the top 5×5 inputs of the matrix that correspond to F and V. Given the

disease free equilibrium,

$$x^* = (E, I_S, I_A, I_H, I_Q, S, R, x, y) = (0, 0, 0, 0, 0, 1, 0),$$

we have that

$$F(x^*) = \begin{bmatrix} 0 & \beta_n S & \beta_n S & 0 & 0 \\ 0 & 0 & 0 & 0 & 0 \\ 0 & 0 & 0 & 0 & 0 \\ 0 & 0 & 0 & 0 & 0 \\ 0 & 0 & 0 & 0 & 0 \end{bmatrix} (x^*) = \begin{bmatrix} 0 & \beta_n & \beta_n & 0 & 0 \\ 0 & 0 & 0 & 0 & 0 \\ 0 & 0 & 0 & 0 & 0 \\ 0 & 0 & 0 & 0 & 0 \\ 0 & 0 & 0 & 0 & 0 \end{bmatrix},$$

$$V(x^*) = \begin{bmatrix} \sigma+\mu & 0 & 0 & 0 & 0 \\ -(1-\Xi)\sigma & \gamma+\eta+\phi+\mu+\delta & 0 & 0 & 0 \\ -\Xi\sigma & 0 & \gamma+\mu & 0 & 0 \\ 0 & -\eta & 0 & \mu+\delta_h+r & 0 \\ 0 & -\phi & 0 & 0 & \gamma+\mu+\delta \end{bmatrix} (x^*)$$

$$= \begin{bmatrix} \sigma+\mu & 0 & 0 & 0 & 0 \\ -(1-\Xi)\sigma & \gamma+\eta+\phi+\mu+\delta & 0 & 0 & 0 \\ -\Xi\sigma & 0 & \gamma+\mu & 0 & 0 \\ 0 & -\eta & 0 & \mu+\delta_h+r & 0 \\ 0 & -\phi & 0 & 0 & \gamma+\mu+\delta \end{bmatrix}.$$

Therefore we have that,

$$V^{-1}(x^*) = \begin{bmatrix} \frac{1}{\sigma+\mu} & 0 & 0 & 0 & 0 \\ \frac{(1-\Xi)\sigma}{(\sigma+\mu)(\gamma+\eta+\phi+\mu+\delta)} & \frac{1}{\gamma+\eta+\phi+\mu+\delta} & 0 & 0 & 0 \\ \frac{\Xi\sigma}{(\sigma+\mu)(\gamma+\mu)} & 0 & \frac{1}{\gamma+\mu} & 0 & 0 \\ 0 & \frac{\eta}{(\mu+\delta_h+r)(\gamma+\eta+\phi+\mu+\delta)} & 0 & \frac{1}{\mu+\delta_h+r} & 0 \\ 0 & \frac{\phi}{(\gamma+\mu+\delta)(\gamma+\eta+\phi+\mu+\delta)} & 0 & 0 & \frac{1}{\gamma+\mu+\delta} \end{bmatrix}$$

$$FV^{-1} = \begin{bmatrix} \frac{(1-\Xi)\sigma\beta_n}{(\sigma+\mu)(\gamma+\eta+\phi+\mu+\delta)} + \frac{\Xi\sigma\beta_n}{(\sigma+\mu)(\gamma+\mu)} & \frac{\beta_n}{\gamma+\eta+\phi+\mu+\delta} & \frac{\beta_a}{\gamma+\mu} & 0 & 0 \\ 0 & 0 & 0 & 0 & 0 \\ 0 & 0 & 0 & 0 & 0 \\ 0 & 0 & 0 & 0 & 0 \\ 0 & 0 & 0 & 0 & 0 \end{bmatrix}$$

Once again FV^{-1} is upper triangular and we can easily see it has only one nonzero eigenvalue, therefore

$$\rho(FV^{-1}) = \mathcal{R}_0 = \frac{(1-\Xi)\sigma\beta_n}{(\sigma+\mu)(\gamma+\eta+\phi+\mu+\delta)} + \frac{\Xi\sigma\beta_n}{(\sigma+\mu)(\gamma+\mu)}.$$

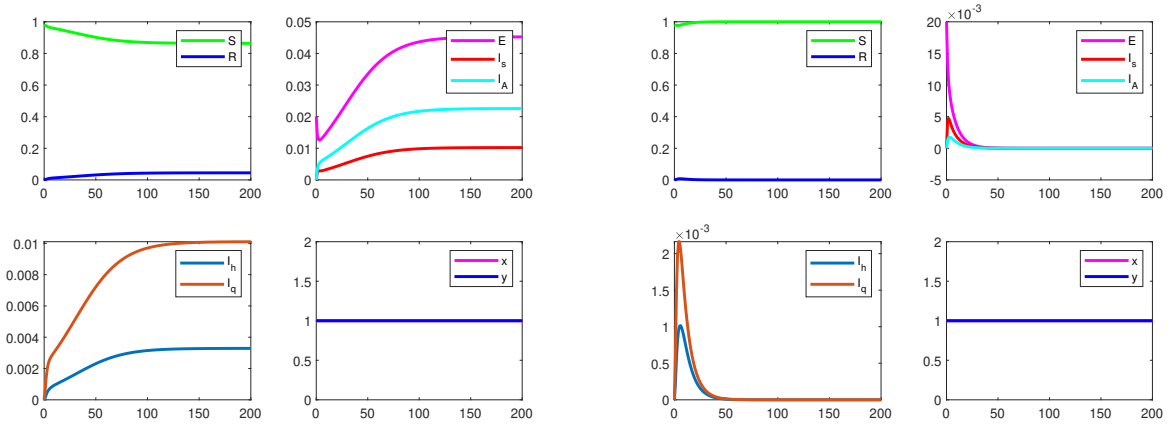

(a) $\mathcal{R}_0 > 1$ (b) $\mathcal{R}_0 < 1$

Figure A.2: For figure (a) we have $\mathcal{R}_0 = 1.1578$ with $\Xi = 0.5$, $\sigma = 0.5$, $\beta_n = 0.8$, $\mu = 0.001$, $\gamma = 0.5$, $\phi = 0.5$, $\eta = 0.1$ and $\delta = 0.005$. For figure (b) we have $\mathcal{R}_0 = 0.6398$ with $\Xi = 0.2$, $\sigma = 0.5$, $\beta_n = 0.5$, $\mu = 0.001$, $\gamma = 0.5$, $\phi = 0.3$, $\eta = 0.1$ and $\delta = 0.005$.

APPENDIX B
BE-SEIMR SENSITIVITY ANALYSIS

Let us now examine $S_V = \Omega(S) - \theta S_V - \psi - \mu S_V$. Drawing from the earlier development of the sensitivity equations for S, we are already familiar with $\Omega(S)'$. Focusing on the smooth component, we find:

$$\begin{aligned} O_{S_V}(\mathbf{p}, \mathbf{x}) &= -\theta S_V - \mu S_V \\ O'_{S_V}(\mathbf{p}^*, \mathbf{x}^*; (\mathbf{M}, \mathbf{S_x}) &= \begin{bmatrix} J_{\mathbf{p}} O_{S_V}(\mathbf{p}^*, \mathbf{x}^*) & | & J_{\mathbf{x}} O_{S_V}(\mathbf{p}^*, \mathbf{x}^*) \end{bmatrix} \begin{bmatrix} M \\ \mathbf{S_x} \end{bmatrix} \\ &= \begin{bmatrix} 0 & 0 & 0 & -S_V^* & \mathbf{0}_{1,15} & | & 0 & -\theta^* - \mu & \mathbf{0}_{1,12} \end{bmatrix} \begin{bmatrix} \mathbf{M} \\ \mathbf{S_x} \end{bmatrix} \\ &= \begin{bmatrix} -S_V^* m_{4,1} + (-\theta^* - \mu) S_{S_V}^{\beta_n} \\ \vdots \\ -S_V^* m_{4,19} + (-\theta^* - \mu) S_{S_V}^{y_0} \end{bmatrix}^T. \end{aligned}$$

Subsequently, for the remaining nonsmooth component, we will investigate:

$$\begin{aligned} \psi &= \beta_v S_V [I_S + I_A \text{mid}(0, y, 1) + \kappa I_A \text{mid}(0, (1-y), 1) + I_V] \\ &= \beta_v S_V I_S + \beta_v S_V I_A \text{mid}(0, y, 1) + \beta_v S_V \kappa I_A \text{mid}(0, (1-y), 1) + \beta_v S_V I_V. \end{aligned}$$

Once more, we will follow a parallel process similar to when we derived Ψ for S. We will start by considering:

$$\begin{aligned} \psi_1 &= \beta_v S_V I_S \\ \psi_2 &= \beta_v S_V I_A \text{mid}(0, y, 1) \\ \psi_3 &= \beta_v S_V \kappa I_A \text{mid}(0, (1-y), 1) \\ \psi_4 &= \beta_v S_V I_V. \end{aligned}$$

From this, we can determine the expression. Similar to before, we will use abbreviated notation, where $\psi_i' = \psi_i'(\mathbf{p}^*, \mathbf{x}^*; (\mathbf{M}, \mathbf{S_x}))$,

$$\psi_1' = \begin{bmatrix} S_V^* I_S^* m_{3,1} + \beta_v^* I_S^* S_{S_V}^{\beta_n} + \beta_v^* S_V^* S_{I_S}^{\beta_n} \\ \vdots \\ S_V^* I_S^* m_{3,19} + \beta_v^* I_S^* S_{S_V}^{y_0} + \beta_v^* S_V^* S_{I_S}^{y_0} \end{bmatrix}$$

$$\psi_2' = \begin{bmatrix} S_V^* I_A^* \text{mid}(0, y^*, 1) m_{3,1} + \beta_v^* I_A^* \text{mid}(0, y^*, 1) S_{S_V}^{\beta_n} + \beta_v^* S_V^* \text{mid}(0, y^*, 1) S_{I_A}^{\beta_n} \\ \vdots \\ S_V^* I_A^* \text{mid}(0, y^*, 1) m_{3,19} + \beta_v^* I_A^* \text{mid}(0, y^*, 1) S_{S_V}^{y_0} + \beta_v^* S_V^* \text{mid}(0, y^*, 1) S_{I_A}^{y_0} \end{bmatrix}$$
$$+ \beta_v^* S_V^* I_A^* \text{slmid}([\mathbf{0}^{20}], [\text{y}, \text{S}_\text{y}], [1, \mathbf{0}^{19}])$$

$$\psi_3' = \begin{bmatrix} S_V^* \kappa I_A^* \text{mid}(0, (1-y^*), 1) m_{3,1} + \beta_v^* \kappa I_A^* \text{mid}(0, (1-y^*), 1) S_{S_V}^{\beta_n} + \beta_v^* S_V^* \kappa \text{mid}(0, (1-y^*), 1) S_{I_A}^{\beta_n} \\ \vdots \\ S_V^* \kappa I_A^* \text{mid}(0, (1-y^*), 1) m_{3,19} + \beta_v^* \kappa I_A^* \text{mid}(0, (1-y^*), 1) S_{S_V}^{y_0} + \beta_v^* S_V^* \kappa \text{mid}(0, (1-y^*), 1) S_{I_A}^{y_0} \end{bmatrix}$$
$$+ \beta_v^* S_V^* \kappa I_A^* \text{slmid}([\mathbf{0}^{20}], [1 - \text{y}, -\text{S}_\text{y}], [1, \mathbf{0}^{19}])$$

$$\psi_4 = \begin{bmatrix} S_V^* I_V^* m_{3,1} + \beta_v^* I_V^* S_{S_V}^{\beta_n} + \beta_v^* S_V^* S_{I_V}^{\beta_n} \\ \vdots \\ S_V^* I_V^* m_{3,19} + \beta_v^* I_V^* S_{S_V}^{y_0} + \beta_v^* S_V^* S_{I_V}^{y_0} \end{bmatrix}.$$

Therefore

$$\begin{aligned} \psi' &= \psi_1' + \psi_2' + \psi_3' + \psi_4' \\ \dot{S}_{S_V} &= -\psi'(\mathbf{p}^*, \mathbf{x}^*; (\mathbf{M}, \mathbf{S_x})) + \Omega'(\mathbf{p}^*, \mathbf{x}^*; (M, \mathbf{S_x})) + O'_{S_V}(\mathbf{p}^*, \mathbf{x}^*; (\mathbf{M}, \mathbf{S_x})). \end{aligned}$$

Turning our attention to $\dot{E}$, we have:

$$\dot{E} = \Psi - \Xi\sigma E - (1 - \Xi)\sigma E - \mu E.$$

Given that we have already LD-differentiated Ψ earlier, our focus will be on the smooth portion:

$$\begin{aligned} O_E(\mathbf{p}, \mathbf{x}) &= -\Xi\sigma E - (1-\Xi)\sigma E - \mu E = -\Xi\sigma E - \sigma E + \Xi\sigma E - \mu E = -\sigma E - \mu E \\ \Rightarrow O'_E(\mathbf{p}^*, \mathbf{x}^*; (M, \mathbf{S_x})) &= \begin{bmatrix} J_\mathbf{p} O_E(\mathbf{p}^*, \mathbf{x}^*) & | & J_\mathbf{x} O_E(\mathbf{p}^*, \mathbf{x}^*) \end{bmatrix} \begin{bmatrix} \mathbf{M} \\ \mathbf{S_x} \end{bmatrix} \\ &= \begin{bmatrix} \mathbf{0}_{1,4} & -E^* & \mathbf{0}_{1,14} & | & 0 & 0 & -\sigma^* - \mu & \mathbf{0}_{1,11} \end{bmatrix} \begin{bmatrix} \mathbf{M} \\ \mathbf{S_x} \end{bmatrix} \\ &= \begin{bmatrix} -E^* m_{5,1} + (-\sigma^* - \mu) S_E^{\beta_n} \\ \vdots \\ -E^* m_{5,19} + (-\sigma^* - \mu) S_E^{y_0} \end{bmatrix}. \end{aligned}$$

Consequently:

$$\dot{S}_E = \Psi'(\mathbf{p}^*, \mathbf{x}^*; (\mathbf{M}, \mathbf{S_x})) + O'(\mathbf{p}^*, \mathbf{x}^*; (\mathbf{M}, \mathbf{S_x}))$$

Moving forward, we consider:

$$\dot{E}_V = \psi - \Xi\sigma E_V - (1-\Xi)\sigma E_V - \mu E_V = \psi - \sigma E_V - \mu E_V$$

Once more, since we have already LD-differentiated ψ in the section pertaining to S_V, our attention will be directed towards the smooth part:

$$\begin{aligned} O_{E_V}(\mathbf{p}, \mathbf{x}) &= -\sigma E_V - \mu E_V \\ \Rightarrow O'_{E_V}(\mathbf{p}^*, \mathbf{x}^*; (\mathbf{M}, \mathbf{S_x})) &= \begin{bmatrix} J_{\mathbf{p}} O_{E_V}(\mathbf{p}^*, \mathbf{x}^*) & | & J_{\mathbf{x}} O_{E_V}(\mathbf{p}^*, \mathbf{x}^*) \end{bmatrix} \begin{bmatrix} M \\ \mathbf{S_x} \end{bmatrix} \\ &= \begin{bmatrix} \mathbf{0}_{1,4} & -E_V^* & \mathbf{0}_{1,14} & | & 0 & 0 & 0 & -\sigma^* - \mu & \mathbf{0}_{1,10} \end{bmatrix} \begin{bmatrix} M \\ \mathbf{S_x} \end{bmatrix} \\ &= \begin{bmatrix} -E_V^* m_{6,1} + (-\sigma^* - \mu) S_{E_V}^{\beta n} \\ \vdots \\ -E_V^* m_{6,19} + (-\sigma^* - \mu) S_{E_V}^{y_0} \end{bmatrix}. \end{aligned}$$

Therefore

$$\dot{S}_{E_V} = \psi'(\mathbf{p}^*, \mathbf{x}^*; (\mathbf{M}, \mathbf{S_x})) + O'(\mathbf{p}^*, \mathbf{x}^*; (M, \mathbf{S_x})).$$

Likewise, for I_S,

$$\dot{I}_V = (1-\Xi)\sigma E_V - \gamma I_V - \eta I_V - \phi I_V - \mu I_V - \delta_v I_V,$$

the equation is smooth and leads to straightforward solution.

$$\begin{aligned} I'_V(\mathbf{p}^*, \mathbf{x}^*; (\mathbf{M}, \mathbf{S_x})) &= \begin{bmatrix} J_{\mathbf{p}} I_V(\mathbf{p}^*, \mathbf{x}^*) & | & J_{\mathbf{x}} I_V(\mathbf{p}^*, \mathbf{x}^*) \end{bmatrix} \begin{bmatrix} \mathbf{M} \\ \mathbf{S_x} \end{bmatrix} \\ &= \begin{bmatrix} \mathbf{0}_{1,4} & (1-\Xi^*)E_V^* & -\sigma^* E_V^* & -I_V^* & -I_V^* & -I_V^* & \mathbf{0}_{1,10} & | & 0 & 0 & 0 & (1-\Xi^*)\sigma^* & 0 & -(\gamma^* + \eta^* + \phi^* + \mu + \delta_v) & \mathbf{0}_{1,8} \end{bmatrix} \begin{bmatrix} \mathbf{M} \\ \mathbf{S_x} \end{bmatrix} \\ &= \begin{bmatrix} (1-\Xi^*)E_V^* m_{5,1} - \sigma^* E_V^* m_{6,1} - I_V(m_{7,1} + m_{8,1} + m_{9,1}) + (1-\Xi^*)\sigma^* S_{E_V}^{\beta} - (\gamma^* + \eta^* + \phi^* + \mu + \delta) S_{I_V}^{\beta} \\ \vdots \\ (1-\Xi^*)E_V^* m_{5,19} - \sigma^* E_V^* m_{6,19} - I_V(m_{7,19} + m_{8,19} + m_{9,19}) + (1-\Xi^*)\sigma^* S_{E_V}^{y_0} - (\gamma^* + \eta^* + \phi^* + \mu + \delta) S_{I_V}^{y_0}. \end{bmatrix} \end{aligned}$$

Once again, we encounter a scenario characterized by smooth dynamics:

$$\dot{I}_A = \Xi\sigma[E + E_V] - \gamma I_A - \mu I_A.$$

This can be solved to find:

$$\begin{aligned} I'_A(\mathbf{p}^*, \mathbf{x}^*; (\mathbf{M}, \mathbf{S_x})) &= \begin{bmatrix} J_{\mathbf{p}} I_A(\mathbf{p}^*, \mathbf{x}^*) & | & J_{\mathbf{x}} I_A(\mathbf{p}^*, \mathbf{x}^*) \end{bmatrix} \begin{bmatrix} \mathbf{M} \\ \mathbf{S_x} \end{bmatrix} \\ &= \begin{bmatrix} \mathbf{0}_{1,4} & \Xi^*(E^* + E_V^*) & \sigma^*(E^* + E_V^*) & 0 & 0 & -I_A^* & \mathbf{0}_{1,9} & | & 0 & 0 & \Xi^*\sigma^* & \Xi^*\sigma^* & 0 & 0 & -\gamma^* - \mu & \mathbf{0}_{1,6} \end{bmatrix} \begin{bmatrix} \mathbf{M} \\ \mathbf{S_x} \end{bmatrix} \\ &= \begin{bmatrix} \Xi^*(E^* + E_V^*) m_{5,1} + \sigma^*(E^* + E_V^*) m_{6,1} - I_A^* m_{9,1} + \Xi^*\sigma^* S_E^{\beta} + \Xi^*\sigma^* S_{E_V}^{\beta} + (-\gamma^* - \mu) S_{I_A}^{\beta} \\ \vdots \\ \Xi^*(E^* + E_V^*) m_{5,19} + \sigma^*(E^* + E_V^*) m_{6,19} - I_A^* m_{9,19} + \Xi^*\sigma^* S_E^{y_0} + \Xi^*\sigma^* S_{E_V}^{y_0} + (-\gamma^* - \mu) S_{I_A}^{y_0}. \end{bmatrix} \end{aligned}$$

As we shift our focus back to the non-smooth realm with I_H, the expression is as follows:

$$\begin{aligned}
\dot{I}_H &= \eta I_S - h(I_H) - \mu I_H - \delta_h I_H \\
&= -\min(rI_H, rH_c) + \eta I_S - \mu I_H - \delta_h I_H \\
&= W(\mathbf{p}, \mathbf{x}) + O(\mathbf{p}, \mathbf{x}) \\
W_{I_H}(\mathbf{p}, \mathbf{x}) &= -\min(rI_H, rH_c) \\
O_{I_H}(\mathbf{p}, \mathbf{x}) &= \eta I_S - \mu I_H - \delta_h I_H.
\end{aligned}$$

For the smooth part we have that

$$\begin{aligned}
O_{I_H}(\mathbf{p}, \mathbf{x}) &= \eta I_S - \mu I_H - \delta_h I_H \\
O'_{I_H}(\mathbf{p}^*, \mathbf{x}^*; (\mathbf{M}, \mathbf{S_x})) &= \begin{bmatrix} J_{\mathbf{p}} O_{I_H}(\mathbf{p}^*, \mathbf{x}^*) & | & J_{\mathbf{x}} O_{I_H}(\mathbf{p}^*, \mathbf{x}^*) \end{bmatrix} \begin{bmatrix} \mathbf{M} \\ \mathbf{S_x} \end{bmatrix} \\
&= \begin{bmatrix} \mathbf{0}_{1,6} & I_S^* & \mathbf{0}_{1,12} & | & \mathbf{0}_{1,4} & \eta^* & 0 & 0 & -\mu - \delta_h & \mathbf{0}_{1,6} \end{bmatrix} \begin{bmatrix} \mathbf{M} \\ \mathbf{S_x} \end{bmatrix} \\
&= \begin{bmatrix} I_S^* m_{7,1} + \eta^* S_{I_S}^{\beta} + (-\mu - \delta_h) S_{I_H}^{\beta} \\ \vdots \\ I_S^* m_{7,19} + \eta^* S_{y_0}^{\beta} + (-\mu - \delta_h) S_{y_0}^{\beta} \end{bmatrix}
\end{aligned}$$

For the nonsmooth part, our approach mirrors the calculation previously performed in the sensitivity derivation for R, albeit with a sign change. Hence, we have:

$$\begin{aligned}
\dot{S}_{I_H} = &-\text{slmin}([\mathrm{r^*I_H^*} \quad \mathrm{I_H^* m_{12,1} + r^* S_{I_H}^{\beta}} \quad \cdots \quad \mathrm{I_H^* m_{12,1} + r^* S_{I_H}^{y_0}}]^{\mathrm{T}}, [\mathrm{r^* H_c} \quad \mathrm{H_c m_{12,1}} \quad \cdots \quad \mathrm{H_c m_{12,19}}]^{\mathrm{T}}) \\
&+ \begin{bmatrix} I_S^* m_{7,1} + \eta^* S_{I_S}^{\beta} + (-\mu - \delta_h) S_{I_H}^{\beta} \\ \vdots \\ I_S^* m_{7,19} + \eta^* S_{y_0}^{\beta} + (-\mu - \delta_h) S_{y_0}^{\beta} \end{bmatrix}
\end{aligned}$$

Much like its unvaccinated counterpart, I_{HV} also falls into the non-smooth category. In this instance, we select:

$$\begin{aligned}
\dot{I}_{HV} &= \eta I_V - h(I_{HV}) - \mu I_{HV} - \chi \delta_h I_{HV} \\
&= -\min(rI_V, rH_c) + \eta I_V - \mu I_{HV} - \chi \delta_h I_{HV} \\
&= W_{I_{HV}}(\mathbf{p}, \mathbf{x}) + O_{I_{HV}}(\mathbf{p}, \mathbf{x}) \\
W_{I_{HV}}(\mathbf{p}, \mathbf{x}) &= -\min(rI_V, rH_c) \\
O_{I_{HV}}(\mathbf{p}, \mathbf{x}) &= \eta I_V - \mu I_{HV} - \chi \delta_h I_{HV}.
\end{aligned}$$

For the non smooth part $W(\mathbf{p}, \mathbf{x})$ we have that

$$\begin{aligned}
W'_{I_{HV}}(\mathbf{p}^*, \mathbf{x}^*) &= -\text{slmin}([\mathrm{r^* I_{HV}^*} \quad \mathrm{J_p r^* I_V^* M + J_x r^* I_V^* S_x}], [\mathrm{r^* H_c} \quad \mathrm{J_p r^* H_c M + J_x r^* H_c S_x}]) \\
&= -\text{slmin}([\mathrm{r^* I_{HV}^*} \quad [\mathbf{0}^{11}, \mathrm{I_{HV}^*}, \mathbf{0}^7]\mathrm{M} + [\mathbf{0}^8, \mathrm{r^*}, \mathbf{0}^5]\mathbf{S_x}], [\mathrm{r^* H_c} \quad [\mathbf{0}^{11}, \mathrm{H_c}, \mathbf{0}^7]\mathrm{M} + \mathbf{0 S_x}]) \\
&= -\text{slmin}([\mathrm{r^* I_{HV}^*} \quad \mathrm{I_{HV}^* m_{12,1} + r^* S_{I_{HV}}^{\beta}} \quad \cdots \quad \mathrm{I_{HV}^* m_{12,1} + r^* S_{I_{HV}}^{y_0}}]^{\mathrm{T}}, \\
&\quad [r^* H_c \quad H_c m_{12,1} \quad \cdots \quad H_c m_{12,19}]^T).
\end{aligned}$$

For the smooth part we have that

$$\begin{aligned} O'_{I_{HV}}(\mathbf{p}^*, \mathbf{x}^*; (M, \mathbf{S_x})) &= \begin{bmatrix} J_{\mathbf{p}} O_{I_{HV}}(\mathbf{p}^*, \mathbf{x}^*) & | & J_{\mathbf{x}} O_{I_{HV}}(\mathbf{p}^*, \mathbf{x}^*) \end{bmatrix} \begin{bmatrix} \mathbf{M} \\ \mathbf{S_x} \end{bmatrix} \\ &= \begin{bmatrix} \mathbf{0}_{1,7} & I_V^* & \mathbf{0}_{1,11} & | & \mathbf{0}_{1,5} & \eta^* & 0 & 0 & -\mu-\chi\delta_h & \mathbf{0}_{1,5} \end{bmatrix} \begin{bmatrix} \mathbf{M} \\ \mathbf{S_x} \end{bmatrix} \\ &= \begin{bmatrix} I_V^* m_{7,1} + \eta^* S_{I_V}^{\beta} + (-\mu-\chi\delta_h) S_{I_{HV}}^{\beta} \\ \vdots \\ I_V^* m_{7,19} + \eta^* S_{I_V}^{y_0} + (-\mu-\chi\delta_h) S_{I_{HV}}^{y_0} \end{bmatrix} \end{aligned}$$

Therefore

$$\begin{aligned} \dot{S}_{I_H} = &-\mathrm{slmin}([\mathrm{r}^* \mathrm{I}_{\mathrm{H}}^* \quad \mathrm{I}_{\mathrm{HV}}^* \mathrm{m}_{12,1} + \mathrm{r}^* \mathrm{S}_{\mathrm{I_{HV}}}^{\beta} \quad \cdots \quad \mathrm{I}_{\mathrm{HV}}^* \mathrm{m}_{12,1} + \mathrm{r}^* \mathrm{S}_{\mathrm{I_{HV}}}^{\mathrm{y_0}}]^{\mathrm{T}}, [\mathrm{r}^* \mathrm{H_c} \quad \mathrm{H_c m_{12,1}} \quad \cdots \quad \mathrm{H_c m_{12,19}}]^{\mathrm{T}}) \\ &+ \begin{bmatrix} I_V^* m_{7,1} + \eta^* S_{I_V}^{\beta} + (-\mu-\chi\delta_h) S_{I_{HV}}^{\beta} \\ \vdots \\ I_V^* m_{7,19} + \eta^* S_{I_V}^{y_0} + (-\mu-\chi\delta_h) S_{I_{HV}}^{y_0} \end{bmatrix} \end{aligned}$$

The quarantine categories exhibit smooth behavior, with the initial one being:

$$\dot{I}_Q = \phi I_S - \gamma I_Q - \mu I_Q - \delta I_Q$$

and can be easily solved resulting in

$$\begin{aligned} I'_Q(\mathbf{p}^*, \mathbf{x}^*; (\mathbf{M}, \mathbf{S_x})) &= \begin{bmatrix} J_{\mathbf{p}} I_Q(\mathbf{p}^*, \mathbf{x}^*) & | & J_{\mathbf{x}} I_Q(\mathbf{p}^*, \mathbf{x}^*) \end{bmatrix} \begin{bmatrix} \mathbf{M} \\ \mathbf{S_x} \end{bmatrix} \\ &= \begin{bmatrix} \mathbf{0}_{[1,7]} & I_S^* & -I_Q^* & \mathbf{0}_{1,9} & | & \mathbf{0}_{1,4} & \phi^* & \mathbf{0}_{1,4} & -\gamma^*-\mu-\delta & \mathbf{0}_{1,4} \end{bmatrix} \begin{bmatrix} \mathbf{M} \\ \mathbf{S_x} \end{bmatrix} \\ &= \begin{bmatrix} I_S^* m_{8,1} - I_Q^* m_{9,1} + \phi^* S_{I_S}^{\beta} + (-\gamma^*-\mu-\delta) S_{I_Q}^{\beta} \\ \vdots \\ I_S^* m_{8,19} - I_Q^* m_{9,19} + \phi^* S_{I_S}^{y_0} + (-\gamma^*-\mu-\delta) S_{I_Q}^{y_0}. \end{bmatrix} \end{aligned}$$

The second quarantine category is

$$\dot{I}_{QV} = \phi I_V - \gamma I_{QV} - \mu I_{QV} - \delta_v I_{QV}$$

and can be easily solved resulting in

$$\begin{aligned} I'_{QV}(\mathbf{p}^*, \mathbf{x}^*; (M, \mathbf{S_x})) &= \begin{bmatrix} J_{\mathbf{p}} I_{QV}(\mathbf{p}^*, \mathbf{x}^*) & | & J_{\mathbf{x}} I_{QV}(\mathbf{p}^*, \mathbf{x}^*) \end{bmatrix} \begin{bmatrix} \mathbf{M} \\ \mathbf{S_x} \end{bmatrix} \\ &= \begin{bmatrix} 0 & 0 & 0 & 0 & 0 & 0 & 0 & I_V^* & -I_{QV}^* & 0 & 0 & 0 & 0 & 0 & 0 & 0 & 0 & 0 & | & 0 & 0 & 0 & 0 & 0 & \phi^* & 0 & 0 & 0 & 0 & -\gamma^*-\mu-\delta_v & 0 & 0 & 0 \end{bmatrix} \begin{bmatrix} M \\ \mathbf{S_x} \end{bmatrix} \\ &= \begin{bmatrix} I_V^* m_{8,1} - I_{QV}^* m_{9,1} + \phi^* S_{I_V}^{\beta} + (-\gamma^*-\mu-\delta) S_{I_{QV}}^{\beta} \\ \vdots \\ I_V^* m_{8,19} - I_{QV}^* m_{9,19} + \phi^* S_{I_V}^{y_0} + (-\gamma^*-\mu-\delta) S_{I_{QV}}^{y_0}. \end{bmatrix} \end{aligned}$$

APPENDIX C
BE-SEIMR MODEL COMPARISON

We have opted to draw parameters from Acuña-Zegarra et al. [1] due to the noteworthy parallels between their non-vaccination model and our initial base model. Here we present their model:

$$\begin{aligned}
\dot{S} &= \mu N - (\frac{\beta_S I_S + \beta_A I_A}{N})S - \mu S + \sigma_R R \\
\dot{E} &= (\frac{\beta_S I_S + \beta_A I_A}{N})S - \mu E - \sigma_E E \\
\dot{I}_S &= \rho\sigma_E E - \mu I_A - \alpha_A I_A \\
\dot{I}_A &= (1-\rho)\sigma_E E - \mu I_A + \alpha_A I_A \\
\dot{R} &= \alpha_S I_S - \theta\alpha_S I_S + \alpha_A I_A - \mu R - \sigma_R R \\
\dot{D} &= \theta\alpha_S I_S.
\end{aligned}$$

In order to get a better understanding of their model we must make a few modifications. As a preliminary step, we must adjust the outputs of their system. We will transform the exact values representing individuals within each compartment into proportions of the population, ranging from zero to one. We will then change their naming conventions to match our own, ensuring consistency in terminology. This results in their model becoming:

$$\begin{aligned}
\dot{S} &= \mu - S\beta_n(I_S + I_A) - \mu S + \zeta R \\
\dot{E} &= S\beta_n(I_S + I_A) - \mu E - \sigma E \\
\dot{I}_S &= (1-\Xi)\sigma E - \mu I_A - \gamma I_A \\
\dot{I}_A &= \Xi\sigma E - \mu I_A + \gamma I_A \\
\dot{R} &= \gamma I_S - \delta I_S + \gamma I_A - \mu R - \zeta R \\
\dot{D} &= \delta I_S.
\end{aligned}$$

While there exist a few minor disparities between the Acuña-Zegarra model and our model, they are of minimal consequence. One such difference is their choice to direct disease related deaths out of the recovered compartment instead of I_S. However, it is important to note that these two flows are identical in value and lead to the same ultimate outcome. The other minor distinction lies in their omission of adding disease related deaths back into the model as births. Given the relatively large population values they employed $N = 26446435$ [1], the impact of this omission on the overall model dynamics is negligible.

BIOGRAPHY OF THE AUTHOR

Cameron Morin is from the small town of Troy, Maine. He then graduated from Mount View High School in 2017, and then graduated with a bachelors in Mathematics along with a minor in religion in 2020 from the University of Maine at Farmington. Cameron Morin is a candidate for the Master of Arts degree in Mathematics from the University of Maine in December 2023.